An Abstract of the Thesis of

David Pidwerbecki for the degree of Doctor of Philosophy in Mechanical Engineering presented on August 29, 1994.
Title: Heat Transfer in the Splash-Zone of a High Temperature Fluidized Bed

Abstract approved: _____
James R. Welty

Experimental results and a predictive correlation are presented describing the heat transfer from a high temperature bubbling fluidized bed of Geldart class D particles to a horizontal tube (brass, 51 mm outside diameter) located in the dense phase, splash-zone, and the freeboard of the bed, respectively. The effects of four different parameters were investigated: the tube location relative to the non-fluidized bed surface was varied, spanning the range from within the dense phase to a location in within the freeboard; particle sizes from 1.1 mm to 2.9 mm mean diameter were used; the effect of bed temperature was studied from 700 K to 1003 K; and the superficial velocity was varied from near minimum fluidization (U_{mf}) to over 2.0 U_{mf}. Specifically reported are the effects of bed temperature on the heat transfer coefficients for a range of superficial velocities, heat transfer coefficients vs. particle size for two representative temperatures, and heat transfer coefficients variations for different tube locations at two representative temperatures. Also presented is a correlation which predicts the heat transfer coefficients in the splash-zone for the range of variables studied.

Temperature effects on the heat transfer coefficients involved studying the significance of four bed operating temperatures (700 K, 810 K, 908 K, and 1003 K) at three tube locations representative of the freeboard, the splash-zone, and the immersed bed. The mean bed particle size was 2.9 mm, and the superficial fluidizing velocity varied from near minimum fluidization conditions (U_{mf}) to over 1.5 U_{mf}.

Particle size effects involved studying an array of experimental conditions which included three particle sizes, of nominal 1.1, 2.0, and 2.9 mm diameter; four bed temperatures (described above), and three tube locations representative of the freeboard, splash-zone, and dense phase of the bed. Convective and blackbody radiative heat transfer coefficient variations are presented as functions of superficial velocity and of particle size for the 1003 K case and the maximum convective and blackbody radiative heat transfer coefficients are tabulated for the other temperatures and particle sizes. The superficial velocity was varied from near minimum fluidization conditions (U_{mf}) to over 2.0 U_{mf}.

Tube location effects on the heat transfer coefficients included obtaining experimental data for the three particle sizes over four bed temperatures at six tube locations ranging from the dense phase to the freeboard within the fluidized bed. The superficial velocity was varied from near minimum fluidization to twice that value. Convective heat transfer coefficients variations for the 810 K and the 1003 K cases and blackbody radiative heat transfer coefficient variations for the 1003 K case are presented.

A correlation based on simple ballistic theory is developed to predict the heat transfer coefficients to a tube in the splash-zone of a bubbling fluidized bed. Due to the inability to correctly predict values for h_{∞}, a conservative RMS error estimate of 30% is recommended when applying the model.

Heat Transfer in the Splash-Zone of a High Temperature Fluidized Bed

by

David Pidwerbecki

A THESIS

submitted to

Oregon State University

in partial fulfillment of
the requirements for the
degree of

Doctor of Philosophy

Completed August 29, 1994

Commencement June 1995

APPROVED:

Redacted for Privacy

Professor of Mechanical Engineering in charge of major

Redacted for Privacy

Professor and Head of department of Mechanical Engineering

Redacted for Privacy

Dean of Graduate School

Date thesis is presented August 29, 1994

Typed by author for David Pidwerbecki

Table of Contents

List of Figures

List of Tables

Heat Transfer in the Splash-Zone of a High Temperature Fluidized Bed

1. Introduction

Fluidization is the operation by which solids are transformed into a fluid like state through suspension in a gas or liquid (21)*. Gas-solid fluidization is used by a wide variety of industries which require the unique properties inherent to the fluidization process, i.e., ease of handling of large volumes of fluidizable solids, nearly isothermal conditions throughout the bed, high rates of heat transfer between the solids and immersed surfaces, and high rates of catalytic conversion between the particles and a chemical feed stock as in fluidized catalytic cracking units used in the petroleum industries. In recent years, there has been increased interest, especially in developing countries, in the utilization of fluidized beds for the combustion of coal for electrical power generation. Some of the advantages that fluidized bed combustors have over conventional coal fired combustors include:

- a higher heat transfer rate is realized between the bed and internal surfaces, reducing the size of the required heat exchange area
- a lower facility operating temperature is possible while maintaining a relatively high overall plant efficiency, allowing the combustion of low-rank coal while producing less nitrous oxides (a major contributor to smog pollution)

* References in Chapter 1 are found in the Thesis Bibliography

- a fluidizing medium can be chosen that will adsorb the sulfur oxides liberated in the combustion process, thereby lowering the exhaust gas scrubbers' load and decreasing the overall sulfur emissions (SO_X) to the atmosphere

Interest in using fluidized bed combustors in developed western countries ebbs and flows with the price of oil, however, since over 80% of the worlds energy resources are coal, western interest in using fluidized beds for electrical power generation is inevitable.

It has been determined that the intermediate-to-large particle sizes ($\geq$ 1 mm) are the most desirable sizes of fluidizing media for the direct burning of coal in fluidized bed combustors. These particles (generally in the Geldart (14) class D particle range) offer the advantages of high thermal mass thus maintaining near uniform temperature when contacting internal surfaces (uniform bed temperature and high heat transfer rates) for a bed operating at a lower operating temperature, yet provide sufficient surface area so that the sulfur liberated in the combustion process can be readily adsorbed.

Many studies (1, 2, 4, 10, 11, 21, 22, 29) have involved heat transfer phenomena for internal surfaces in the dense phase of fluidized beds, however there is a dearth of studies in the literature that address the heat transfer phenomena between the fluidized bed and surfaces in the splash-zone, especially for the intermediate to larger particle sizes. The operating characteristics of the splash-zone, the region between the dense phase of the fluidized bed and the freeboard region, are of practical importance to designers in terms of off-design thermal output of power plants. Generally, a fluidized bed combustor is operated so that the exchanger surface is nearly immersed in the dense phase during the peak power consumption hours; however, during low load periods the bed surface is lowered, allowing more exchanger surface to be exposed to the lean phase of the fluidized bed, thus decreasing the thermal output of the plant.

This is the only known investigation which includes direct simultaneous measurement of both the total and radiative heat transfer coefficients from a high temperature bubbling fluidized bed to a horizontal tube located at various levels ranging from the dense phase to the relatively particle unaffected freeboard. The two-phase fluid flow behavior of fluidized beds is so chaotic that an analysis of the heat transfer, from first principles, is presently impossible. This work also proposes the only known correlation which accurately predicts the convective heat transfer to a horizontal tube located in the splash-zone and the freeboard for the conditions of general interest in the design of coal fired fluidized bed combustors. The experimental conditions investigated included particle sizes of 1.1, 2.0, and 2.9 mm nominal diameter; bed operating temperatures of 700, 810, 908, and 1003 K; superficial velocities ranging from minimum fluidization (U_{mf}) to approximately 2.0 U_{mf}; and tube locations ranging from well within the dense phase to the relatively particle-free freeboard region.

This manuscript is composed of four papers, submitted to archival journals, three of which address the independent experimental parameters (Chapters 2 - 4). The first paper (Chapter 2) addresses temperature effects; the second paper (Chapter 3) describes heat transfer as related to different particle sizes, and the third paper (Chapter 4) addresses the tube location effects. A correlation was developed and is presented (Chapter 5) which predicts the heat transfer coefficients within the splash-zone for the range of variables investigated.

2. Splash-Zone Heat Transfer in Bubbling Fluidized Beds - an Experimental Study of Temperature Effects

2.1 ABSTRACT

Experimental results are reported for the heat transfer between a high temperature fluidized bed and a horizontal tube located within the splash-zone. Of specific interest in this study is the effect of bed temperature. Four bed operating temperatures, 700 K, 810 K, 908 K, and 1003 K, were investigated. At each temperature, five circumferential local time averaged values of the total and black body radiative heat transfer coefficients were measured for three tube locations. The tube was located at 406 mm, 64 mm, and -127 mm relative to the packed bed-freeboard interface. These locations are representative of a tube in the freeboard, splash-zone, and totally immersed in the bed, respectively. The tube outside diameter was 51 mm, the mean bed particle size was 2.9 mm, and the superficial fluidizing velocity varied from near minimum fluidization conditions (U_{mf}) to over 1.5 U_{mf}. The work was performed in the Oregon State University high temperature fluidized-bed test facility.

2.2 KEYWORDS

Fluidized Beds, Temperature Effects, High Temperature, Freeboard, Splash-zone

2.3 INTRODUCTION

In recent years, there has been considerable interest in the utilization of fluidized-bed combustion of coal for electrical power generation. Gas-solid fluidized bed combustors offer excellent heat transfer characteristics as well as a great potential for the utilization of low-rank high-sulfur coal in an environmentally acceptable way. Fluidized-bed combustors are often designed with horizontal arrays of heat transfer tubes positioned such that a portion of the tubes are submerged in the dense phase of the fluidized bed and the remaining tubes are in the freeboard space above the bed. The heat transfer coefficients to tubes located within the dense phase of a fluidized bed may be an order of magnitude greater than that due to gas convection alone. Tubes located in the splash-zone are in the transition region between the dense phase and the pure gas phase. This variation in behavior can be used to adjust the operating power level of fluidized bed combustors. During turndown (reduced superficial fluidizing velocity) operation, the dense phase surface of a fluidized bed will drop, placing more tubes in the freeboard, thereby causing the thermal output of the tube array to decrease. Many investigators have studied dense phase heat transfer characteristics, but there is a dearth of information regarding heat transfer in the freeboard region of high temperature fluidized beds. Some results have been reported dealing with heat transfer in the freeboard, utilizing ambient temperature fluidized beds [Refs. 1-10]. Fewer studies have examined these phenomena at near combustion temperatures [Refs. 11-17]. This paper the first in a series of three which investigates circumferential local and weighted average convective and black body radiative heat transfer characteristics of a horizontal tube located in the freeboard over a range of fluidizing velocities and tube locations. The particular interest in this paper is the effect of bed temperature upon heat transfer characteristics.

2.4 EXPERIMENTAL APPARATUS AND FACILITY

An instrumented tube capable of measuring both the circumferential local, total, and black body radiative heat transfer coefficients, developed by Alavizadeh et al. [18] and Lei [19], was employed to evaluate the effect of the different parameters. Figure 2-1 illustrates the instrumented tube used to measure both heat transfer coefficients simultaneously. The tube is made of bronze with an outside diameter of 51 mm and an inside diameter of 32 mm. High precision commercially available microfoil thermopile detectors were used as the heat transfer measuring gages. Three total and three radiative gages were located 90^{o} apart, along the axis of the tube. The total heat flux gages were bonded to the outside tube surface with a high thermal conductivity epoxy and then covered with 0.127 mm thick stainless steel shim stock which was sanded to a dull finish and stretched tightly over the tube. A thin layer of a high thermal conductivity paste was deposited between the shim stock and the gages to reduce thermal contact resistance. The radiation heat flux gages, developed by Alavizadeh et al [18] and Lei [19], are located 10 cm away from and at the same circumferential locations and orientations as the total heat flux gages. The radiation heat flux gages were epoxied to the bottom of a carefully milled cavity in the tube surface and covered by a silicon window. The inner surfaces of the cavity, including the gage, were painted with a known high absorptivity paint, hence, all radiative heat transfer coefficients reported are black body values. The silicon window was machined to have the same curvature as the outside of the tube. Silicon [19] was found to be the superior window material when silicon, sapphire, crystal quartz, and fused quartz were considered as potential window materials. Details of the instrument calibration procedures can be found in Refs. 18,19, and 20.

Figure 2-2 shows a schematic of the Oregon State University high temperature fluidized bed test facility. Combustion and fluidization air is compressed by a roots style positive displacement compressor and piped to an industrial propane burner. Propane flow is regulated to the burner and is burned in a refractory lined combustion chamber. The hot combustion gases are directed by a plenum into a .3 m by .6 m test section through a nickel based alloy distributor plate. The distributor plate consists of two flat alloy plates with a 9 x 17 square hole array. The hole diameters are 7.9 mm and the centerline to centerline hole pitch is 25.4 mm. Sandwiched between the plates is a 40 mesh inconel 800 screen.

The instrumented tube was located 84 cm from the distributor plate and 34 cm from one of the 30 cm side walls of the test section. It was located so that the gages were located as near as possible to the center of the test section. The instruments are cooled by circulating water. A rotary union allowed adjustment of the instrumented tube to the desired angular positions for data collection. The test section walls were instrumented with five type-K thermocouples, three located in the fluidizing region, one on the wall of the disengaging zone, and one on the ceiling of the disengaging zone.

A high precision data acquisition system was used to record and reduce the circumferential local heat fluxes and surface temperatures in order to calculate the circumferential local heat transfer coefficients at each position on the instrumented tube. The system also recorded the bed temperature and the surface wall temperatures of the test section.

2.5 EXPERIMENTS

Experiments were conducted at four bed temperatures, 700 K, 810 K, 908 K and 1003 K. The tube was positioned in six locations relative to the packed bed freeboard

interface, three of which are reported, 406 mm, 64 mm, and -127 mm. The fluidization velocity was varied from near minimum fluidization (U_{mf}) to over 1.5 U_{mf}. A granular industrial fluidizing medium with a nominal 2.9 mm particle size was used as the bed material. The particle size was determined by mechanical sifting and using the cut between a Number 5 and Number 6 standard Tyler Screen. The chemical composition of the particles consists of 53.5% silica, 43.8% alumina, 2.3% titania, and .4% other substances. The particle thermal properties are characteristic of industrial fluidizing mediums, with a detailed listing by Chung [21].

Data were taken with the heat flux gages positioned at 0^o, 45^o, 90^o, 135^o, and 180^o relative to the lower stagnation point. The total heat transfer coefficient and the black body radiative heat transfer coefficient were experimentally determined. The convective heat transfer coefficients reported were calculated from the measured data using an experimentally measured emissivity of 0.37 for the stainless steel shim stock.

2.6 ERROR ANALYSIS

The overall error in the total heat transfer coefficient was determined to be + 8%, - 14% and the overall error in the radiative heat transfer coefficient was determined to be + 13%, - 12%. The three sources of error in the total heat flux measurements were: (1) errors due to conduction along the stainless steel shim surface, (2) errors caused by non uniform surface temperature in the bubble contact region, and (3) calibration and data collection procedure errors. Three sources of error in the radiative heat flux measurements include: (1) errors due to conduction from the silicon window to the gage sensing area, (2) errors caused by non uniform heat flux on the gages, and (3) calibration and data collection procedure errors.

The decrease in temperature across the stainless steel shim stock to the total heat flux gages was found to be less than 1.8 K at a tube wall temperature of 478 K. Neglecting the temperature difference, a two dimensional steady state heat conduction analysis was performed and it was found that approximately 2% of the heat flux absorbed at the shim's upper surface was not conducted to the active area of the sensor. The error introduced by conduction from the silicon window to the radiative heat flux sensor was determined to be + 1%.

A laminar thermal boundary layer analysis was conducted to investigate the effect of non uniform surface temperature in the bubble contact region on the performance of the total heat flux gage. This analysis applies when the gage is covered by gas bubbles. A reduction of approximately 4% in the total heat flux measurements was found by using the data for the bubble contact fraction suggested by Catipovic [22]. The maximum error associated with non uniform heat fluxes experienced by the radiative gages was determined to be ± 2.5%.

The root-sum-square (rss) method given by Doebelin [23] was used to determine the errors in the total heat flux gages calibration and in data collection. Using the manufacture's uncertainty values and estimating the uncertainties in reading bed temperatures, the random error in evaluating the total heat transfer coefficient was found to be approximately ± 8%. The overall error in the total heat transfer coefficients was determined by summing the three sources, resulting in an overall uncertainty of + 8%, - 14%. The random error for the radiative heat transfer coefficient was determined to be ± 9%, hence, the overall error associated with the radiative heat transfer coefficients is + 13%, - 12%.

Two other sources of error are introduced by the experimental procedure; the error of measuring the superficial fluidization velocity and the error of measuring the distance from the packed bed height to the tube centerline. The maximum error in

measuring the superficial fluidization velocity was determined to be ±.02 m/s. Because of the large mass of the test facility, it took considerable time to heat up the facility to the experimental test temperatures. During the warm up time and the experimental data collection time, particles were elutriated from the bed, increasing the distance from the packed bed height to the tube centerline. For the data shown, the maximum decrease in bed depth experienced during the experimental runs was -32 mm. This occurred when the bed temperature was 1003 K, the tube to packed bed distance being 64 mm, and at the maximum superficial velocity of 3.23 m/s.

2.7 RESULTS AND DISCUSSION

Figures 2-3 through 2-5 show the effects of superficial velocity on the circumferential weighted averaged convective and black body radiative heat transfer coefficients for the tube to packed bed distances (-127 mm, 64 mm, and 406 mm) and the bed temperatures (700 K, 810 K, 908 K, and 1003 K) investigated. The greatest convective heat transfer coefficients occurred when the tube was located within the dense phase of the bubbling fluidized bed. Figure 2-3 indicates that the minimum values of the convective and radiative heat transfer coefficients are experienced near the minimum fluidization velocity.

The spread in the data is expected to be large when the superficial velocity is near minimum fluidization. It was observed that the bed was not always uniformly fluidized, but could be locally fluidized when the superficial velocity was near minimum fluidization. The local fluidization occurred randomly, causing some areas of the bed to behave similarly to a packed bed with thermal gradients. These phenomena caused erratic heat transfer behavior and a corresponding large spread in the data in this operating region. The minimum fluidization velocity was measured with pressure taps

located on the test section walls and was visually confirmed using a sight glass located on the ceiling of the test section. The best estimates of the values are shown in Table 2-1.

Because of the difficulties in measuring minimum fluidization velocities, the abscissas of Figs. 2-3 through 2-11 are superficial velocity, as opposed to the nondimensionalized velocity ratio U/U_{mf}. The convective heat transfer coefficients ranged from 113 to 137 W/m^2 K and the radiative heat transfer coefficients ranged from 8 to 22 W/m^2 K at the minimum fluidization velocity for the temperatures investigated. As the superficial velocity was increased, the convective heat transfer coefficients reached their maximum values between 2.4 to 2.7 m/s. The maximum convective heat transfer coefficients ranged between 172 to 182 W/m^2 K. When the superficial velocity was increase even further, the convective heat transfer coefficients decreased and tended to reach similar asymptotic limits of approximately 165 W/m^2 K. This decrease is attributed to a decrease in the bed density, increase in bubble contact fraction, and an enlarging of the lower stagnation bubble. The radiative heat transfer coefficients tended to increase as the superficial velocity was increased from minimum fluidization until a maximum asymptotic value was reached for each temperature. The maximum radiative heat transfer coefficient values were achieved between the superficial velocities of 2.4 to 2.7 m/s varying between 12 to 33 W/m^2 K. As expected, the radiative heat transfer coefficients increased with increasing bed temperature. When averaged over the ranges of superficial velocities, radiation was found to comprise 6.9%, 9.9%, 13.0%, and 16.9% of the total heat transfer at 700 K, 810 K, 908 K, and 1003 K respectively.

Figure 2-4 shows the weighted average convective and black body radiative heat transfer coefficients versus fluidization velocity for the centerline of the instrumented tube located 64 mm above the packed bed. Convective heat transfer coefficient values increased from minima at U_{mf} to maxima at the higher superficial velocities (a factor of

approximately 2.5). All curves for the individual temperatures tend to converge to asymptotic limits at the higher superficial velocities. The minimum fluidization convective heat transfer coefficients range from 39 to 51 W/m^2 K (approximately 34 to 37% of the immersed tube values) and converge to an asymptotic value of approximately 125 W/m^2 K (approximately 71% of the maximum and 76% of the asymptotic immersed tube values) at the higher superficial velocities. The slopes of the convective heat transfer variations are highest for the lower bed temperatures and decrease in a monatomic fashion for the higher bed temperatures.

The radiative heat transfer coefficients are lowest at the respective minimum fluidization velocities and increase slightly for higher superficial velocities. Minimum fluidization radiative heat transfer coefficients ranged from 12 to 23 W/m^2 K and the maximum values ranged from 13 to 33 W/m^2 K. The radiative trends are as expected with radiative heat transfer coefficients increasing with increasing bed temperature. When averaging the radiative heat transfer coefficients over the range of velocities, it was found that radiation comprised 14.6%, 16.2%, 21.0%, and 27.0% of the total heat transfer at 700 K, 810 K, 908 K, and 1003 K respectively. It appears, that at higher fluidization velocities the void fraction is low and the net radiation impinging upon the tube is due to the expanded bed, with the surrounding wall temperatures having little effect. This environment will essentially simulate the dense phase of the bed, with the magnitude of the radiation heat transfer coefficient being comparable to that of the dense phase of the fluidized bed.

Figure 2-5 shows the weighted average of the convective and black body radiative heat transfer coefficients for a tube located in the freeboard, 406 mm above the packed bed surface. Both radiative and convective heat transfer coefficients increase linearly with superficial velocity. Values of the convective heat transfer coefficient vary from 28 to 40 W/m^2 K at minimum fluidization and increase linearly to a converged

maximum value of approximately 50 W/m^2 K at superficial velocities above 3.3 m/s, except for the 700 K case, where the maximum convective heat transfer coefficient was 33 W/m^2 K when the superficial velocity reached 2.50 m/s. Radiative heat transfer coefficient values varied from minima of 5, 8, 13, and 23 W/m^2 K at U_{mf} to maxima of 8, 15, 23, and 32 W/m^2 K at the maximum superficial velocities attained for 700 K, 810 K, 908 K, and 1003 K respectively. The radiative components comprised much larger percentages of the total heat transfer than were true for the other two bed heights listed. Radiation comprises 21.0, 23.9, 34.5, and 48.2 percent of the total heat transfer when averaged over the range of superficial velocities for temperatures 700 K, 810 K, 908 K, and 1003 K, respectively. At this location, the facility design has effects upon the black body radiative values, hence, radiative values reported at this location should be considered representative and specific only for this experimental facility.

Figures 2-6, 2-8, and 2-10 show the convective and black body radiative local heat transfer coefficients as functions of superficial velocity for the different bed heights at a bed temperature of 810 K. These figures are representative of the data obtained for all bed temperatures investigated. Fig. 2-6 shows local heat transfer coefficient values when the tube is immersed within the dense phase of the fluidized bed. At all circumferential locations, except the lower stagnation point, the local convective heat transfer coefficients are minima at the minimum fluidization velocity, rise to a maximum, and then decrease as the superficial velocity is increased. The lower stagnation point experiences a maximum local convective heat transfer coefficient at minimum fluidization, and subsequently decreases as the superficial velocity is increased. This is largely attributed to the growth of the lower stagnation point bubble. The maximum local convective heat transfer coefficient values for all superficial velocities, except minimum fluidization, occur at the 90^o location. At minimum fluidization, the maximum local convective heat transfer coefficient occurs at the lower

stagnation point. The effects of the stagnant "lee stack" on the top portion of the tube are apparent for the lower superficial velocities. At minimum fluidization, the upper stagnation point local convective heat transfer coefficient is 22 percent of the maximum local convective heat transfer coefficient reached at a superficial velocity of approximately 2.6 m/s (1.26 U_{mf}). Local black body radiative heat transfer coefficients are smallest at minimum fluidization velocities and increase to a common asymptotic limit of approximately 19 W/m^2 K for superficial velocities greater than 2.3 m/s.

Figure 2-7 represents the weighted average of the circumferential heat transfer coefficients for the tube located within the dense phase of the fluidized bed. This figure, along with similar figures for the other temperatures investigated, was used in the construction of Fig. 2-3.

Figure 2-8 shows the local convective and black body radiative heat transfer variations for the tube located 64 mm above the packed bed level. Heat transfer at all circumferential locations show similar trends; the local convective heat transfer coefficients are smallest at the minimum fluidization velocity and increase with the superficial velocity. Maximum values of the local convective heat transfer coefficient were experienced at the lower stagnation point, except at minimum fluidization. At minimum fluidization conditions, the maximum convective heat transfer coefficient is located at the upper stagnation point, in direct contrast with the tube located within the dense phase of the fluidized bed. Within this region of the splash-zone, the void fraction is low enough so that there are significant particle effects, yet still high enough so that the lee stack on the upper stagnation point is regularly replaced, causing high heat transfer coefficients at lower fluidization velocities. The local radiative heat transfer coefficients exhibit minimum values at minimum fluidization velocities and increase to an asymptote of approximately 19 W/m^2 K for superficial velocities above 2.5 m/s. Figure 2-9 represents the weighted average of the local heat transfer

coefficients shown in Fig. 2-8. Note that Fig. 2-9, along with similar figures for the other temperatures studied, were used to construct Fig. 2-4.

Fig. 2-10 shows the local convective and black body radiative heat transfer coefficients for the tube located 406 mm above the packed bed. For this case, the highest local convective heat transfer coefficient occurred at the lower stagnation point for all velocities except minimum fluidization. At minimum fluidization, the maximum local convective heat transfer coefficient was found to be at the 45^{o} location, only slightly greater than the value at the lower stagnation point. The lowest local convective heat transfer coefficient occurred at the 135^{o} location at all velocities. An examination of behavior at the upper stagnation point indicates that particles start to significantly influence the heat transfer at this location at superficial velocities above 2.6 m/s (1.26 U_{mf}). All black body radiative heat transfer coefficients exhibit similar behavior in that they are at or near minimum values at the minimum fluidization velocities and reach their maximum values at the maximum fluidization velocities studied. When the superficial velocity is near 2.4 m/s, the radiative heat transfer coefficients at 0^{o} and 45^{o} show marked increases, while values at the other circumferential locations vary in a predictably smooth manner.

By the nature of the configuration of the instrumented tube, each of the radiation sensors has a view angle, that is, the radiation incident upon the tube over a finite circumferential angular location will be averaged by the gages. It has been determined that the maximum view angle of each gage is approximately 15^{o} when measured with respect to a normal to the gage surface. At low superficial velocities, the radiation incident upon the tube at the 0^{o} and 45^{o} location will be due to the bed and the vessel walls. As the superficial velocity is increased, the bed will expand, and eventually the radiation incident upon those locations will be due primarily to the bed. These phenomena are shown in Fig. 2-10.

Below a superficial velocity of 2.4 m/s, the radiative heat transfer coefficient for the 0^o location is approximately 11 W/m^2 K and above a superficial velocity of 2.6 m/s, the coefficient is approximately 20 W/m^2 K, a 180 percent increase. The 45^o location exhibits similar trends, with an increase of the radiative heat transfer coefficient from 10 W/m^2 K to 18 W/m^2 K over the same range of superficial velocities. The variations at other circumferential locations over the entire range of superficial velocities studied is not as pronounced, and is likely a result of both an increase in particle radiation and the slight increase in vessel wall temperatures experienced as the superficial velocities increased.

Figure 2-11 represents the weighted average of the circumferential heat transfer coefficients found in Fig. 2-10. Figure 2-10, along with similar figures for the other temperatures investigated, was used to construct Fig. 2-5.

2.8 SIGNIFICANCE OF RESULTS

Coal comprises over 80% of the earth's energy resources and the most effective application of coal involves direct burning. In recent years, there has been significant interest in the use of large particle fluidized beds as the means of combusting coal in an efficient, environmentally safe manner. By the nature of the gas/particle/surface interactions, the heat transfer rates between a fluidized bed and immersed surfaces can be an order of magnitude higher than that of pure gas convection alone. These high energy transport rates allow power plants to operate at lower than normal temperatures, decreasing the amount of NO_X produced. Also, fluidized beds provide the added benefit that by using limestone or dolomite as the fluidizing medium, much of the sulfur liberated in the coal combustion process will be absorbed by the fluidizing medium, thus making them attractive for burning low-rank high-sulfur coal.

The operating characteristics of the splash-zone, the region between the dense phase of the fluidized bed and the freeboard region, are of practical importance to designers in terms of off-design thermal output of power plants. The two phase fluid flow behavior of fluidized beds is so chaotic that an analysis of the heat transfer, from first principles, is presently impossible. Numerical simulations and empirical models have limited success, but each must be validated by experimental results. The results reported are the only ones known to include direct simultaneous measurement of both total and radiative heat transfer coefficients for a horizontal tube located in the splash-zone of a high temperature fluidized bed.

2.9 CONCLUSIONS

Reported in this paper are convective and radiative experimental values of heat transfer coefficients for a tube located in the dense phase, the splash-zone, and the freeboard regions of a high temperature fluidized bed.

The greatest convective heat transfer occurred within the dense phase of the fluidized bed (-127 mm location). Maximum values in this immersed case ranged from 172 to 182 W/m^2 K for superficial velocities between 2.4 to 2.7 m/s and over the range of temperatures studied. The radiative heat transfer coefficients were smallest at U_{mf} and increased to asymptotic limits at higher superficial velocities. Maximum values of the radiative heat transfer coefficients ranged from 12 to 33 W/m^2 K.

The tube located at 64 mm above the packed bed height exhibited characteristics of both the dense phase of the fluidized bed and the freeboard region. Circumferentially-averaged convective heat transfer coefficients increase from their minima at U_{mf} to maximum values at the higher superficial velocities. Minimum values ranged from 39 to 51 W/m^2 K and increased to an asymptotic limit of

approximately 125 W/m^2 K at the higher superficial velocities. The radiation heat transfer coefficients ranged from minimum values between 12 to 23 W/m^2 K to maximum values between 13 to 33 W/m^2 K. The maximum values indicated that the bed had expanded sufficiently so that the surroundings had little effect on the radiant contribution; thus the radiant transfer mechanisms were similar to those found in the dense phase of the bed. The 406 mm tube location exhibited characteristics of a tube in the freeboard region of a fluidized bed. Both the convective and radiative heat transfer coefficients increased linearly with superficial velocity. The convective heat transfer coefficient ranged from minimum values of 28 to 40 W/m^2 K at U_{mf} to maximum values of 33 to 52 W/m^2 K at the maximum superficial velocity studied at 700 K and 1003 K, respectively. The radiative heat transfer coefficient varied from minimum values of 5 to 23 W/m^2 K at U_{mf} to maximum values of 8 to 32 W/m^2 K.

Circumferentially-averaged heat transfer coefficients, which are of primary interest in design, were achieved by weighted averaging the local radiative and convective heat transfer coefficients measured over a range in tube locations and temperatures. Local values for the three tube locations and a bed temperature of 810 K are presented in this paper. Heat transfer performance at this temperature is representative of the behavior at the other temperatures.

2.10 ACKNOWLEDGMENTS

We wish to express our appreciation to the National Science Foundation (Grant Number CTS-8803077) for supporting this research.

2.11 NOMENCLATURE

d_p	mean particle diameter, mm
U_{mf}	minimum fluidization velocity, m/s
X	tube centerline to slumped bed surface distance, mm
Θ	angle from the lower stagnation point, deg

Table 2-1.

Minimum Fluidization Velocities for Various Temperatures and Bed Depths, d_p = 2.9 mm

Temperature (K)	Tube to Slumped Bed Distance (mm)	Bed Depth (mm)	U_{mf} (m/s)
700	406	305	1.97
810			2.08
908			2.15
1003			2.14
700	64	647	1.98
810			2.07
908			2.13
1003			2.10
700	-133	838	2.00
810			2.07
908			2.11
1003			2.12

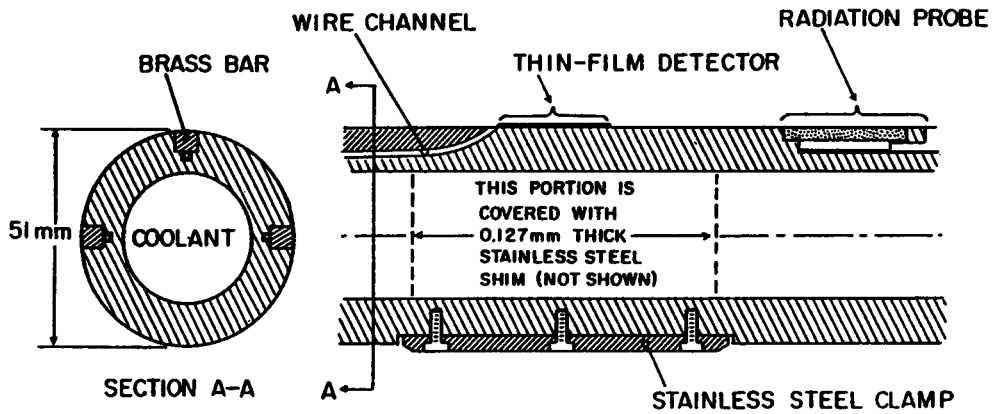

Fig. 2-1 Instrumented tube for total and radiative heat flux measurements

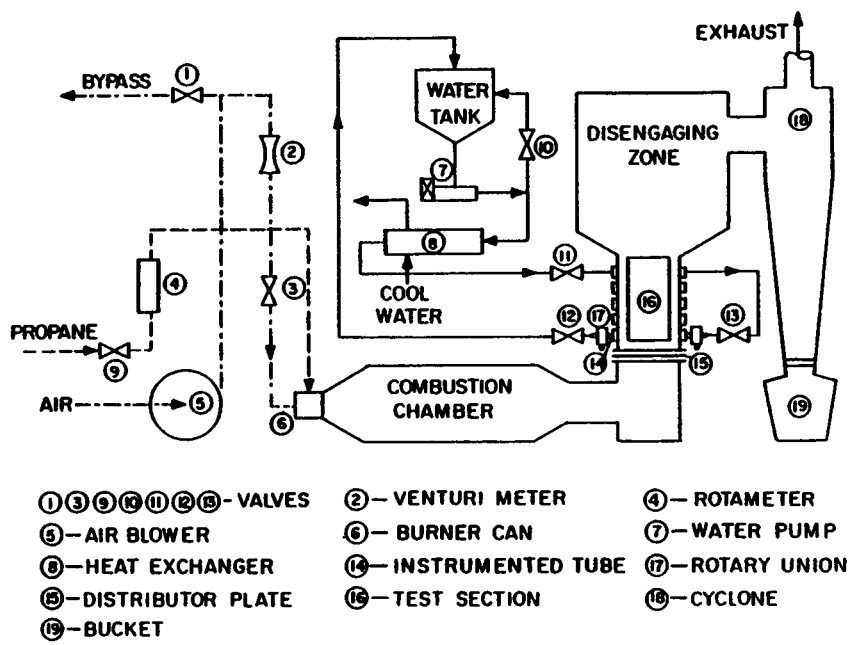

Fig. 2-2 Oregon State University high temperature fluidized bed test facility

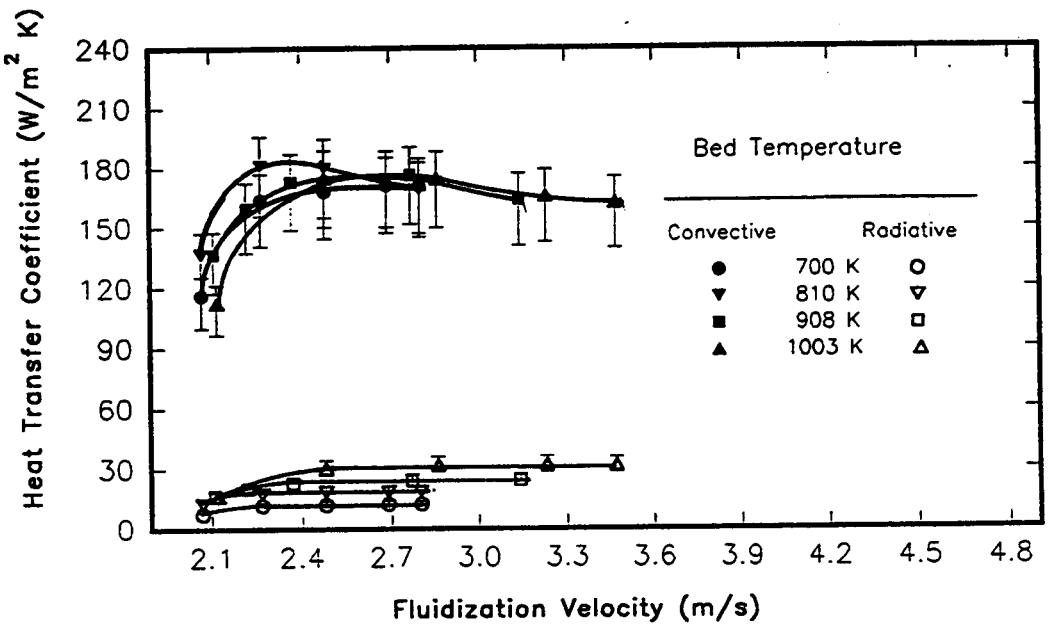

Fig. 2-3 Circumferencial averaged convective and radiative heat transfer coefficients d_p = 2.9 mm and tube to slumped bed surface distance = -127 mm

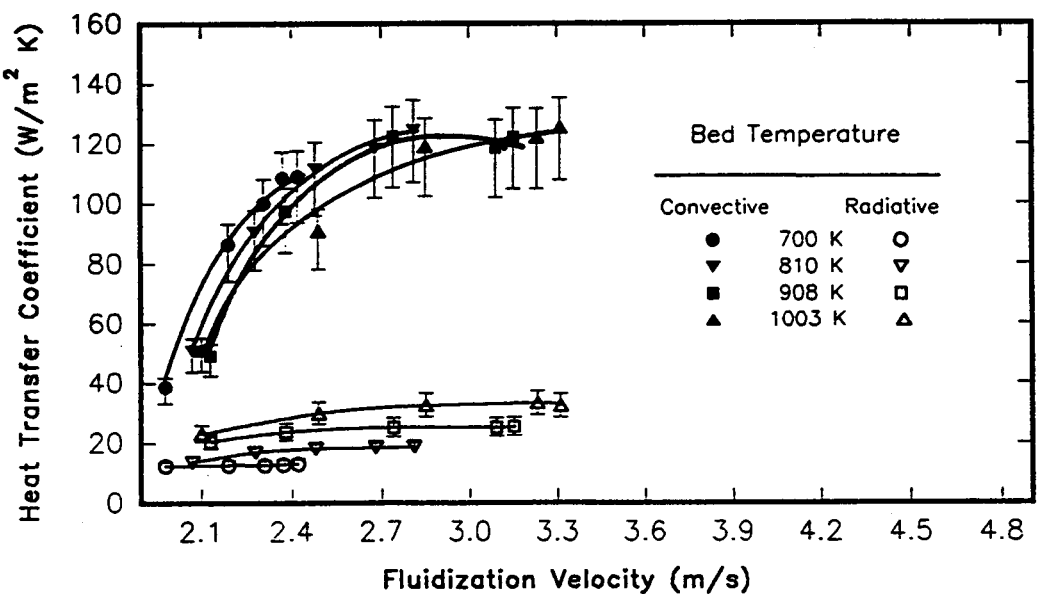

Fig. 2-4 Circumferencial averaged convective and radiative heat transfer coefficients d_p = 2.9 mm and tube to slumped bed surface distance = 64 mm

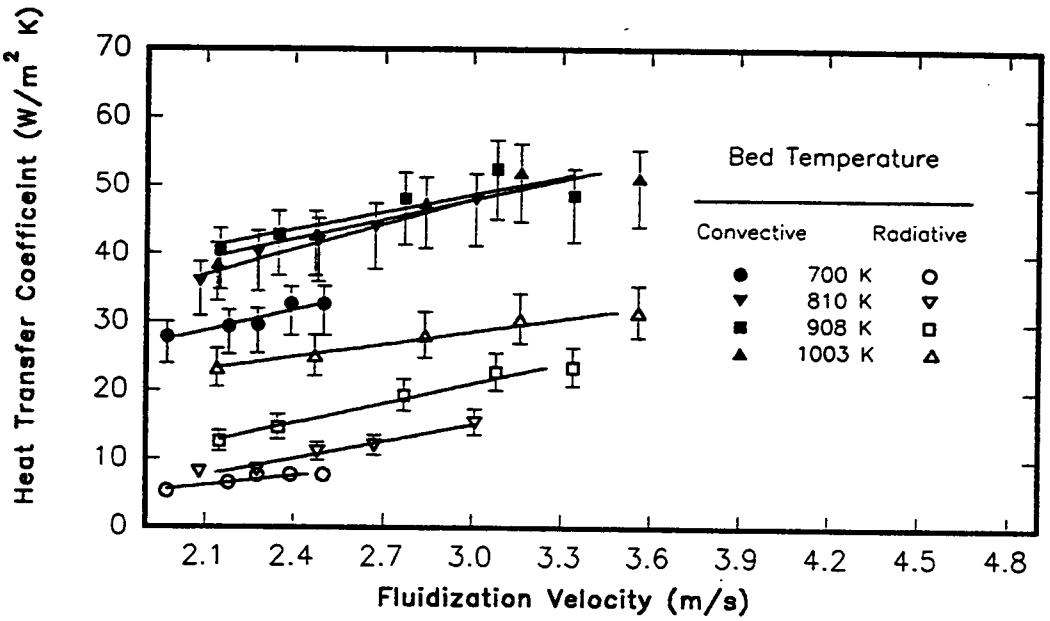

Fig. 2-5 Circumferencial average convective and radiative heat transfer coefficients $d_p = 2.9$ mm and tube to slumped bed surface distance = 406 mm

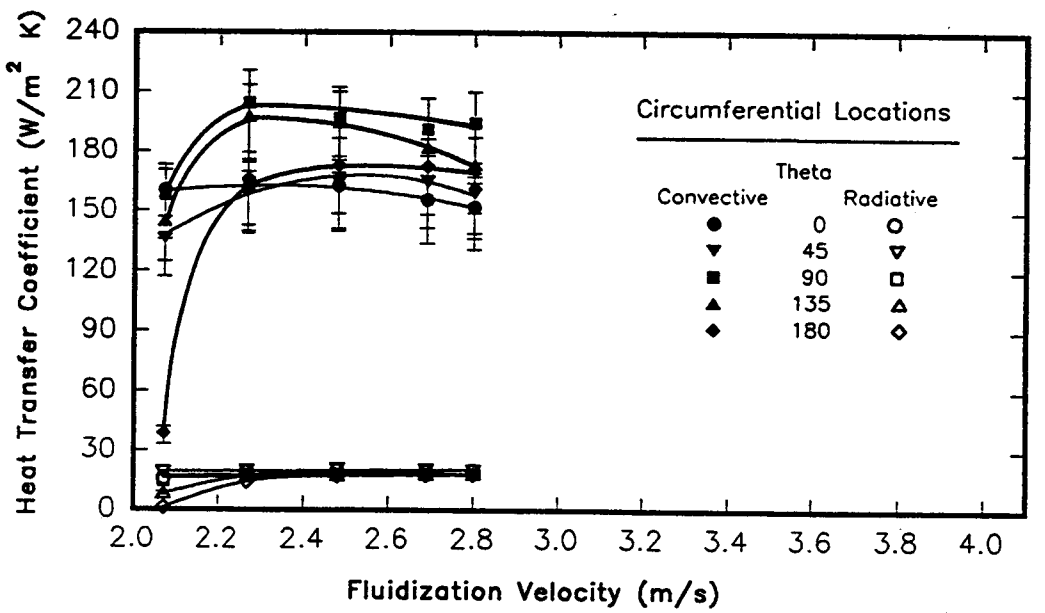

Fig. 2-6 Convective and radiative circumferencial heat transfer coefficients $d_p = 2.9$ mm, $T_{bed} = 810$ K, and $U_{mf} \approx 2.07$ m/s
Tube to slumped bed surface distance is - 127 mm

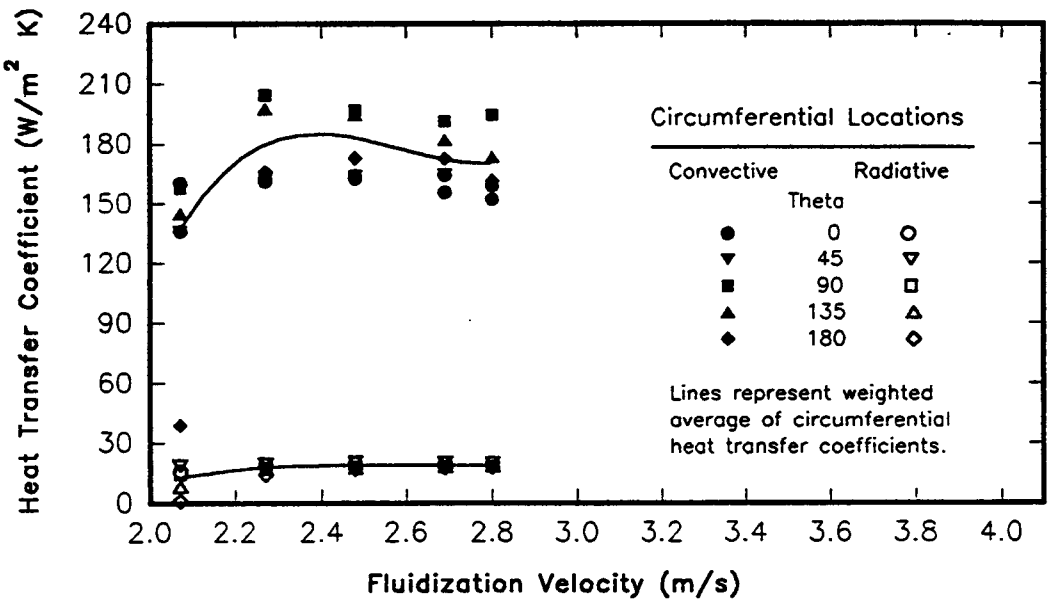

Fig. 2-7 Average convective and radiative circumferencial heat transfer coefficients
$d_p = 2.9$ mm, $T_{bed} = 810$ K, and $U_{mf} \approx 2.07$ m/s
Tube to slumped bed surface distance is - 127 mm

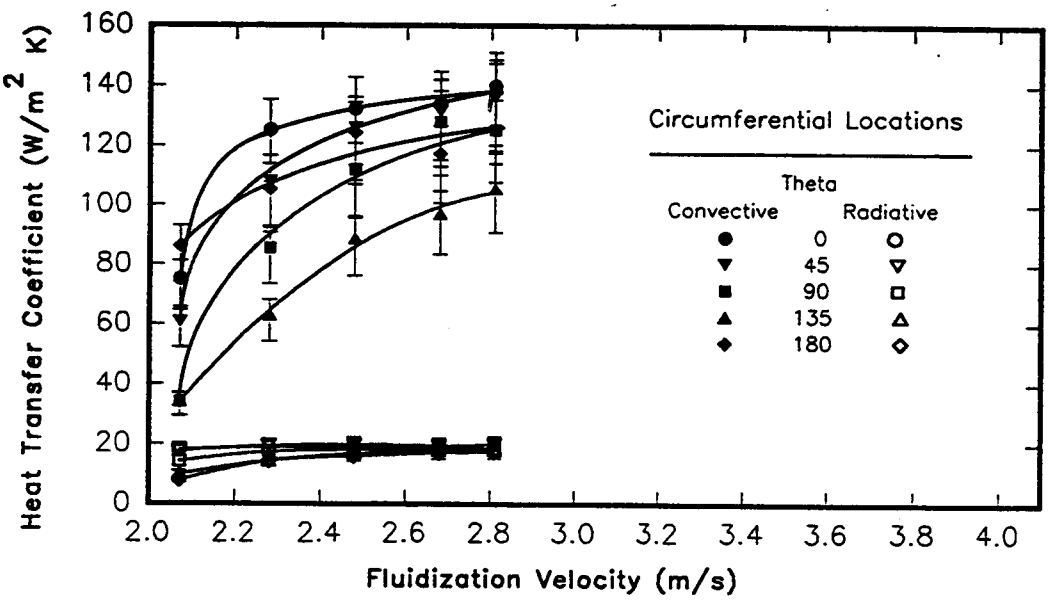

Fig. 2-8 Convective and radiative circumferencial heat transfer coefficients
$d_p = 2.9$ mm, $T_{bed} = 810$ K, and $U_{mf} \approx 2.07$ m/s
Tube to slumped bed surface distance is 64 mm

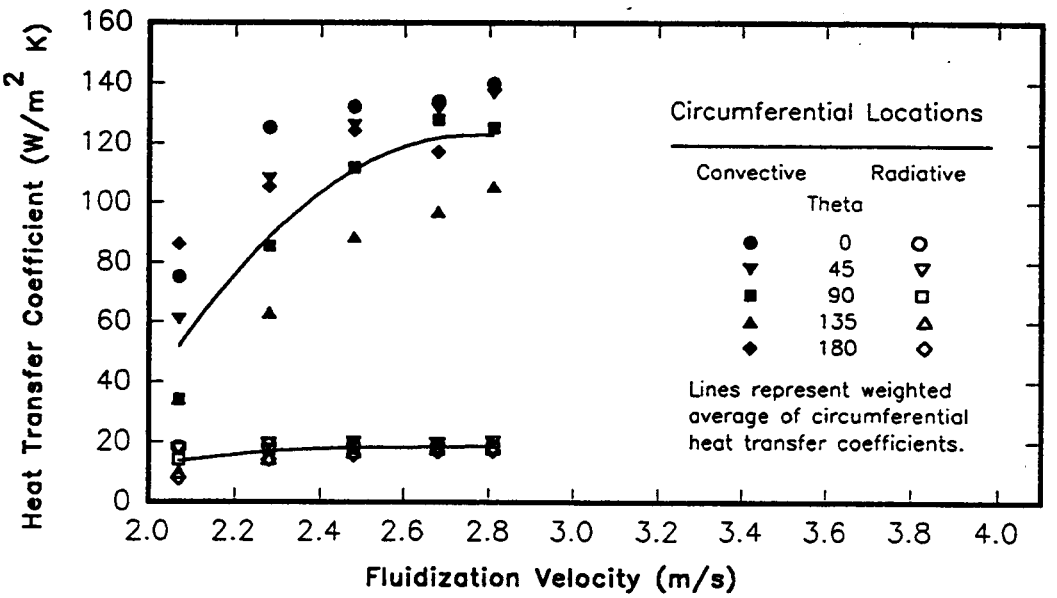

Fig. 2-9 Average convective and radiative circumferencial heat transfer coefficients
$d_p = 2.9$ mm, $T_{bed} = 810$ K, and $U_{mf} \approx 2.07$ m/s
Tube to slumped bed surface distance is 64 mm

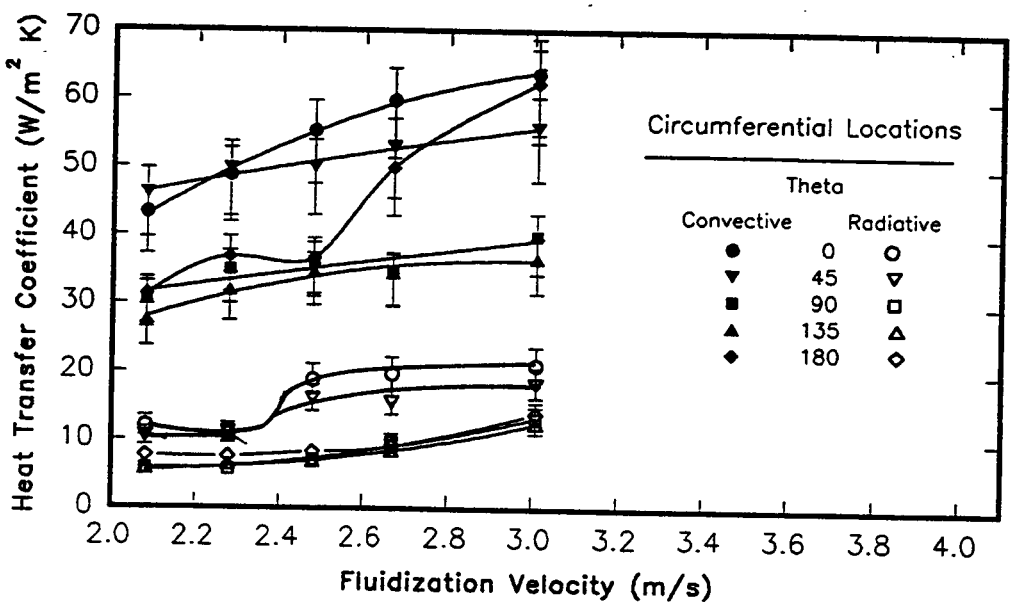

Fig. 2-10 Convective and radiative circumferencial heat transfer coefficients
$d_p = 2.9$ mm, $T_{bed} = 810$ K, and $U_{mf} \approx 2.07$ m/s
Tube to slumped bed surface distance is 406 mm

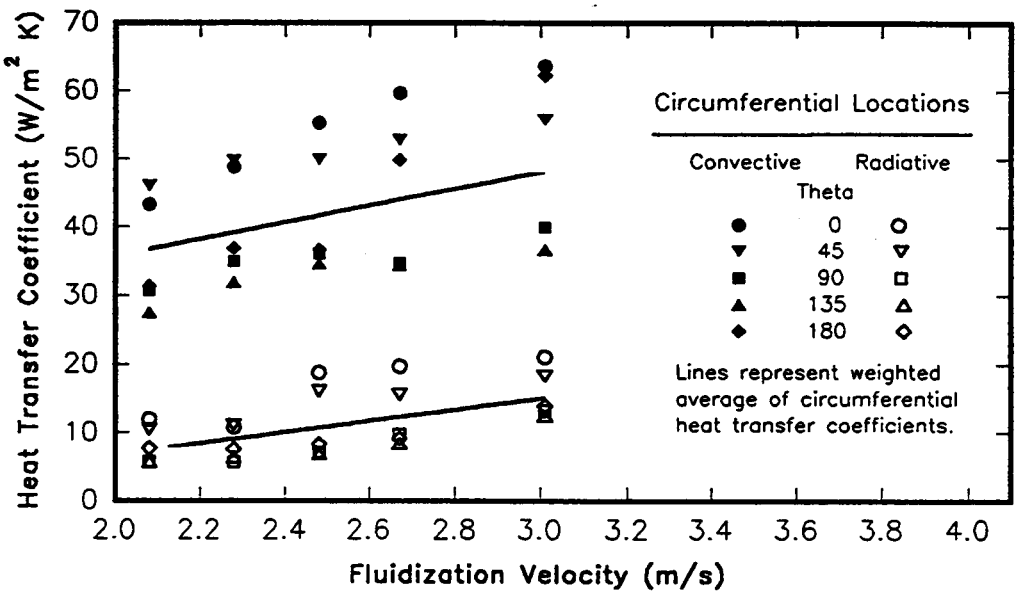

Fig. 2-11 Average convective and radiative circumferencial heat transfer coefficients
d_p = 2.9 mm, T_{bed} = 810 K, and $U_{mf} \approx$ 2.07 m/s
Tube to slumped bed surface distance is 406 mm

2.12 REFERENCES

1. Biyikli, S., Tuzla, K., and Chen, J.C., 1989, A Phenomenological Model for Heat Transfer in Freeboard of Fluidized Beds, Can. J. of Chem. Eng., Vol 67, April, pp 230-236.

2. Biyikli, S., Tuzla, K., and Chen, J.C., 1987, Particle Contact Dynamics on Tubes in the Freeboard Region of Fluidized Beds, AIChE J., Vol. 33, No. 7, July, pp 1225-1227.

3. Biyikli, S., Tuzla, K., and Chen, J.C., 1983, Heat Transfer Around a Horizontal Tube in Freeboard Region of Fluidized Beds, AIChE J., Vol. 29, No. 5, Sept., pp 712-716.

4. Dyrness, A., Glicksman, L.R., and Yule, T., 1992, Heat Transfer in the Splash Zone of a Bubbling Fluidized Bed, Int. J. Heat Mass Transfer, Vol. 35, No. 4, pp 847-859.

5. George, S.E. and Grace, J.R., 1982, Heat Transfer to Horizontal Tubes in the Freeboard Region of a Gas Fluidized Bed, AIChE J., Vol. 28, No. 5, pp 759-765.

6. George, S.E. and Grace, J.R., 1979, Hear Transfer to Horizontal Tubes in Freeboard Region of a Gas Fluidized Bed, AIChE Meeting, San Francisco, No. 7E.

7. Hongshen, G., et al., 1987, A Model and Experiments for Heat Transfer of Single Horizontal Tube in the Freeboard of Fluidized Bed, Proc. of the 1987 Intl. Conf. on Fluidized Bed Combustion, ed. J.P. Mustonen, Vol 2, pp 1159-1164, Sponsored by ASME, Boston, MA.

8. Shi, M.H., 1987, Heat Transfer to Horizontal Tube and Tube Bundle in Freeboard Region of a Gas Fluidized Bed, Proc. of the 1987 ASME.JSME Thermal Eng. Joint Conf., eds. P.J. Martso and I. Tanasawa, Vol. 4, pp 113, Honolulu, HI, March 22-27.

9. Wood, R.T., Kuwata, M., and Staub, F.W., 1980, Heat Transfer to Horizontal Tube Banks in the Splash Zone of a Fluidized Bed of Large Particles, Fluidization ed. R. Grace and J.M. Matsen, pp 235-243, Plenum, NY.

10. Xavier, A.M. and Davidson, J.F., 1981, Heat Transfer to Surfaces Immersed in Fluidized Beds and in the Freeboard Region, AIChE Symposium Series, Vol.77, No. 208, pp 368-373.

11. Bardakci, T. and Molayem, B., 1989, Experimental Studies of Heat Transfer to Horizontal Tubes in a Pilot-Scale Fluidized-Bed Combustor, Canadian J. of Chem. Engr., Vol. 67, April, pp 348-351.

12. Biyikli, S., Tuzla, K., and Chen, J.C., 1987, Freeboard Heat Transfer in High-Temperature Fluidized Beds, Powder Technology, Vol. 53, pp 187-194.

13. Byam, J., Pillai, K.K., and Roberts, A.G., 1981, Heat Transfer to Cooling Coils in the Splash Zone of a Pressurized Fluidized Bed Combustor, AIChE Symposium Series, Vol. 77, No. 208, pp 351-358.

14. Görmar, H., Renz, U., and Verweyen, N., 1989, Heat Transfer to the Cooled Freeboard of a Fluidized Bed, Proc. of the 1989 Intl. Conf. on Fluidized Bed Combustion, ed. A.M. Manaker, Vol. 2, pp 1241-1244, Sponsored by ASME, San Francisco, CA, Apr 30 - May 3.

15. Kortleven, A., Bast, J., and Meulink, J., 1984, Heat Transfer for Horizontal Tubes in the Splash Zone of a 0.6 x 0.6 m AFBC Research Facility, Proc. of the XVI Intl. Center of Heat and Mass Trans. Conf., Yugoslavia.

16. Mitor, V.V., Matsnev, V.V., and Sorokin, A.P., 1986, Investigation of Hat Transfer in Bed and Freeboard of Fluidized Bed Combustors, Proc. of the Eighth Intl. Heat Trans. Conf., eds. C.L. Tien, V.P. Carey, and J.K. Ferrell, Vol. 5, pp 2611-2615, San Francisco, CA.

17. Renz, U., von Wedel, G., and Reinartz, A., 1987, Heat Transfer Characteristics of the FBC at Aachen Technical University, Proc. of the 1987 International Conf. on Fluidized Bed Combustion, ed. J.P. Mustonen, Vol. 1, pp 619-623, Sponsored by ASME, Boston, MA, May 3-7.

18. Alavizadeh, N., Adams, R.L., Welty, J.R., and Goshayeshi, A., 1984, An Instrument for Local Radiative Heat Transfer Measurement in a Gas Fluidized Bed at Elevated Temperature, New Experimental Techniques in Heat Transfer, 22nd National Heat Transfer Conf. and Exhibition, ASME HTD-Vol. 31, pp 1-8.

19. Lei, D.H.-Y., An Experimental Study of Radiative and Total Heat Transfer between a High Temperature Fluidized Bed and an Array of Immersed Tubes. Ph.D. Thesis, Dept. Mech. Eng., Oregon State Univ., January 1988.

20. Alavizadeh, N., 1985, An experimental Investigation of Radiative and Total Heat Transfer Around a Horizontal Tube, Ph.D. Thesis, Dept. Mech. Eng., Oregon State Univ.

21. Chung, T.-Y., Welty, J.R., 1990, Heat Transfer Characteristics for Tubular Arrays in a High-Temperature Fluidized Bed: An Experimental Study of Bed Temperature Effects, Exper. Therm. and Fluid Sci., Vol. 3, pp 388-394.

22. Catipovic, N.M., Heat Transfer to Horizontal Tubes in Fluidized Beds, Ph.D. Thesis, Dept. of Chem. Eng., Oregon State Univ., March 1979.

23. Doeblin, E. O., Measurement Systems Application and Design, rev. ed., McGraw-Hill, New York, 1975.

3. Heat Transfer to a Horizontal Tube in the Splash-zone of a Bubbling Fluidized Bed, an Experimental Study of Particle Size Effects.

3.1 ABSTRACT

The experimental results of an investigation involving particle size effects on the heat transfer for a horizontal tube located in the splash-zone of a high temperature bubbling fluidized bed are reported. This paper is the second of a series [1] which investigates specific operating parameters of bubbling fluidized beds. The array of experimental conditions for this work involved three particle sizes, of nominal 1.1, 2.0, and 2.9 mm diameter; four bed temperatures, 700 K, 810 K, 908 K, and 1003 K; and three tube locations, -127 mm, 64 mm, and 406 mm relative to the tube centerline to non-fluidized bed surface. The tube locations are representative of a tube totally immersed in the bed, located in the splash-zone, and located in the freeboard, respectively. Convective and blackbody radiative heat transfer coefficient variations are presented as functions of the nondimensionalized velocity ratio and of the particle size for the 1003 K case. Maximum convective and blackbody radiative heat transfer coefficients are tabulated for the other temperatures and particle sizes. The tube outside diameter was 51 mm and the superficial velocity was varied from near minimum fluidization conditions (U_{mf}) to over 2.0 U_{mf}.

3.2 KEYWORDS

Fluidized Beds, Particle Size Effects, High Temperature, Freeboard, Splash-zone

3.3 INTRODUCTION

Coal comprises over 80% of the earth's energy resources and the most effective application of coal involves direct burning. Gas-solid fluidized bed combustion offers great potential for the burning of low-rank, high-sulfur coal in an environmentally acceptable manner. Fluidized bed combustors are often designed so that horizontal tube arrays, generating steam for electrical power generation, are located in a bubbling air suspension of burning crushed coal and an inert material (dolomite or limestone for high sulfur coal and silica sand, or its own ash for low rank coal). The combustor is generally designed so that a portion of the tube array is exposed to essentially pure gas convection (no particle convective effects, the "freeboard region"), with a portion of the tube array fully immersed in the dense phase of the fluidized bed (with both particle and gas convective effects) and with the remaining portion located in the transition region (the "splash-zone" of the fluidized bed).

Many investigators have studied dense phase fluidized bed gas and particle convection heat transfer to horizontal tubes, and the pure gas convection heat transfer to a horizontal tube in cross flow is very well documented. There is, however, a dearth of published information concerning heat transfer to horizontal tubes located in the splash-zone of fluidized beds. Some results have been reported dealing with heat transfer in the splash-zone and the freeboard utilizing ambient temperature fluidized beds [Refs. 2-11]. Fewer studies have examined these phenomena at near combustion temperatures [Refs. 12-18]. This paper examines the circumferential, weighted average convective and blackbody radiative heat transfer coefficients to a horizontal tube located in the dense phase, splash-zone, and freeboard regions of a bubbling fluidized bed for a range of superficial velocities, temperatures, and particle sizes. The effect of particle size on the heat transfer characteristics is of particular interest.

3.4 EXPERIMENTAL APPARATUS AND FACILITY

Figure 3-1 shows a schematic of the high temperature fluidized bed test facility. Combustion and fluidization air is compressed and piped to an industrial propane burner, burned in a refractory lined combustion chamber, and directed by a plenum into a refractory lined 0.6 m wide by 0.3 m deep by 1.2 m tall test section through a nickel based alloy distributor plate. The distributor plate consists of two flat alloy plates with a 9 x 17 square hole array. The hole diameters are 7.9 mm and the centerline to centerline hole pitch is 25.4 mm. Sandwiched between the plates is a 40 mesh inconel 800 screen.

An instrumented tube developed by Alavizadeh et al. [19] and Lei [20] (see Fig. 3-2) was used to measure both the circumferential local, total, and blackbody radiative heat transfer coefficients simultaneously. A rotary union allowed the rotational adjustment of the instrumented tube to the desired angular positions for data collection while the tube was cooled by circulating water. The test section walls were instrumented with five Type-K thermocouples, three located in the fluidizing region, one on the wall of the disengaging zone, and one on the ceiling of the disengaging zone.

A high precision data acquisition system was used to record and reduce the heat fluxes and surface temperatures which were employed to calculate the circumferential local heat transfer coefficients at each position on the instrumented tube. The system also recorded the bed temperature and the surface wall temperatures of the test section.

The instrumented tube is made of bronze with an outside diameter of 51 mm and an inside diameter of 32 mm. Six high precision commercially available microfoil thermopile detectors (three total and three radiative, located 90^{o} apart along the tube axis) were used as the heat transfer measuring gages. The total heat flux gages were affixed to the outside tube surface with a high thermal conductivity epoxy and tightly covered with a 0.127 mm thick stainless steel shim stock which was sanded to a dull

finish. A thin layer of a high thermal conductivity paste was sandwiched between the shim stock and the gages to reduce thermal contact resistance. The radiation heat flux gages were axially located 10 cm from the total heat flux gages at the same circumferential locations and orientations. The radiation heat flux gages were epoxied to the bottom of a cavity which was carefully milled in the tube surface. The inner surfaces of the cavity, including the gage, were painted with a known high absorptivity paint, hence, all radiative heat transfer coefficients reported are blackbody values. The cavity was covered by a silicon window which was machined to have the same curvature as the outside of the tube. Silicon [20] was found to be the superior window material when silicon, sapphire, crystal quartz, and fused quartz were considered as potential window materials. Details of the instrument calibration procedures can be found in Refs. 19,20, and 21.

3.5 EXPERIMENTS

The experiments consisted of an examination of the effects of four different variables; temperature, particle size, tube location, and superficial velocity on the heat transfer between a high temperature bubbling fluidized bed and a horizontal tube located in the dense phase, splash-zone, and freeboard. This is the second in a series of papers, each of which emphasizes the different variables investigated. The emphasis of this paper is particle size effects on the heat transfer characteristics in the aforementioned regions of the bubbling fluidized bed.

A granular industrial fluidizing medium was used as the bed material. Three particle sizes were examined with nominal 1.1 mm, 2.0 mm, and 2.9 mm diameters. The particle sizes were determined by a mass averaging for the 1.1 mm diameter, and by mechanical sifting and using the cut between a Number 8 and Number 10 standard

Tyler Screen for the 2.0 mm diameter and a Number 4 and Number 5 standard Tyler Screen for the 2.9 mm diameter. The chemical composition of the particles is 53.5% silica, 43.8% alumina, 2.3% titania, and .4% other substances. The particle thermal properties are characteristic of industrial fluidizing mediums, with a detailed listing by Chung and Welty [21].

Four bed temperatures, 700 K, 810 K, 908 K and 1003 K were examined and the tube was positioned at six locations relative to the packed bed/freeboard interface, three of which are reported. The tube was kept at a fixed location of 711 mm from the distributor plate and 340 mm (both distances are tube centerline to surface values) from one of the 300 mm side walls of the test section. It was located so that the total and radiative gages were located equidistant from the nearest side wall. The packed bed depth was varied from 305 mm, to 647 mm, to 838 mm which accounted for a tube-to-packed-bed-distance of 406 mm, 64 mm, and -127 mm. These relative tube locations are representative tube locations in the freeboard, splash-zone, and dense phase of the fluidized bed, respectively. The fluidization velocity was varied from near minimum fluidization (U_{mf}) to over 2.0 U_{mf}.

Data were taken with the heat flux gages positioned at 0^{o}, 45^{o}, 90^{o}, 135^{o}, and 180^{o} relative to the lower stagnation point. The total heat transfer coefficient and the black body radiative heat transfer coefficient were experimentally determined. The convective heat transfer coefficients reported were calculated from the total and blackbody radiative heat transfer coefficients using an experimentally measured emissivity of 0.37 for the stainless steel shim stock.

3.6 ERROR ANALYSIS

The error involved in measuring the total heat transfer coefficient was determined to be + 8%, - 14%. The three sources of error include: (1) errors due to conduction along the stainless steel shim surface, (2) errors caused by non uniform surface temperature in the bubble contact region, and (3) calibration and data collection procedure errors.

The decrease in temperature across the stainless steel shim stock to the total heat flux gages was found to be less than 1.8 K at a tube wall temperature of 478 K. Neglecting the temperature difference, a two- dimensional steady state heat conduction analysis was performed and it was found that approximately 2% of the heat flux absorbed at the shim's upper surface was not conducted to the active area of the sensor.

A laminar thermal boundary layer analysis was conducted to investigate the effect of non uniform surface temperature in the bubble contact region on the performance of the total heat flux gage. This analysis applies when the gage is covered by gas bubbles. A reduction of approximately 4% in the total heat flux measurements was found by using the data for the bubble contact fraction suggested by Catipovic [23].

The root-sum-square (rss) method given by Doebelin [24] was used to determine the errors in the total heat flux gage calibration and in data collection. Using the manufacturer's uncertainty values and estimating the uncertainties in reading bed temperatures, the random error in evaluating the total heat transfer coefficient was found to be approximately ± 8%. The overall error in the total heat transfer coefficients was determined by summing the three sources, resulting in an overall uncertainty of + 8%,- 14%.

The error in measuring the blackbody radiative heat transfer coefficient was determined to be + 13%, -.12%. Three sources of error in the radiative heat flux measurements include: (1) errors due to conduction from the silicon window to the gage

sensing area, (2) errors caused by non uniform heat flux on the gages, and (3) calibration and data collection procedure errors.

The error introduced by conduction from the silicon window to the radiative heat flux sensor was determined to be + 1%. The maximum error associated with non uniform heat fluxes experienced by the radiative gages was determined to be ± 2.5%. The random error for the radiative heat transfer coefficient was determined to be ± 9%, hence, the overall error associated with the radiative heat transfer coefficients is + 13%,-12%.

Two other sources of error includes the error involved in measuring the superficial fluidization velocity and the error in the measurement of the distance from the packed bed height to the tube centerline. The maximum error in measuring the superficial fluidization velocity was determined to be ±.02 m/s. Because of the considerable time to heat up the facility to the experimental test temperatures, particles were elutriated from the bed which increased the distance from the packed bed to the tube. For the data shown, the maximum decrease in bed depth experienced during the experimental runs was -32 mm. This occurred when the bed temperature was 1003 K, the tube to packed bed distance being 64 mm, and at the maximum superficial velocity of 3.23 m/s.

3.7 RESULTS AND DISCUSSION

Figures 3-3 through 3-6 show the effects of particle size on the heat transfer between a bubbling fluidized bed operating at 1003 K for three superficial velocities and for the three tube locations. Figure 3-3 presents the convective heat transfer results and figs. 3-4 through 3-6 show blackbody radiative heat transfer coefficients. Tables 3-1 and 3-2 give the maximum convective and blackbody radiative heat transfer

coefficients, respectively, for the matrix of parameters investigated. Tables 3-3 and 3-4 give the minimum fluidization velocities and superficial non-dimensional velocity ratios (or non-dimensional velocity range) which are representative of the superficial velocity (velocities) at which the maximum heat transfer coefficients occurred.

Figure 3-3 indicates that there are two general trends for a tube located in the dense phase (-127 mm location) of the fluidized bed operating at the parameters investigated. The first general trend is that the greatest convective heat transfer coefficient for all three particle sizes occurred with the tube located in the dense phase of the fluidized bed. At this location, the 1.1 mm particle size produced the largest convective heat transfer coefficient and showed the greatest spread in the values, but the values for all three particle sizes fell within the error limits of each other. The nominal convective heat transfer coefficient for the for the tube in the dense phase of the 1.1 mm particles and for the range of non-dimensional superficial velocities investigated was 261 W/m^2 K. The 2.0 mm and 2.9 mm particle-size-data indicate little variation in the heat transfer coefficients for the non-dimensional superficial velocities investigated. Nominal values for the convective heat transfer coefficients for the 2.0 and 2.9 mm particles in the dense phase are 197 W/m^2 K and 170 W/m^2 K, respectively.

Another general result is that particle size effects on the convective heat transfer are most pronounced for the tube located within the bed. The 2.0 mm particle convective heat transfer coefficients are approximately 75 percent of the values for the 1.1 mm particles and the 2.9 mm particle coefficients are approximately 65 percent of the 1.1 mm particle values. Values of convective heat transfer coefficients for the 2.0 and 2.9 mm particles for all ranges of non-dimensional superficial velocity ratios are closer to each other than when compared to the 1.1 mm particle results. This result indicates that the predominant mode of heat transfer for the larger particles is gas convection, while both particle and gas convective components for the 1.1 mm particles

are significant. Figure 3-3 is a cross plot of fig. 3-7 (the source of the raw data used to generate figs. 3-3 through 3-6), which shows convective heat transfer coefficient variations vs. non-dimensional superficial velocity ratio. Figure 3-7 shows that the greatest convective heat transfer coefficients are found in the dense phase of the fluidized bed and reconfirms the differences between the 2.0 and 2.9 mm particle heat transfer characteristics compared with those for the 1.1 mm particles.

For a tube located in the splash zone (64 mm location), the convective heat transfer coefficient is considerably less than for a tube located in the dense phase. Because of the increased void fraction in the splash zone, the particle convective component of convective heat transfer coefficient decreases. The 1.1 mm particle size shows the greatest absolute difference and percentage decrease in convective heat transfer coefficient (approximately 130 W/m^2 K difference, or about a 50 percent decrease) when compared with the tube located in the dense phase. The 2.0 mm particles also show a decrease of about 50 percent, but the actual heat transfer coefficient difference is considerably less (approximately 95 W/m^2 K). The 2.9 mm particles show the least variation (approximately 33 percent), and absolute heat transfer coefficient decrease (about 60 W/m^2 K).

The convective heat transfer coefficient increases with increasing superficial velocity, indicating that the void fraction in the splash-zone decreases, increasing particle convective effects on the tube while also increasing the gas convective effects. It is also noted that the convective heat transfer coefficients are similar for all three particle sizes. The above trends are explained by the fact that gas convection is the prominent heat transfer mode for increasingly larger particles, and the residence time of the particles on the tube surface is significantly less for a tube located in the splash-zone than for a tube located the dense phase, hence the particle convective effects tend to become less important and closer to the same value for all particle sizes as the tube-to-

bed surface distance increases. The results shown are for the tube located well within the splash-zone for all three particle sizes and superficial velocity ratios. The decreasing particle size effect over the same non-dimensional superficial velocity ratios (1.2-1.5 U/U_{mf}) is similar to the trends found when the tube-to-bed surface distance was increased in the splash-zone/freeboard (see Pidwerbecki [1]). Figure 3-7 confirms the findings that particle size effects decrease for a tube located in the splash-zone and that the convective coefficients increase with increasing superficial velocity.

The tube located in the freeboard (406 mm location) demonstrated the lowest convective heat transfer values of the three positions and, due to the very low particle densities at this location, the particle convective effects are minimized. The slight increase in heat transfer with superficial velocity is due to an increase in the pure gas convective effects. Figure 3-7 shows the slight increase in convective heat transfer coefficients with the non-dimensional superficial velocity ratio for the three particle sizes. This figure reconfirms that particle convective effects are negligible at this location in the freeboard.

Figure 3-7 shows convective and blackbody radiative heat transfer coefficients vs. non-dimensional superficial velocity ratio for three particle sizes and three tube locations for a bed temperature of 1003 K. This figure indicates how convective heat transfer coefficients relate to blackbody radiative heat transfer coefficients for the different tube locations over a range of non-dimensional superficial velocity ratios. Blackbody radiative heat transfer coefficients seem to be relatively small when compared to convective heat transfer coefficients for the tube located in the dense phase, but become an increasingly larger fraction of the total heat transfer with the tube located in the splash zone and in the freeboard. The dense-phase radiant values are slightly lower than those reported by Lei [20] due to the tube location. The tube was located in the dense phase where a large bubble could periodically expose the tube surface to the

surroundings, lowering the radiant values. The radiation values, however, are still in the expected range reported by Baskakov [25]. It should be kept in mind that values for the blackbody radiative heat transfer coefficients for the tube located in the freeboard (406 mm location) are system specific, and should be considered representative. Figures 3-8 and 3-9 clearly show the blackbody radiative heat transfer coefficients with velocity ratio which are also shown to scale in fig. 3-7.

Figures 3-4 through 3-6 show the blackbody radiative heat transfer coefficient variations with respect to particle size for the tube located in the various regions of the fluidized bed. Figure 3-4 indicates that, for a tube located in the dense phase, particle size has some effect on the radiative heat transfer coefficients, but the superficial velocity ratio has greater influence. At the lower superficial velocity ratio (U/U_{mf} = 1.2), particle size has a significant effect on the radiative heat transfer. At these lower velocities, the blackbody radiative heat transfer coefficient was minimum for the 1.1 mm particles with a value of 25 W/m^2 K, reached a maximum for the 2.9 mm particles at 31.6 W/m^2 K; and exhibited a value of 29 W/m^2 K for the 2.0 mm particles. This is due to the greater thermal mass of the larger particles which results in a more constant particle temperature during their residence times near the tube surface. At higher superficial velocities, blackbody radiative heat transfer coefficients tend to increase in value with increasing velocities, indicating that particles have a shorter surface residence times. The 2.0 mm and 2.9 mm particles exhibited essentially the same radiative heat transfer coefficients as the superficial velocity increased, indicating that particle temperatures remained essentially constant; that is, the thermal masses of the particles are large when compared to the transient energy loss during their short residence times on the tube surface.

The data shown in fig. 3-5 show that radiative energy transfer in the splash-zone did not vary appreciably with particle size over the range of velocities studied and that the blackbody radiative heat transfer coefficients were similar to those found in the dense phase of the bed. These results indicate that the void fraction was sufficiently small at this location such that the surroundings (experimental facility specific geometry) had only a modest radiative contribution to the heat transfer, yet the particle residence time on the tube surface was short enough so that the particles do not cool appreciably. The 2.0 mm particles did show slightly lower radiative heat transfer values, but the values are within the error limits for the other particle sizes.

Figure 3-6 shows blackbody radiative heat transfer coefficients for a tube located in the freeboard of the experimental facility. General trends indicate that the radiant heat transfer contribution is less than either the splash-zone or the dense phase of the fluidized bed, however, values are of the same order of magnitude. Figures 3-4 through 3-6 were obtained by cross plotting data from figs. 3-8 and 3-9 which represent blackbody radiative heat transfer coefficients as a functions of superficial velocity. Figures 3-8 and 3-9 also show that radiative heat transfer coefficients are of similar magnitudes for tubes located both in the splash zone and in the dense phase of the fluidized bed, and they are generally lower in the freeboard.

The general trends of values in Tables 3-1 and 3-2 indicate that at the lower bed operating temperature, 700K, the radiant contribution is small relative to that for convection. Neglecting freeboard values, maximum blackbody radiative heat transfer coefficients are on the order of 10-18 percent of the maximum convective heat transfer coefficients with the tube located in the dense phase of the fluidized bed, and are between 12 and 26 percent of the maximum convective heat transfer coefficients for the tube located in the splash-zone at the higher temperatures. Tabulated values indicate that particle size has little effect on the maximum radiative heat transfer coefficients for

the tube located in the splash zone and the dense phase of the fluidized bed for the temperatures of 908K and 1003K.

3.8 SIGNIFICANCE OF RESULTS

The operating characteristics of the splash-zone, the region between the dense phase of the fluidized bed and the freeboard region, are of practical importance to designers in terms of off-design thermal output of coal fired power plants. This paper addresses particle size effects within the splash-zone. The two phase fluid flow behavior of fluidized beds is so chaotic that an analysis of the heat transfer, from first principles, is presently impossible. Numerical simulations and empirical models have had limited success, but each must be validated by experimental results. The results reported herein are the only ones known to include direct simultaneous measurement of both total and radiative heat transfer coefficients for a horizontal tube located in the splash-zone of a high temperature fluidized bed.

3.9 CONCLUSIONS

The largest convective heat transfer coefficients were found in the dense phase of the fluidized bed. The maximum convective heat transfer coefficient for the 1.1 mm particles varied from 277 W/m^2 K at 700 K, to 258 W/m^2 K at a temperature of 908 K. The maximum convective heat transfer coefficients for the 2.0 mm particles varied from 173 to 200 W/m^2 K at 810 K and 1003 K, respectively and for the 2.9 mm particles varied from 171 to 185 W/m^2 K at 700 K and 810 K, respectively. The maximum convective heat transfer values for each of the particle sizes investigated fell within the experimental error limits of each other over all the superficial velocities and temperatures.

Convective heat transfer behavior of the 2.0 and 2.9 mm particles were similar and consistent with the characteristics of Geldart class D particles, while the 1.1 mm particles exhibited characteristics which are a combination of by both Geldart class B and class D particle behavior. For velocities between 1.2 to 1.5 U/U_{mf}, particle size effects are significant, and velocity effects show only minor influence. Over the range of velocities studied there was approximately a 17% difference between the nominal convective heat transfer coefficient for the 2.0 and 2.9 mm particles, yet the difference between the nominal convective heat transfer coefficients for the 2.0 and 1.1 mm particles was approximately 33% and the difference between nominal convective heat transfer coefficients for the 2.9 and 1.1 mm particles is approximately 54%.

For a tube located in the splash-zone, the particle effects diminish, but the superficial velocities have some effect upon the convective heat transfer coefficients. Since the gas convective component of the convective heat transfer coefficient is dominant for the larger particles, the 2.0 and 2.9 mm particles did not experience as large a decrease in the convective heat transfer coefficient when compared with the 1.1 mm particles, causing the overall convective heat transfer coefficients for the three particle sizes to have similar values for the tube located in the splash-zone. As the non-dimensional superficial velocity ratio was increased some change in the convective heat transfer coefficient was observed for all three particle sizes. This was a result of a decrease in the void fraction of the particles surrounding the tube with a corresponding increase in both the particle convective and gas convective contributions to the total. For the tube located in the freeboard (406 mm), the results indicate that the bed particles have minimal effect, and the slight increase in the convective heat transfer is attributed to the increase in gas convection alone.

The maximum blackbody radiative heat transfer occurred either within the splash-zone or the dense phase of the fluidized bed but, the maximum values for either

location are generally very similar. These values, however, are small in comparison to the maximum convective heat transfer coefficients. For the tube located in the dense phase of the fluidized bed operating at a temperature of 1003 K and between the non-dimensional superficial velocity ratios of 1.2-1.5 U/U_{mf}, the 2.0 and 2.9 mm particle blackbody radiative heat transfer coefficient values were approximately 30 W/m^2 K, whereas, for the 1.1-mm particles a nominal value of approximately 27 W/m^2 K was measured. With the tube located in the splash-zone and operating at the same conditions, the blackbody radiative heat transfer coefficient for the 1.1-mm particles was approximately 34 W/m^2 K, for the 2.0-mm particles the coefficient value was approximately 28 W/m^2 K, and for the 2.9 mm particles the coefficient value was approximately 32 W/m^2 K. Blackbody coefficients are all within the error bars of each other, indicating that particle size has little effect on the radiation incident upon a tube located in the splash-zone. The blackbody radiative heat transfer coefficients for the tube located in the freeboard are specific to the fluidized bed test facility employed in this work. The values measured may be considered representative of typical values. Results indicates that the blackbody radiative heat transfer coefficients are likely to be of the same order, but somewhat less than those measured in the dense phase or the splash-zone of the fluidized bed.

3.10 NOMENCLATURE

d_p - Average particle size, mm

U - Average Superficial Fluidizing Velocity, m/s

U_{mf} - Minimum Superficial Fluidizing Velocity, m/s

T_{bed} - Average Bed Temperature, K

3.11 ACKNOWLEDGMENTS

We wish to express our appreciation to the National Science Foundation, Grant Number CTS-8803077, for supporting this research.

Table 3-1.

Maximum Convective Heat Transfer Coefficient vs. Particle Size
Convective Coefficients (W/m^2 K)

Tube Location	Particle Size(mm)	700 K	810 K	908 K	1003 K
406 mm	1.1	45	49	50	54
	2.0	40	45	47	56
	2.9	33	49	52	52
64 mm	1.1	226	230	219	182
	2.0	142	150	138	139
	2.9	110	124	126	126
-127 mm	1.1	277	273	258	269
	2.0	179	173	182	200
	2.9	171	185	181	181

Table 3-2.

Maximum Blackbody Radiative Heat Transfer Coefficient vs. Particle Size
Radiative Coefficients (W/m^2 K)

Tube Location	Particle Size(mm)	700 K	810 K	908 K	1003 K
406 mm	1.1	7.9	11.9	13.5	23.5
	2.0	7.7	13.7	21.5	28.4
	2.9	7.8	15.5	23.8	31.8
64 mm	1.1	12.8	19.2	26.2	35.0
	2.0	11.0	17.0	23.2	30.6
	2.9	12.8	18.8	25.4	33.3
-127 mm	1.1	12.7	19.5	25.6	33.3
	2.0	12.5	18.8	25.3	33.0
	2.9	12.7	19.0	24.7	32.2

Table 3-3.

Non Dimensional Velocity Ratio for the Maximum Convective Heat Transfer Coefficient listed in Table 3-1

Tube Location	Particle Size	700 K Umf	700 K U/Umf	810 K Umf	810 K U/Umf	908 K Umf	908 K U/Umf	1003 K Umf	1003 K U/Umf
406 mm	1.1	.45	2.23	.49	2.03	.50	1.99	.50	2.21
	2.0	1.59	1.44	1.67	1.56	1.68	2.41	1.68	2.00
	2.9	1.97	1.28	2.08	1.45	2.15	1.56	2.10	1.69
64 mm	1.1	.46	2.18	.49	2.03	.49	2.04	.50	2.22
	2.0	1.59	1.43	1.67	1.57	1.68	1.60-1.77	1.68	1.80-1.93
	2.9	1.98	1.22	2.07	1.36	2.13	1.23-1.56	2.11	1.39-1.53
-127 mm	1.1	.46	1.55-2.15	.49	1.38-2.04	.50	1.40-2.00	.50	1.42-2.18
	2.0	1.64	1.19-1.33	1.68	1.20-1.33*	1.68	1.22-1.33*	1.69	1.26-1.38*
	2.9	2.00	1.16-1.22	2.07	1.12-1.18*	2.11	1.18-2.24*	2.12	1.23-1.30*

When more than one non-dimensional superficial velocity is listed, those values represent a range of non dimensional superficial velocities over which the listed maximum convective heat transfer coefficient is representative.

Asterisk values indicates the range of non-dimensional superficial velocities does not include the maximum experimentally studied superficial velocity, otherwise, the upper bound represents the maximum non-dimensional superficial velocity studied.

Table 3-4.

Non Dimensional Velocity Ratio for the Maximum Blackbody Radiative Heat Transfer Coefficient listed in Table 3-2

Tube Location	Particle Size	700 K U_{mf}	700 K U/U_{mf}	810 K U_{mf}	810 K U/U_{mf}	908 K U_{mf}	908 K U/U_{mf}	1003 K U_{mf}	1003 K U/U_{mf}
406 mm	1.1	.45	2.23	.49	2.03	.50	1.88-1.99	.50	1.90-2.21
	2.0	1.59	1.44	1.67	1.48-1.56	1.68	2.32-2.41	1.68	1.88-2.00
	2.9	1.97	1.20-1.28	2.08	1.44	2.15	1.56	2.10	1.69
64 mm	1.1	.46	1.60-2.18	.49	1.40-2.03	.49	1.48-2.04	.50	1.41-2.22
	2.0	1.59	1.32-1.43	1.67	1.35-1.57	1.68	1.50-1.77	1.68	1.57-1.93
	2.9	1.98	1.05-1.22	2.07	1.26-1.36	2.13	1.25-1.56	2.11	1.35-1.53
-127 mm	1.1	.46	1.80-2.15	.49	1.73-2.04	.50	1.99	.50	2.08-2.18
	2.0	1.64	1.21-1.33	1.68	1.32-1.51	1.68	1.61-1.73	1.69	1.50-1.86
	2.9	2.00	1.15-1.22	2.07	1.14-1.33	2.11	1.31-1.49	2.12	1.29-1.63

When more than one non-dimensional superficial velocity is listed, those values represent a range of non-dimensional superficial velocities over which the listed maximum convective heat transfer coefficient is representative. All the values include the maximum non-dimensional superficial velocity studied.

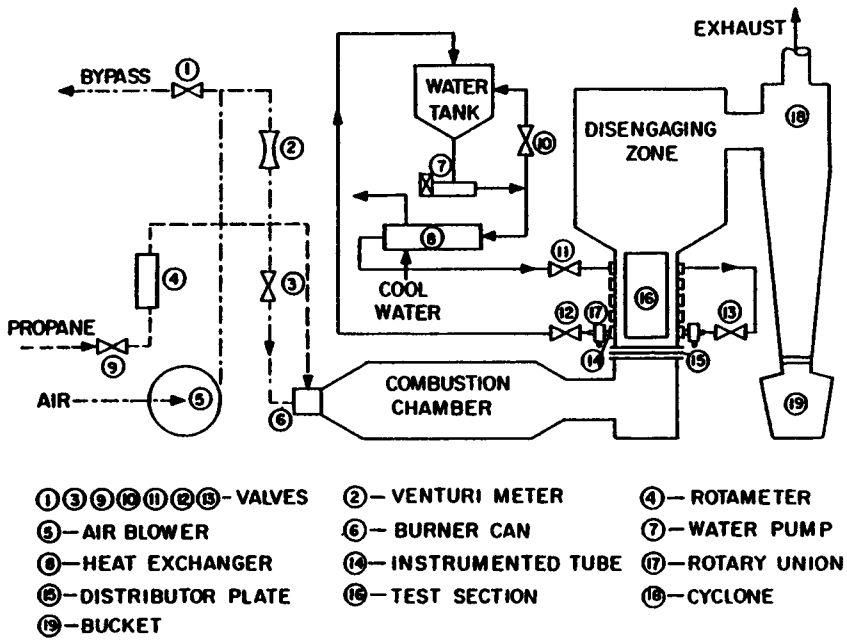

Fig. 3-1 Oregon State University high temperature fluidized bed test facility

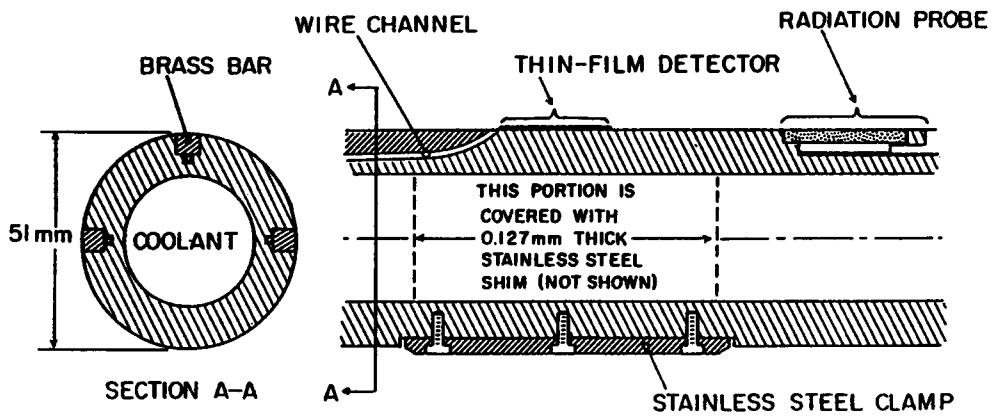

Fig. 3-2 Instrumented tube for total and radiative heat flux measurements

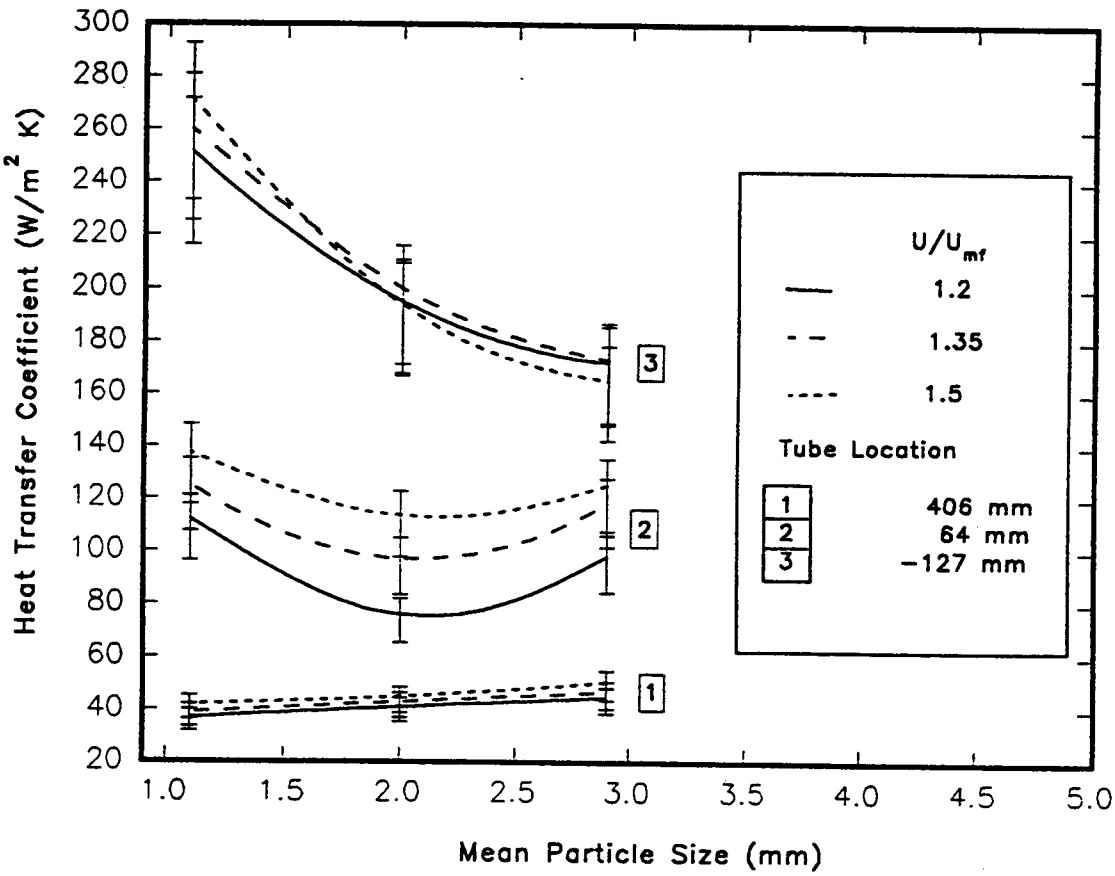

Fig. 3-3 Convective Heat Transfer Coefficients vs. Particle Size, T_{bed} = 1003 K

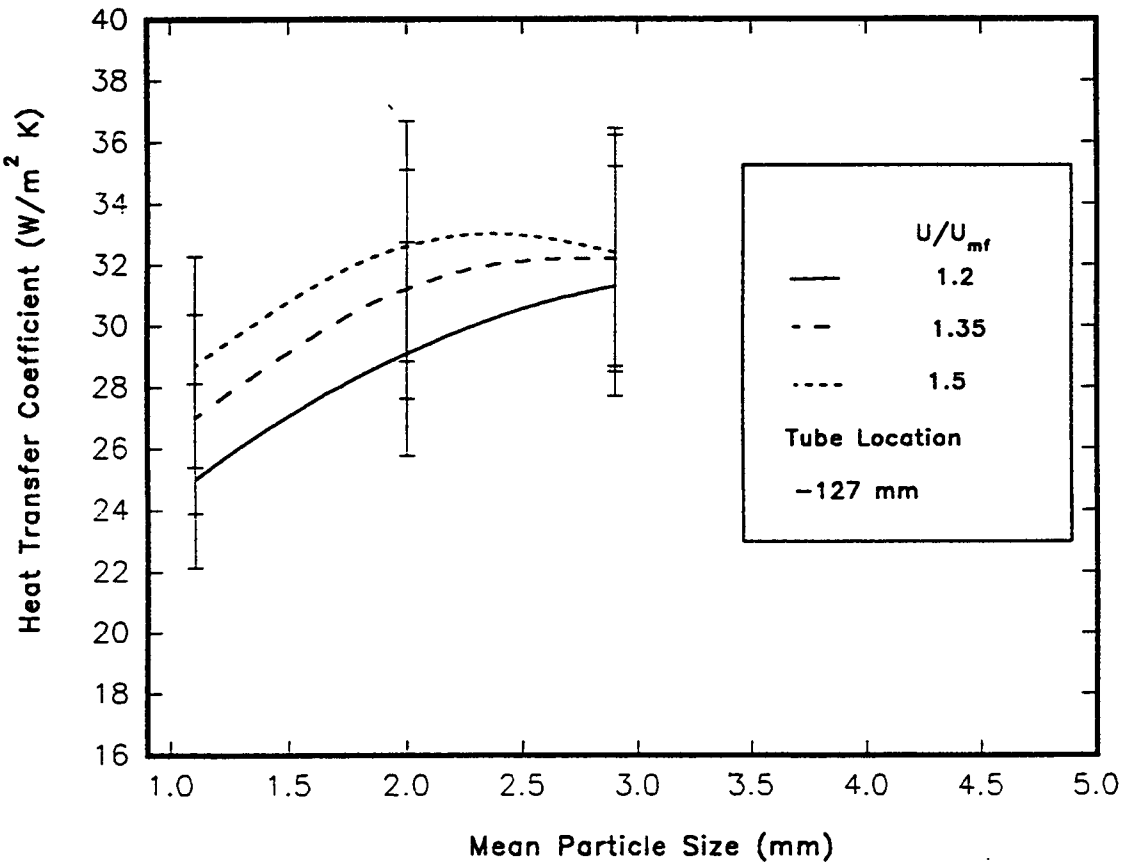

Fig. 3-4 Radiative Heat Transfer Coefficients vs. Particle Size, T_{bed} = 1003 K, tube to slumped bed surface distance = -127 mm

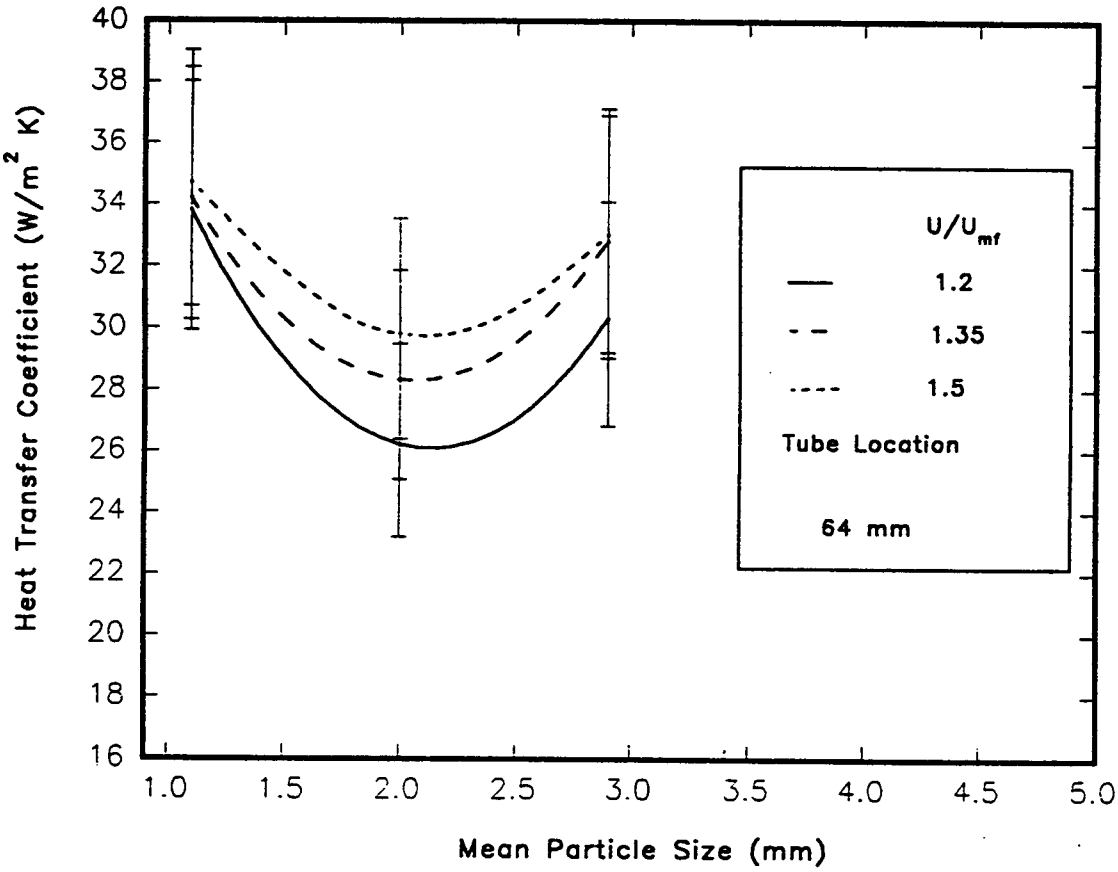

Fig. 3-5 Radiative Heat Transfer Coefficients vs. Particle Size, T_{bed} = 1003 K, tube to slumped bed surface distance = 64 mm

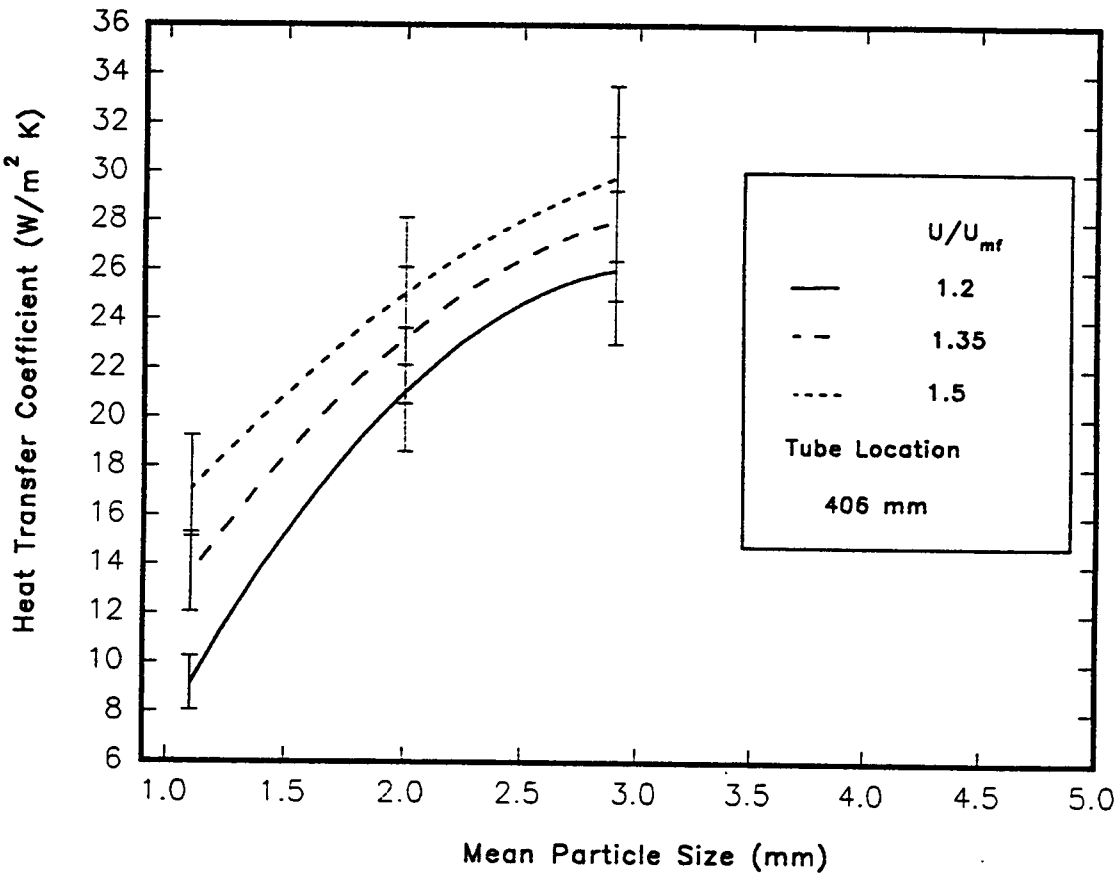

Fig. 3-6 Radiative Heat Transfer Coefficients vs. Particle Size, T_{bed} = 1003 K, tube to slumped bed surface distance = 406 mm

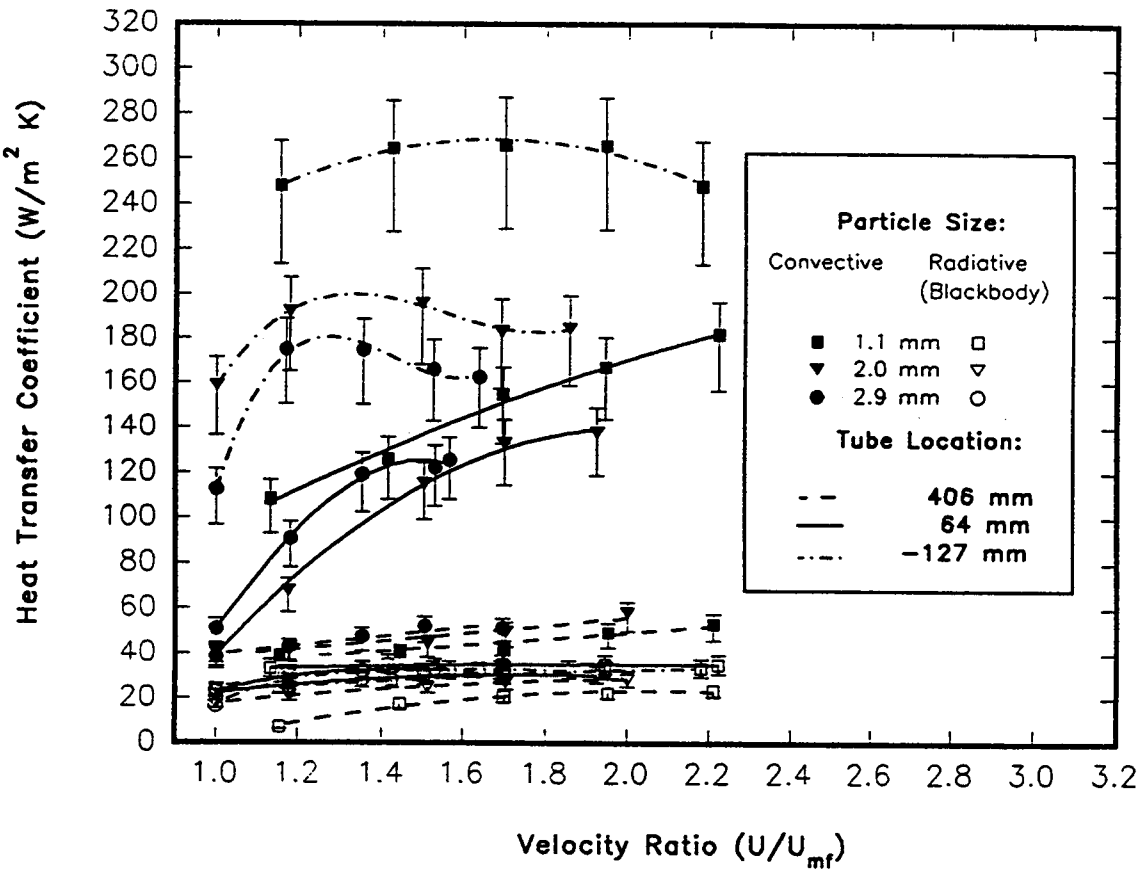

Fig. 3-7 Convective and Radiative Heat Transfer Coefficients vs. Velocity Ratio, T_{bed} = 1003 K

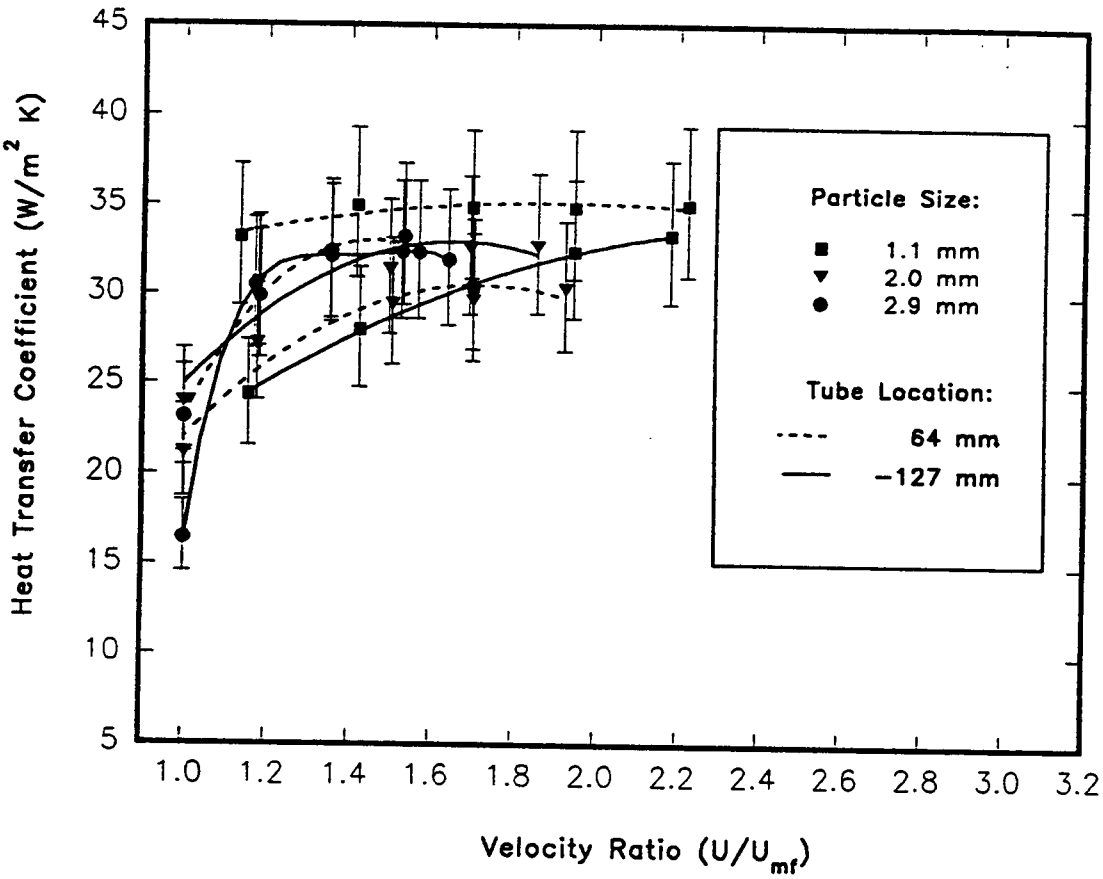

Fig. 3-8 Radiative Heat Transfer Coefficients vs. Velocity Ratio, T_{bed} = 1003 K

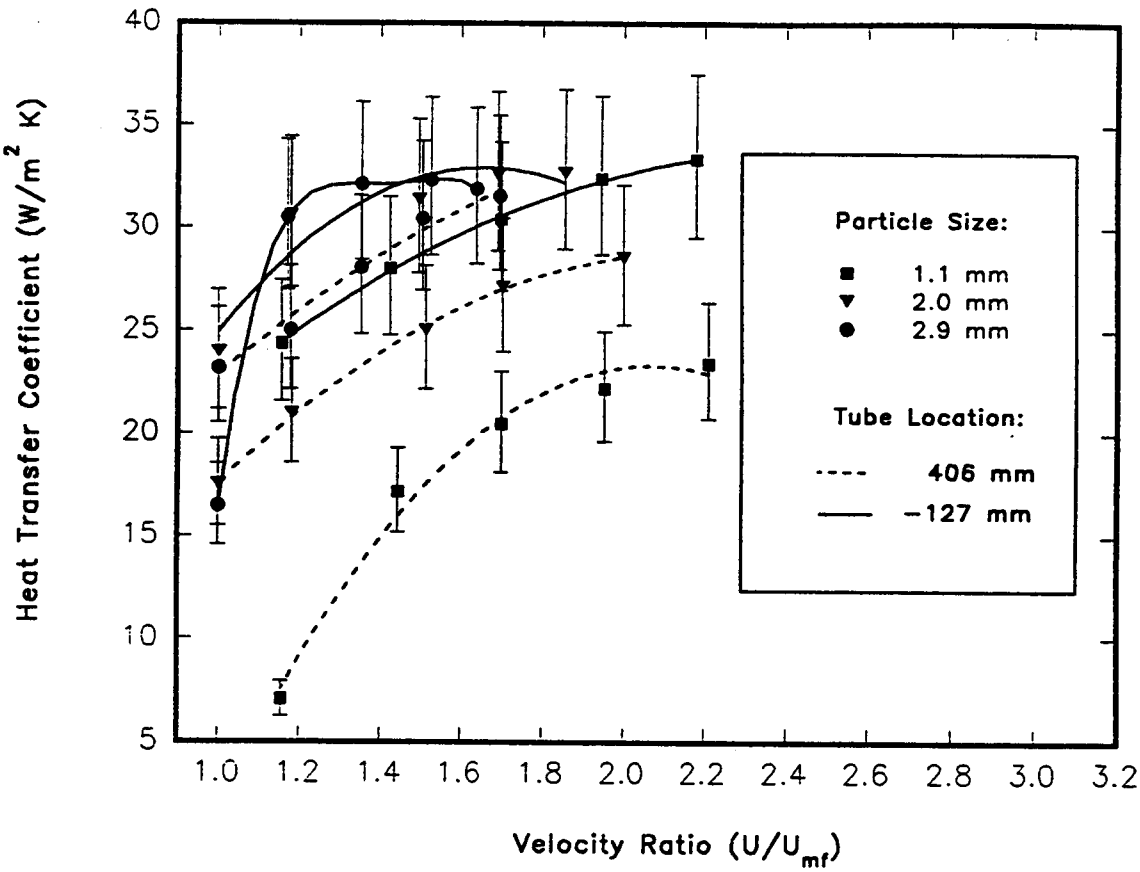

Fig. 3-9 Radiative Heat Transfer Coefficients vs. Velocity Ratio, T_{bed} = 1003 K

3.12 REFERENCES

1. Pidwerbecki, D., Welty, J.R., Splash-zone Heat Transfer in Bubbling Fluidized Beds - an Experimental Study of Temperature Effects, accepted for publication in *Journal of Experimental and Thermal Fluid Science* 1994.

2. Biyikli, S., Tuzla, K., and Chen, J.C., A Phenomenological Model for Heat Transfer in Freeboard of Fluidized Beds, Can. *J. of Chem. Eng.*, **67**, 230-236, April 1989.

3. Biyikli, S., Tuzla, K., and Chen, J.C., Particle Contact Dynamics on Tubes in the Freeboard Region of Fluidized Beds, *AIChE J.*, **33** (7), 1225-1227, July 1987.

4. Biyikli, S., Tuzla, K., and Chen, J.C., Heat Transfer Around a Horizontal Tube in Freeboard Region of Fluidized Beds, *AIChE J.*, **29** (5), 712-716, Sept. 1983.

5. Dyrness, A., Glicksman, L.R., and Yule, T., Heat Transfer in the Splash Zone of a Bubbling Fluidized Bed, *Int. J. Heat Mass Transfer*, **35** (4), 847-859, 1993.

6. George, S.E. and Grace, J.R., Heat Transfer to Horizontal Tubes in the Freeboard Region of a Gas Fluidized Bed, *AIChE J.*,**28** (5), 759-765, 1982.

7. George, S.E. and Grace, J.R., Hear Transfer to Horizontal Tubes in Freeboard Region of a Gas Fluidized Bed, AIChE Meeting, San Francisco, No. 7E, 1979.

8. Hongshen, G., et al., A Model and Experiments for Heat Transfer of Single Horizontal Tube in the Freeboard of Fluidized Bed, Proc. of the 1987 Intl. Conf. on Fluidized Bed Combustion, ed. J.P. Mustonen, Vol 2, pp 1159-1164, Sponsored by ASME, Boston, MA., 1987.

9. Shi, M.H., Heat Transfer to Horizontal Tube and Tube Bundle in Freeboard Region of a Gas Fluidized Bed, Proc. of the 1987 ASME.JSME Thermal Eng. Joint Conf., eds. P.J. Martso and I. Tanasawa, Vol. 4, pp 113, Honolulu, HI, March 22-27, 1987.

10. Wood, R.T., Kuwata, M., and Staub, F.W., Heat Transfer to Horizontal Tube Banks in the Splash Zone of a Fluidized Bed of Large Particles, *Fluidization*, R. Grace and J.M. Matsen Eds., pp 235-243, Plenum, NY, 1980.

11. Xavier, A.M. and Davidson, J.F., Heat Transfer to Surfaces Immersed in Fluidized Beds and in the Freeboard Region, AIChE Symposium Series, Vol.77, No. 208, pp 368-373, 1981.

12. Bardakci, T. and Molayem, B., Experimental Studies of Heat Transfer to Horizontal Tubes in a Pilot-Scale Fluidized-Bed Combustor, *Canadian J. of Chem. Engr.*, **67**, 348-351, April 1989.

13. Biyikli, S., Tuzla, K., and Chen, J.C., Freeboard Heat Transfer in High-Temperature Fluidized Beds, *Powder Technology*, **53**, 187-194, 1987.

14. Byam, J., Pillai, K.K., and Roberts, A.G., Heat Transfer to Cooling Coils in the Splash Zone of a Pressurized Fluidized Bed Combustor, AIChE Symposium Series, Vol. 77, No. 208, pp 351-358, 1981.

15. Gormar, H., Renz, U., and Verweyen, N., Heat Transfer to the Cooled Freeboard of a Fluidized Bed, Proc. of the 1989 Intl. Conf. on Fluidized Bed Combustion, A.M. Manaker Ed., Vol. 2, pp 1241-1244, Sponsored by ASME, San Francisco, CA, Apr 30 - May 3, 1989.

16. Kortleven, A., Bast, J., and Meulink, J., Heat Transfer for Horizontal Tubes in the Splash Zone of a 0.6 x 0.6 m AFBC Research Facility, Proc. of the XVI Intl. Center of Heat and Mass Trans. Conf., Yugoslavia, 1984.

17. Mitor, V.V., Matsnev, V.V., and Sorokin, A.P., Investigation of Heat Transfer in Bed and Freeboard of Fluidized Bed Combustors, Proc. of the Eighth Intl. Heat Trans. Conf., C.L. Tien, V.P. Carey, and J.K. Ferrell Eds., Vol. 5, pp 2611-2615, San Francisco, CA, 1986.

18. Renz, U., von Wedel, G., and Reinartz, A., Heat Transfer Characteristics of the FBC at Aachen Technical University, Proc. of the 1987 International Conf. on Fluidized Bed Combustion, J.P. Mustonen Ed., Vol. 1, pp 619-623, Sponsored by ASME, Boston, MA, May 3-7, 1987.

19. Alavizadeh, N., Adams, R.L., Welty, J.R., and Goshayeshi, A., An Instrument for Local Radiative Heat Transfer Measurement Around a Horizontal Tube Immersed in a Fluidized Bed, *J. Heat Transfer*, **112** (2), 486-491, 1990.

20. Lei, D.H.-Y., An Experimental Study of Radiative and Total Heat Transfer between a High Temperature Fluidized Bed and an Array of Immersed Tubes. Ph.D. Thesis, Dept. Mech. Eng., Oregon State Univ., January 1988.

21. Alavizadeh, N., An experimental Investigation of Radiative and Total Heat Transfer Around a Horizontal Tube, Ph.D. Thesis, Dept. Mech. Eng., Oregon State Univ, 1985.

22. Chung, T.-Y., Welty, J.R., Heat Transfer Characteristics for Tubular Arrays in a High-Temperature Fluidized Bed: An Experimental Study of Bed Temperature Effects, *Exper. Therm. and Fluid Sci.*, **3**, 388-394, 1990.

23. Catipovic, N.M., Heat Transfer to Horizontal Tubes in Fluidized Beds, Ph.D. Thesis, Dept. of Chem. Eng., Oregon State Univ., March 1979.

24. Doeblin, E. O., *Measurement Systems Application and Design*, rev. ed., McGraw-Hill, New York, 1975.

25. Baskakov, A.P., Radiative Heat Transfer in Fluidized Beds, in *Fluidization 2nd. Edition*, J.F. Davidson et al. Eds., pp 465-472, Academic Press, London, 1985.

4. Heat Transfer to a Horizontal Tube in the Splash-Zone of a Bubbling Fluidized Bed, an Investigation of Tube Location Effects. Part I: Experimental Results

4.1 ABSTRACT

The effects of tube location on experimentally determined heat transfer coefficients associated with a horizontal tube located in the splash-zone of a high temperature bubbling fluidized bed are reported. The experimental results of this study are presented in Part I of a two-part series; and a modeling study of this situation will be presented in Part II (Chapter 5). This paper is the third of a series (Pidwerbecki 1994 a, b) related to specific operating parameters of bubbling fluidized beds. The array of experimental parameters investigated in this work include three particle sizes of nominal 1.1, 2.0, and 2.9 mm diameter; four bed temperatures of 700 K, 810 K, 908 K, and 1003 K; and six tube locations ranging from the dense phase of the bed to the freeboard. The superficial velocity was varied from near minimum fluidization (U_{mf}) to over 2.0 U_{mf}. Convective heat transfer coefficient variations for the 810 K and the 1003 K cases and blackbody radiative heat transfer coefficient variations for the 1003 K cases are presented.

4.2 KEY WORDS

splash-zone, high temperature, fluidized bed, horizontal tube

4.3 INTRODUCTION

The heat transfer to horizontal tubes located in the splash-zone is of interest in many applications of fluidized beds; an application of current interest is in the design of coal fired-electrical power generation plants. Fluidized bed combustors are often designed so that a portion of the tube array is exposed to essentially pure gas convection (no particle convective effects, the "freeboard region"), another portion of the tube array is fully immersed in the dense phase of the fluidized bed (with both particle and gas convective effects) and the remaining portion is located in the transition region (the "splash-zone" of the fluidized bed). The technical literature includes a number of fluidized bed studies where a horizontal tube is located in the dense phase (Alavizadeh et al. 1990, Alavizadeh 1985, Catipovic 1979, Lei 1988, Chung and Welty 1990), however, there is a scarcity of published information concerning heat transfer to horizontal tubes located in the splash-zone. Of the studies dealing with splash-zone heat transfer, most have utilized ambient temperature fluidized beds (Biyikli et al. 1989 a, 1987 and 1983, Dyrness et al. 1993, George and Grace 1982 and 1979, Hongshen et al. 1987, Shi 1987, Wood et al. 1980), and a few have examined these phenomena at typical combustion temperatures (Bardakci and Molayem 1989, Biyikli et al. 1989 b, Byam et al. 1981, Gormar et al. 1989, Kortleven et al. 1984, Mitor et al. 1986, Renz et al. 1987). Part I of this work presents the experimental results for the circumferential, weighted average convective and black body radiative heat transfer coefficients for a horizontal tube located in the dense phase, splash-zone, and freeboard regions of a bubbling fluidized bed. Of particular interest is the effect of tube location upon the heat transfer characteristics within the splash-zone. Part II (Chapter 5) of this study presents a correlation which can be used to predict the convective heat transfer to a single tube in the splash-zone.

4.4 EXPERIMENTAL APPARATUS AND FACILITY

Figure 4-1 shows a diagram of the high temperature fluidized bed test facility. A Roots style rotary vane compressor provided air to an industrial propane burner/combustion chamber where the high temperature combustion products were directed into a refractory lined 0.6 m wide by 0.3 m deep by 1.2-m-tall test section. The distributor plate, consisting of two perforated nickel alloy plates sandwiching a 40 mesh inconel 800 screen, was located between the combustion chamber and the test section. The perforation pattern was a 9 x 17 square hole array with a 25.4 mm centerline to centerline pitch and with 7.9-mm hole diameters.

Figure 4-2 illustrates the instrumented tube (developed by Alavizadeh et. al. 1990 and Lei 1988) which was used to measure both the circumferential local total and local blackbody radiative heat transfer coefficients simultaneously. The instrumented tube was made of bronze with an outside diameter of 51 mm and an inside diameter of 32 mm. Six commercially available high precision microfoil thermopile detectors (three total and three radiative, located 90^{o} apart along the tube axis) were used as the heat flux measuring gages. The total heat flux gages were attached to the outside tube surface with a high thermal conductivity epoxy and tightly covered with a 0.127-mm-thick stainless steel shim stock. A thin layer of high thermal conductivity paste was sandwiched between the shim stock and the gages to minimize the thermal contact resistance. The shim stock was sanded to a dull finish prior to the tube being placed in the fluidized bed insuring that the emmisivity of the shim stock remained constant throughout the experiments. The radiation heat flux gages, as described by Lei (1988), were located 10 cm axially from the total heat flux gages at the same circumferential locations and orientations. The radiation gages were epoxied to the bottom of a carefully milled cavity in the tube surface. The inner surfaces of the cavity, including

the gages, were painted with a known high absorptivity paint, hence, all radiative heat transfer coefficients reported are blackbody values. The cavity was covered by a silicon window (Lei 1988) which was machined to have the same curvature as the outside of the tube. Details of the instrument calibration procedures can be found in Alavizadeh (1985). The test section walls were instrumented with five type-K thermocouples, three located in the fluidizing region, one on the wall of the disengaging zone, and one on the ceiling of the disengaging zone. A high precision data acquisition system was used to record and reduce the local heat flux and surface temperature data which were employed to calculate the circumferential local heat transfer coefficients at each position on the instrumented tube. The system also recorded the bed temperature and the surface wall temperatures of the test section. A rotary union allowed the desired rotational adjustment of the instrumented tube for data collection while cooling water circulated inside the tube.

4.5 EXPERIMENTS

A granular industrial fluidizing medium with a chemical composition of 53.5% silica, 43.8% alumina, 2.3% titania, and 0.4% other substances, and of nominal 1.1 mm, 2.0 mm, and 2.9 mm diameters was used as the bed material. Particle sizes were determined by a mass average of the various particle size components for the 1.1 mm diameter particles; by mechanical sifting and using the cut between a Number 8 and Number 10 standard Tyler Screen for the 2.0 mm diameter particles, and by mechanical sifting and using the cut between a Number 4 and Number 5 standard Tyler Screen for the 2.9 mm diameter particles. The particle thermal properties are characteristic of industrial fluidizing media, with a detailed listing by Chung and Welty (1990).

Heat transfer coefficients were obtained for four bed temperatures, for three particle sizes, and for six approximate tube locations relative to the packed bed/freeboard interface, -127 mm (immersed), 0 mm, 64 mm, 133 mm, 273 mm, and 406 mm (approximately the freeboard). The tube location was maintained at 711 mm above the distributor plate, 340 mm from one of the 300 mm side walls of the test section (both distances are tube centerline to surface values), and positioned so that the total and radiative gages were equidistant from the nearest end wall. The packed-bed depth was varied from 305 mm to 838 mm which accounted for the tube-to-packed-bed-distance variation from 406 mm to -127 mm. The fluidization velocity was varied from near minimum fluidization (U_{mf}) to over 2.0 U_{mf}.

The local total heat transfer coefficients and local blackbody radiative heat transfer coefficients were determined with the heat flux gages positioned at 0^{o}, 45^{o}, 90^{o}, 135^{o}, and 180^{o} relative to the lower stagnation point. The local values were integrated, using Simpsons rule, to determine the average total and blackbody radiative heat transfer coefficients. Convective heat transfer coefficients reported were determined from the total and blackbody radiative heat transfer coefficients using an experimentally measured emissivity of 0.37 for the sanded stainless steel shim stock.

4.6 ERROR ANALYSIS

An error analysis indicated that the total heat transfer coefficients could be determined within +8%, -14% of full scale values. The three major sources of error include: (1) errors due to conduction along the stainless steel shim surface, (2) errors caused by non uniform surface temperature in the bubble contact region, and (3) calibration and data collection procedure errors.

The analysis of the error due to conduction involved determining the lateral and radial conduction contributions. The decrease in temperature across the stainless steel shim stock to the total heat flux gages was found to be less than 1.8 K at a tube wall temperature of 478 K. Neglecting the temperature difference, a two- dimensional steady state heat conduction analysis was performed and it was found that approximately 2% of the heat flux absorbed at the upper surface of the shim was not conducted to the active area of the sensor.

In order to determine the errors which could result from the gages being subjected to non-uniform surface temperature in the bubble contact region, a laminar thermal boundary layer analysis was performed. This analysis applies when the gage is covered by gas bubbles. A reduction of approximately 4% in the total heat flux measurements was found using the data for the bubble contact fraction suggested by Catipovic (1979).

The root-sum-square (rss) method given by Doebelin (1975) was used to determine the errors in the total heat flux gage calibration and in data collection. Using the manufacturer's uncertainty values and estimating the uncertainties in reading bed temperatures, the random error in evaluating the total heat transfer coefficient was found to be approximately ± 8%. The overall error in the total heat transfer coefficients was determined by summing the three sources, resulting in an overall uncertainty of +8%,-14% of full scale value with 95% confidence.

The error in measuring the blackbody radiative heat transfer coefficient was determined to be +13%, -12% of full scale values. The three sources of error in the radiative heat flux measurements include: (1) errors due to conduction from the silicon window to the gage sensing area, (2) errors caused by non uniform heat flux on the gages, and (3) calibration and data collection procedure errors.

The error due to conduction from the silicon window to the sensor was determined to be + 1%. The maximum error associated with non uniform heat fluxes experienced by the radiative gages was estimated to be ± 2.5%. The random error for the radiative heat transfer coefficient (uncertainty in the gages, bed temperature measurements, etc.) was determined to be ± 9%, hence, the overall error associated with the radiative heat transfer coefficients is +13%,-12% (95% confidence).

Other sources of error include the error in measuring the superficial fluidization velocity and the error in measuring the distance between the packed bed height and the tube centerline. The maximum error in measuring the superficial fluidization velocity was determined to be ±.02 m/s. The experimental facility was quite massive, and required considerable time to heat up to the test temperatures. During this time, some particles were elutriated from the bed causing an increase in the distance from the packed bed to the tube centerline. The maximum decrease in bed depth, or increase in distance between the bed and the tube, was 32 mm. This condition occurred while fluidizing the 2.9 mm particles at a bed temperature of 1003 K when the distance between the tube and the packed bed was 64 mm, and when the superficial velocity was at its maximum value of 3.23 m/s (1.56 U_{mf}). These corrections are taken into account for all values reported, where the tube locations are averaged between the beginning (the experimental set point location) and the end of each run.

The experimental facilities are of a similar scale and operating conditions as most commercial fluidized boilers and the convection results can be considered representative. Blackbody radiation results, however, are strong functions of the facility configuration (side wall temperatures, surface properties, etc.), thus all splash-zone and freeboard results should be considered typical but not general. The radiant results obtained when

the tube was located in the dense phase (-127 mm location) are well within the range of those predicted by Baskakov (1985) and can be considered general.

4.7 RESULTS AND DISCUSSION

Figures 4-3 through 4-8 show convective heat transfer coefficient variations for several different particle sizes, tube locations, superficial fluidizing velocities, and for the bed temperatures of 810 K and 1003 K. Tube location is defined as the distance from tube centerline to non-fluidized (slumped) bed surface. Note that the points shown on these figures are not experimentally determined data points, but are cross plots of the raw data. An example of the raw data is shown in Fig. 4-9, for the 2.0 mm particles at the various tube locations, superficial velocities, and a temperature of 700 K. The superficial velocity values were chosen so that uniform bubbling fluidization within the bed was insured. All convective results showed similar trends which are summarized as follows:

- The maximum convective heat transfer coefficients occurred when the tube was located in the dense phase of the fluidized bed. For a particular particle size the values did not vary appreciably over the range of superficial velocities examined. The convective heat transfer coefficients at the slumped bed/splash-zone interface (0 mm location) were comparable to those in the dense phase.
- The convective heat transfer coefficients reached their minimum values when the tube was located the greatest distance from the slumped bed surface. At these locations, the heat transfer coefficients did not vary appreciably over the range of superficial velocities examined, indicating that particle effects on the convective heat transfer were negligible. These minimum convective heat transfer coefficients were much higher (by approximately a factor of 3) than those values determined by

the commonly accepted correlations for determining the pure gas heat transfer to a cylinder in cross flow.

- Over the range of superficial velocities investigated, as the superficial velocity increased the particle effects on the convective heat transfer increased, and as the tube height above the bed was increased, the convective heat transfer coefficients always decreased.

Figures 4-3 and 4-4 show convective heat transfer variations as functions of tube location for the 1.1 mm particles at three superficial velocities. The dense phase and the freeboard convective coefficients did not vary appreciably over the range of superficial velocities presented, but there was a clear difference in behavior for the tube located slightly above the splash-zone/dense phase interface (0 mm location). The 1.1 mm particles have hydrodynamic characteristics of both Geldart class B and D particles, that is, significant bed expansion can occur before large bubbles or bubble channels form within the bed. This phenomenon produces a larger bed expansion at the higher superficial velocities, resulting in the heat transfer characteristics for the tube near the splash-zone/dense phase interface at the higher superficial velocities to be similar to those within the dense phase of the bed. Above a splash-zone height of 25 mm, the differences in the convective heat transfer coefficients were significant, indicating the heat transfer to be a strong function of both the tube location and the superficial velocity in the splash-zone. These figures indicate that the convective heat transfer coefficient decreases in a monatonic manner with increasing tube height within the splash-zone and that, for a given tube location within the splash-zone, the greater the superficial velocity the higher the convective heat transfer coefficients. Freeboard convective heat transfer coefficients are approximately three times those predicted by the commonly used empirical correlations for a tube in cross flow at the average superficial velocities, indicating that the freeboard is a highly turbulent flow region. Temperature effects are

small when compared with tube location and superficial velocity effects, especially at the higher superficial velocities. The values indicated in Figs. 4-3 and 4-4 correspond closely to those presented by Biyikli, et. al. (1987) and George and Grace (1982).

Figures 4-5 and 4-7 and Figs. 4-6 and 4-8 show the convective heat transfer variations for tube located in the splash-zone for the 2.0 mm and 2.9 mm particles, respectively. These particle sizes fall into the Geldart class D range and the figures confirm that they behave very similarly both hydrodynamically and thermally. As with the 1.1 mm particles, heat transfer variations are not apparent in the dense phase or the freeboard, but they are significantly different in the splash-zone. Convective heat transfer coefficient variations are similar for the same non-dimensionalized superficial velocities for both particle sizes and for both temperatures throughout the splash-zone; the heat transfer coefficients are higher at the lower tube locations and for higher superficial velocities. The minimum convective heat transfer coefficients are approximately 2 times those predicted by the correlations for a cylinder in pure gas cross flow.

Figures 4-10 and 4-11 show how the convective heat transfer coefficients for the three particle sizes varies with tube location for a non-dimensional superficial velocity ratio of 1.2 and for bed temperatures of 1003 K, and 810 K, respectively. These figures indicate that the 2.0 and 2.9 mm particles behave similarly both thermally and hydrodynamically, and noticeably different from the 1.1 mm particles. Within the dense phase, the 2.0 and 2.9 mm particles have essentially the same heat transfer coefficients. The 1.1 mm particles display convective heat transfer coefficients which are approximately 40 percent greater than for the larger particles. These figures indicate that the convective heat transfer coefficients do not vary with particle size above a splash-zone height of approximately 250 mm for $U/U_{mf} = 1.2$. Here, the particle convective effects tend to flatten and reach asymptotic limits between 45 - 50 W/m^2 K.

Figure 4-12 shows similar results for the three particle sizes for a superficial velocity ratio of 1.5 and a bed temperature of 1003 K.

Figures 4-13 through 4-15 show variations in the blackbody radiative heat transfer coefficients for different tube locations, superficial velocities, and particle sizes. Figure 4-16 compares particle size effects for a non-dimensional velocity of $U/U_{mf} = 1.2$. These results should only be considered representative; they are specific for the experimental facility used in this work. The figures do indicate some features of interest:

- The maximum blackbody radiative heat transfer coefficient occurred for the tube located slightly above the dense phase/splash-zone interface. These results indicate that the void fraction is sufficiently small at this location within the splash-zone so that the surroundings have only a modest radiative contribution to the heat transfer, yet the particle residence time on the tube surface is short enough so that they do not cool appreciably. Bed temperature effects are very important, superficial velocity effects are of modest importance (especially near minimum fluidization), and particle size effects are minimal, with the maximum blackbody radiative heat transfer coefficient of approximately 35 W/m^2 K for the superficial velocities studied and for a bed temperature of 1003 K. The maximum values correspond very well with those predicted by Baskakov (1985).
- The minimum blackbody radiative heat transfer coefficient occurs for a tube located within the freeboard where the void fraction is very large and the radiant contribution of the surroundings and the bed are both significant. The minimum black body radiative heat transfer coefficient is also dependent upon the superficial velocity and particle size, decreasing as the superficial velocity particle size decreases.
- Within the splash-zone, the black body radiative heat transfer coefficients decrease

monatonically from the maximum values found near the dense phase/splash-zone interface. The coefficients are dependent upon particle size, tube location and superficial velocity.

Tables 4-1 through 4-4 give the maximum convective and black body radiative heat transfer coefficients at the corresponding superficial velocities for the different variables investigated. Tables 4-1 and 4-3 indicate that the maximum convective heat transfer coefficient is a function of particle size, tube location, and superficial velocity, but is less dependent on bed temperature. For the range of variables investigated, the maximum convective heat transfer was obtained within the dense phase of the fluidized bed at the smallest particle size. The maximum convective heat transfer coefficients are generally found over a range of superficial velocities which vary with the particle size. Tables 4-2 and 4-4 indicate that the maximum black body radiative heat transfer coefficient is strongly dependent upon bed temperature and to a lesser degree upon superficial velocity, but has little dependence upon particle size. The figures and tables were produced by cross plotting figures similar to Fig. 4-9. Because the figures and the tables do not represent actual experimental data points, no error bars are shown.

4.8 CONCLUSIONS

This paper is Part I of a study which describes the effects of tube location, bed temperature, particle size, and superficial velocity on the heat transfer to a horizontal tube located in the splash-zone of a high temperature bubbling fluidized bed. In part II (Chapter 5), a model to predict those values will be presented.

The coupled effects of particle size, superficial velocity, and tube location had the greatest influence on the convective heat transfer coefficients to the horizontal tube. Temperature variations had less affect. The greatest overall heat transfer coefficients

measured in this study occurred when the tube was located in the dense phase of the fluidized bed for the 1.1 mm particles. The 2.0 and 2.9 mm particles displayed similar behavior for convective heat transfer, but the convective heat transfer coefficients for these cases were approximately 70 percent of the value measured for the 1.1 mm particles. The smallest convective heat transfer coefficients occurred when the tube was located in the freeboard (the tube located the greatest distance from the bed).

The freeboard convective heat transfer coefficients were greater (approximately two to three times) than the values predicted by the correlations for a cylinder in single phase cross flow of a gas at the same temperature and bulk flow rate. This is attributed to the large freeboard turbulence caused by bubbles bursting at the bed surface. No quantitative studies or correlations were found which could be used to strengthen this hypothesis, but it is known that the gas flow rate through the bubbles in a fluidized bed of this particle size can be anywhere from approximately 3 to 10 times the bulk flow rate (Dyrness and Glicksman 1993, Kunii and Levenspiel 1991). A first-order analysis indicates that theses flow rates could cause freeboard convective coefficients to be within the range of those values measured.

Superficial velocity, temperature, and tube location had the greatest influence on the radiative heat transfer coefficients, whereas particle size had minimal effect. The maximum radiative heat transfer coefficients were found when the tube was located slightly above the slumped bed level and the minimum coefficients were observed when the tube was located in the freeboard. When the tube is located slightly above the slumped-bed surface, the particle residence time is short enough that hot particles are nearly always in contact with the tube surface, yet the void fraction is small enough so that the surroundings have little affect on the radiant values. Since the radiation heat transfer coefficients for the tube located in the splash-zone are so system specific, the values measured in this study should only be considered representative and not general.

The in bed radiant coefficients can be considered general, and are well within the limits determined by Baskakov (1985).

4.9 NOMENCLATURE

d_p - Nominal Particle Diameter, mm

T_{bed} - Average Fluidized Bed Temperature, K

U - Average Superficial Fluidizing Velocity, m/s

U_{mf} - Minimum Superficial Fluidizing Velocity, m/s

4.10 ACKNOWLEDGMENTS

We wish to express our appreciation to the National Science Foundation, Grant Number CTS-8803077, for supporting this research.

Table 4-1.

Maximum Convective Heat Transfer Coefficient vs. Tube Location

Convective Coefficients ($W/m^2 K$)

Particle Size(mm)	Tube Location	700 K	810 K	908 K	1003 K
1.1	406 mm	45	49	52	54
	273 mm	75	83	76	76
	133 mm	151	155	159	168
	64 mm	226	230	219	182
	0 mm	258	265	277	256
	-127 mm	277	273	258	269
2.0	406 mm	40	45	47	56
	273 mm	43	60	90	93
	133 mm	87	107	122	131
	64 mm	142	147	138	139
	0 mm	173	177	180	176
	-127 mm	179	173	182	200
2.9	406 mm	33	49	52	52
	273 mm	41	56	77	80
	133 mm	70	90	106	112
	64 mm	110	124	122	126
	0 mm	154	147	152	163
	-127 mm	171	185	181	181

Table 4-2.

Maximum Black body Radiative Heat Transfer Coefficient vs. Tube Location

Radiative Coefficients ($W/m^2 K$)

Particle Size(mm)	Tube Location	700 K	810 K	908 K	1003 K
1.1	406 mm	7.5	12.3	14.2	23.2
	273 mm	10.0	15.7	21.3	30.8
	133 mm	12.3	19.0	25.6	34.0
	64 mm	12.8	19.2	26.2	35.1
	0 mm	13.3	21.0	27.5	36.3
	-127 mm	12.7	19.8	25.6	33.0
2.0	406 mm	7.5	14.0	21.2	28.4
	273 mm	11.0	15.0	21.0	27.5
	133 mm	10.8	15.7	22.1	29.0
	64 mm	10.8	17.0	23.2	34.0
	0 mm	11.3	17.6	24.1	33.3
	-127 mm	12.2	18.2	25.1	32.5
2.9	406 mm	7.8	15.4	23.4	31.8
	273 mm	9.0	18.5	26.1	33.3
	133 mm	11.5	18.9	26.1	33.0
	64 mm	12.9	18.8	25.3	33.3
	0 mm	12.5	18.8	26.0	34.0
	-127 mm	12.7	19.0	24.7	32.2

Table 4-3.

Non Dimensional Velocity Ratio for the Maximum Convective Heat Transfer Coefficient listed in Table 4-1

Particle Size	Tube Location	700 K U_{mf}	700 K U/U_{mf}	810 K U_{mf}	810 K U/U_{mf}	908 K U_{mf}	908 K U/U_{mf}	1003 K U_{mf}	1003 K U/U_{mf}
1.1	406 mm	.45	2.22	.46	2.03	.50	1.98	.50	2.21
	273 mm	.46	2.17	.46	2.17	.51	1.95	.50	2.18
	133 mm	.46	2.14	.49	2.03	.50	1.97	.50	2.21
	64 mm	.46	2.18	.49	1.83-2.03	.49	2.04	.50	2.22
	0 mm	.46	1.67-2.05*	.49	1.70-1.93*	.51	1.97	.50	2.20
	-127 mm	.46	1.80-2.15*	.49	1.67-1.93*	.50	1.40-2.00	.50	1.60-1.81*
2.0	406 mm	1.59	1.44	1.63	1.56	1.68	1.80	1.68	2.00
	273 mm	1.59	1.44	1.63	1.60	1.69	1.79	1.68	1.93
	133 mm	1.59	1.44	1.63	1.54	1.68	1.75-1.80	1.68	1.83-1.92
	64 mm	1.59	1.43	1.63	1.59	1.68	1.60-1.71*	1.68	1.83-1.92
	0 mm	1.58	1.17-1.41	1.67	1.11-1.25*	1.68	1.31-1.38*	1.68	1.29-1.39*
	-127 mm	1.64	1.19-1.33	1.67	1.20-1.33*	1.68	1.25-1.36*	1.69	1.30-1.38*
2.9	406 mm	1.97	1.26	2.08	1.45	2.15	1.56	2.10	1.69
	273 mm	2.01	1.24	2.04	1.43	2.15	1.53	2.11	1.67
	133 mm	1.99	1.23	2.07	1.39	2.14	1.44-1.50	2.14	1.66
	64 mm	1.98	1.22	2.07	1.36	2.13	1.27-1.55	2.11	1.45-1.56
	0 mm	2.00	1.13-1.18*	2.06	1.12*	2.11	1.25-1.40*	2.12	1.18-1.25*
	-127 mm	2.00	1.16-1.22	2.07	1.12-1.18*	2.11	1.18-2.25*	2.12	1.26-1.30*

When more than one non-dimensional superficial velocity is listed, those values represent a range of non-dimensional superficial velocities over which the listed maximum convective heat transfer coefficient is representative.

Asterisk values indicates the range of non-dimensional superficial velocities does not include the maximum experimentally studied superficial velocity, otherwise, the upper bound represents the maximum non-dimensional superficial velocity studied.

Table 4-4.

Non Dimensional Velocity Ratio for the Maximum Black body Radiative Heat Transfer Coefficient listed in Table 4-2

Particle Size	Tube Location	700 K		810 K		908 K		1003 K	
		U_{mf}	U/U_{mf}	U_{mf}	U/U_{mf}	U_{mf}	U/U_{mf}	U_{mf}	U/U_{mf}
1.1	406 mm	.45	2.23	.46	2.12	.50	1.98	.50	1.96-2.20
	273 mm	.46	2.16	.46	2.17	.51	1.95	.50	1.98-2.19
	133 mm	.46	1.80-2.14	.49	1.87-2.02	.50	1.67-1.88*	.50	1.90-2.00*
	64 mm	.46	1.65-1.86*	.49	1.55-2.02	.49	1.55-1.77*	.50	1.80-2.07*
	0 mm	.46	1.35-1.85*	.49	1.70-1.93*	.51	1.14-1.42*	.50	1.50-1.78*
	-127 mm	.46	1.72-1.97*	.49	1.67-1.93*	.50	1.98	.50	2.18
2.0	406 mm	1.59	1.43	1.63	1.60	1.68	1.80	1.68	2.00
	273 mm	1.59	1.30-1.43	1.63	1.60	1.69	1.79	1.68	1.93
	133 mm	1.59	1.30-1.43	1.63	1.38-1.55	1.69	1.54-1.80	1.68	1.80-1.93
	64 mm	1.59	1.30-1.43	1.63	1.38-1.51*	1.68	1.56-1.77	1.68	1.66-1.92
	0 mm	1.58	1.15-1.41	1.67	1.35-1.53	1.68	1.44-1.76	1.68	1.63-1.92
	-127 mm	1.64	1.30-1.33	1.67	1.36-1.52	1.68	1.29-1.73	1.69	1.60-1.85
2.9	406 mm	1.97	1.22-1.25	2.08	1.44	2.15	1.55	2.10	1.68
	273 mm	2.01	1.23	2.04	1.43	2.15	1.53	2.11	1.67
	133 mm	1.99	1.24	2.07	1.39	2.14	1.37-1.50	2.14	1.50-1.67
	64 mm	1.98	1.22	2.07	1.36	2.13	1.27-1.55	2.11	1.35-1.53
	0 mm	2.00	1.15-1.20	2.06	1.17-1.36	2.11	1.35-1.47	2.12	1.40-1.60
	-127 mm	2.00	1.15-1.22	2.07	1.17-1.36	2.11	1.31-1.48	2.12	1.29-1.63

When more than one non-dimensional superficial velocity is listed, those values represent a range of non-dimensional superficial velocities over which the listed maximum black body radiative heat transfer coefficient is representative.

Asterisk values indicates the range of non-dimensional superficial velocities does not include the maximum experimentally studied superficial velocity, otherwise, the upper bound represents the maximum non-dimensional superficial velocity studied.

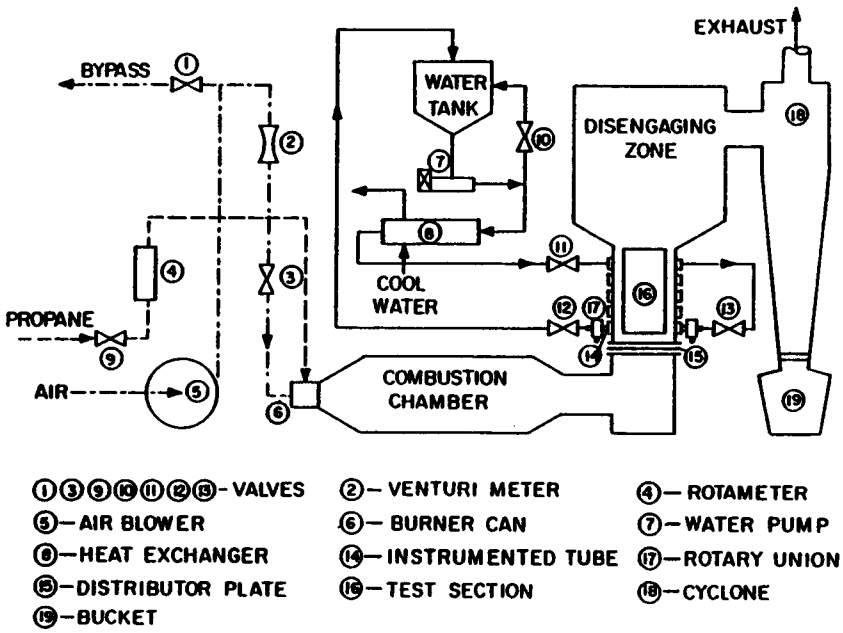

Fig. 4-1 Oregon State University high temperature fluidized bed test facility

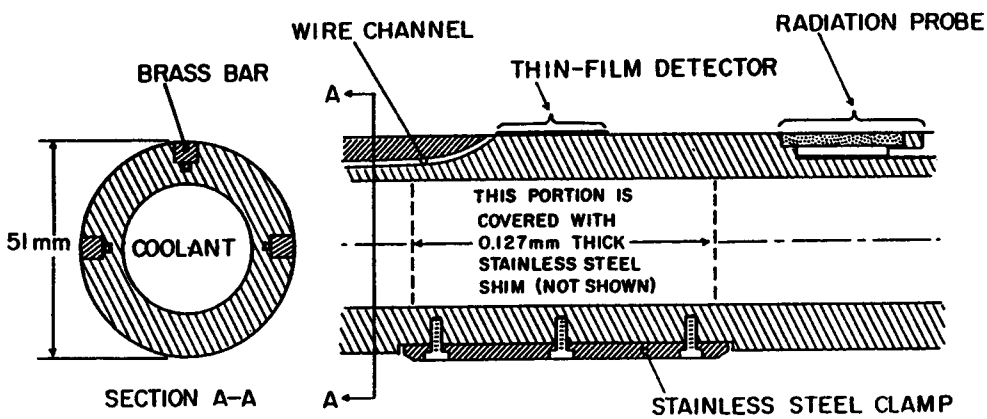

Fig. 4-2 Instrumented tube for total and radiative heat flux measurements

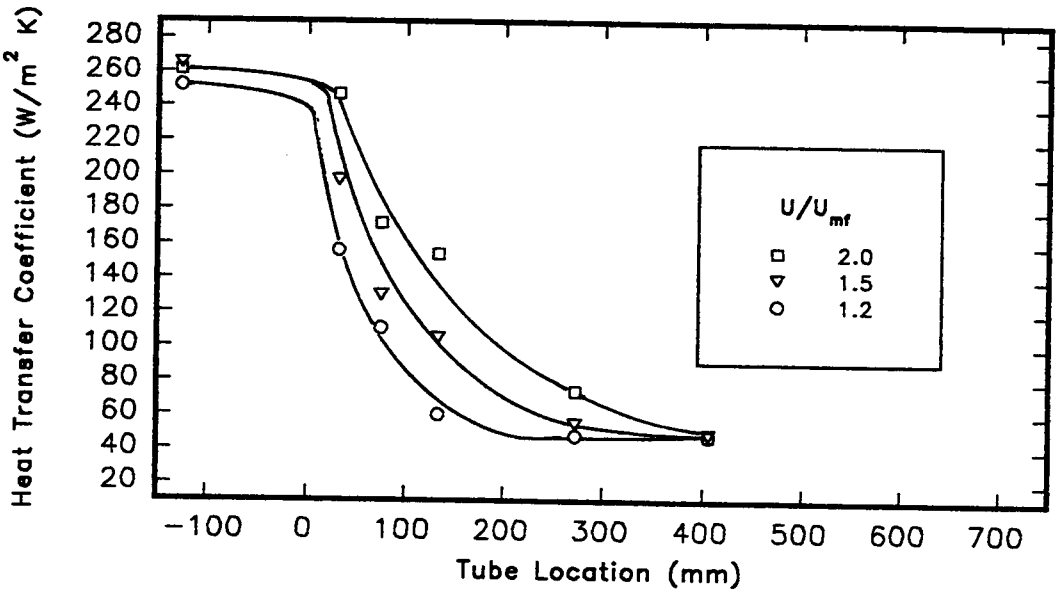

Fig. 4-3 Convective heat transfer coefficients vs. tube location for T_{bed} = 1003 K and for mean particle size d_p = 1.1 mm

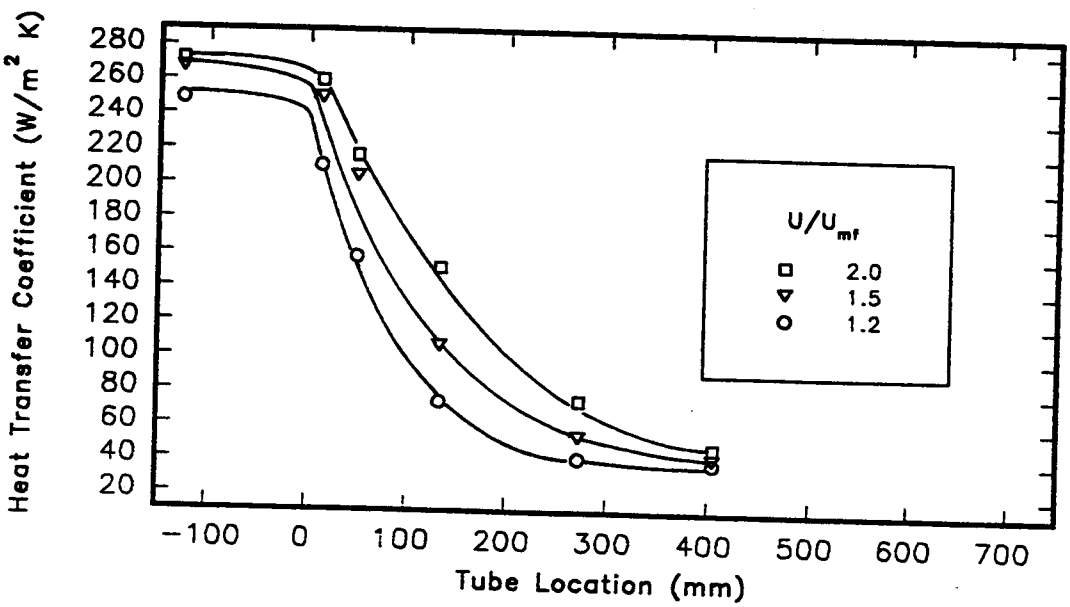

Fig. 4-4 Convective heat transfer coefficients vs. tube location for T_{bed} = 810 K and for mean particle size d_p = 1.1 mm

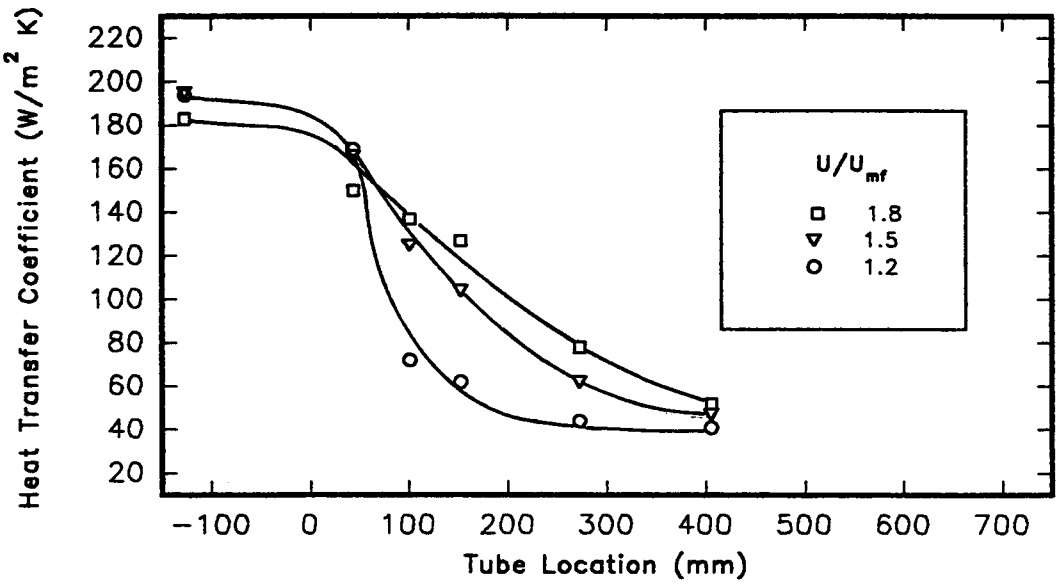

Fig. 4-5 Convective heat transfer coefficients vs. tube location for T_{bed} = 1003 K and for mean particle size d_p = 2.0 mm

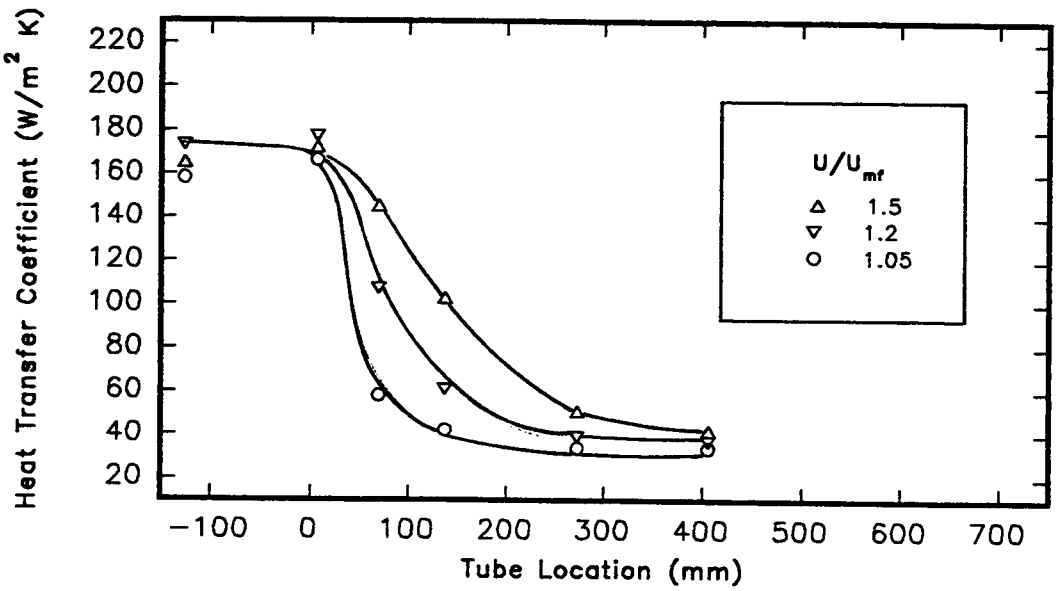

Fig. 4-6 Convective heat transfer coefficients vs. tube location for T_{bed} = 810 K and for mean particle size d_p = 2.0 mm

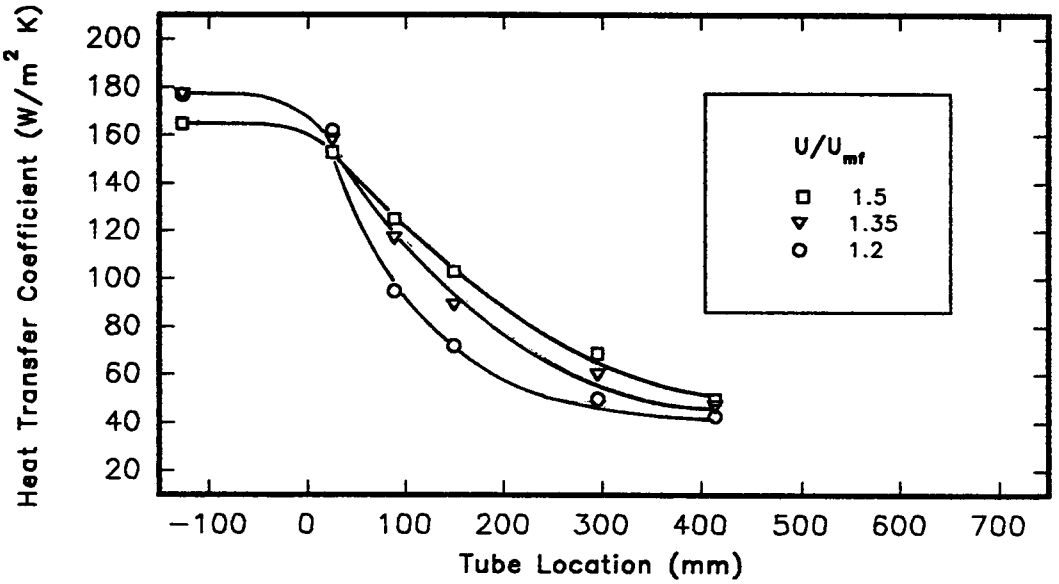

Fig. 4-7 Convective heat transfer coefficients vs. tube location for T_{bed} = 1003 K and for mean particle size d_p = 2.9 mm

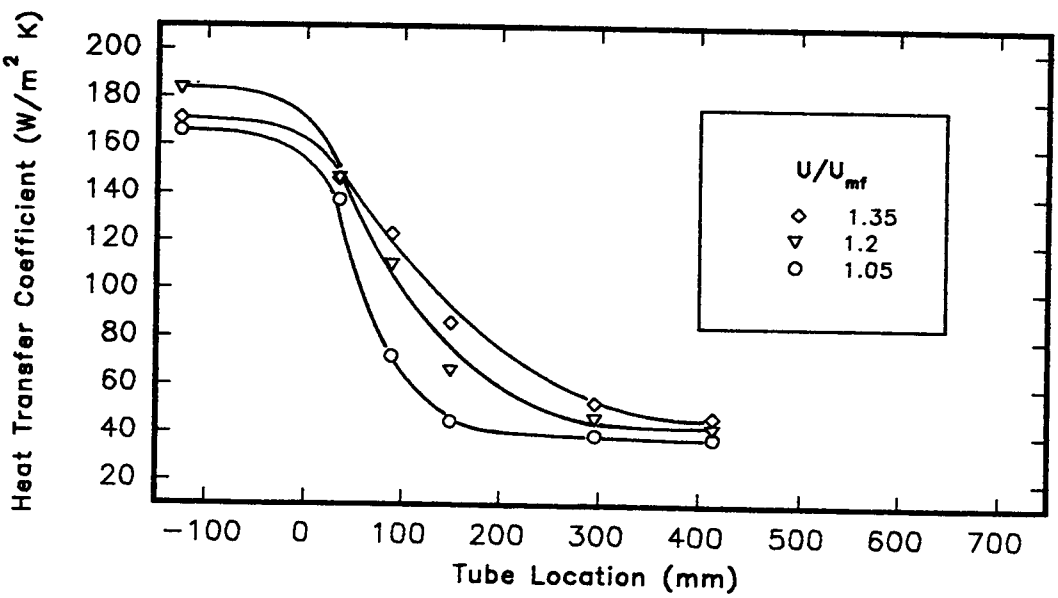

Fig. 4-8 Convective heat transfer coefficients vs. tube location for T_{bed} = 810 K and for mean particle size d_p = 2.9 mm

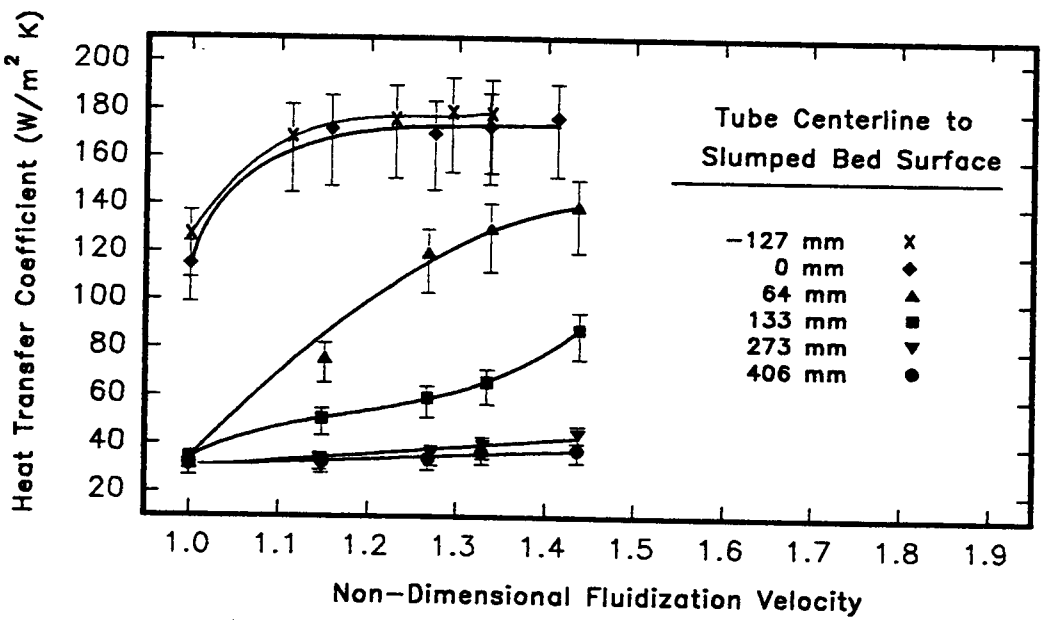

Fig. 4-9 Convective heat transfer coefficients vs. superficial velocity for T_{bed} = 700 K and for mean particle size d_p = 2.0 mm

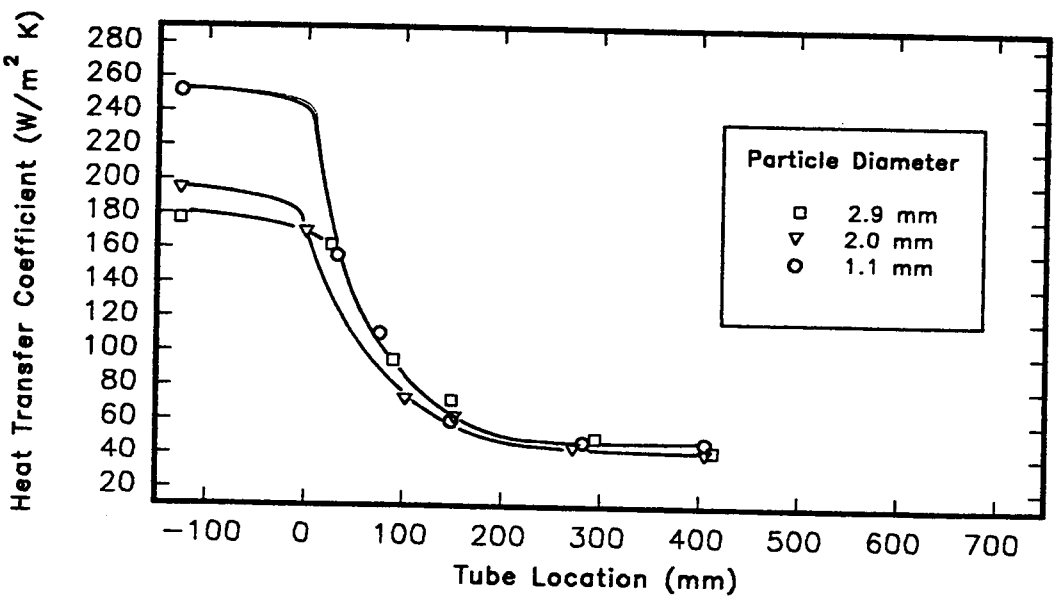

Fig. 4-10 Convective heat transfer coefficients vs. tube location for T_{bed} = 1003 K and for U/U_{mf} = 1.2

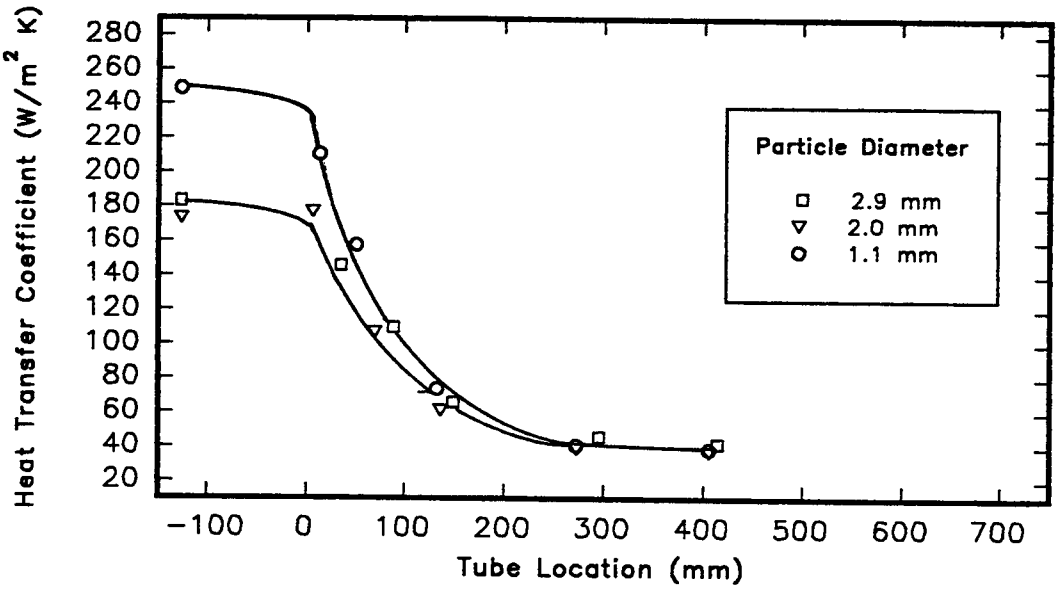

Fig. 4-11 Convective heat transfer coefficients vs. tube location for T_{bed} = 810 K and for U/U_{mf} = 1.2

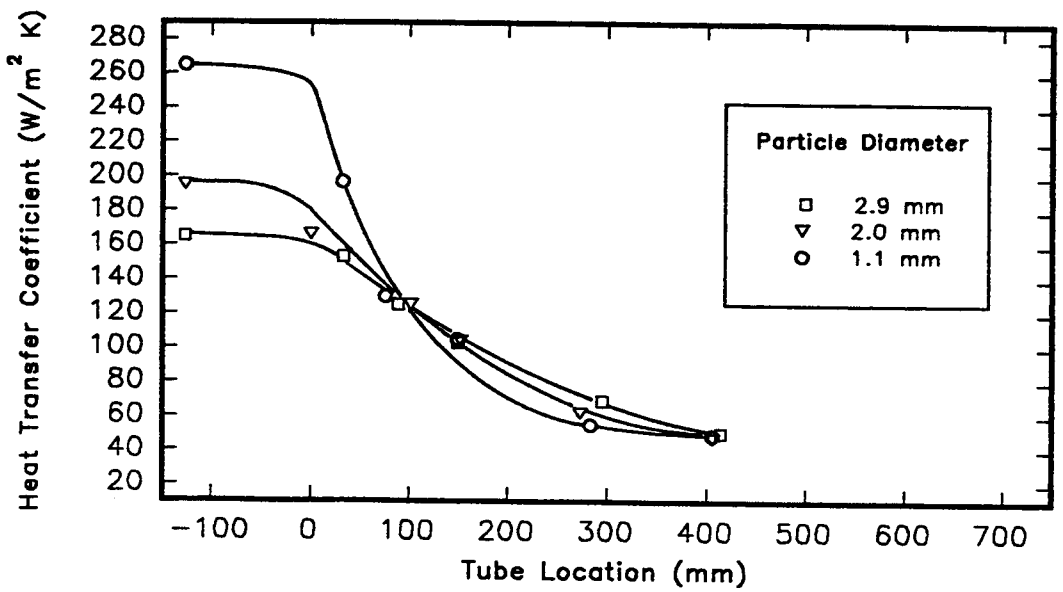

Fig. 4-12 Convective heat transfer coefficients vs. tube location for T_{bed} = 1003 K and for U/U_{mf} = 1.5

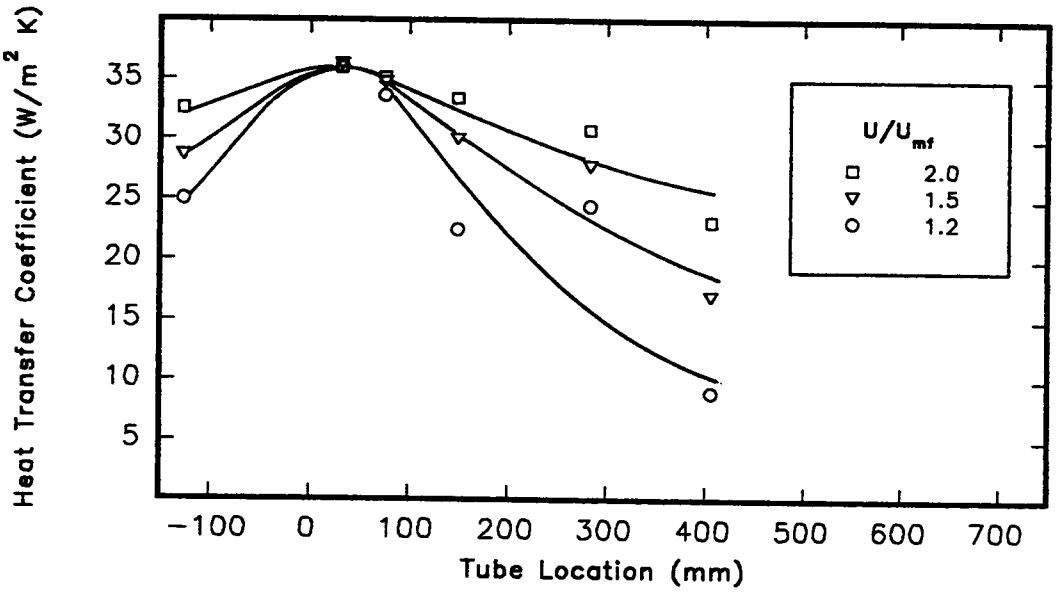

Fig. 4-13 Black body radiative heat transfer coefficients vs. tube location for T_{bed} = 1003 K and for mean particle size d_p = 1.1 mm

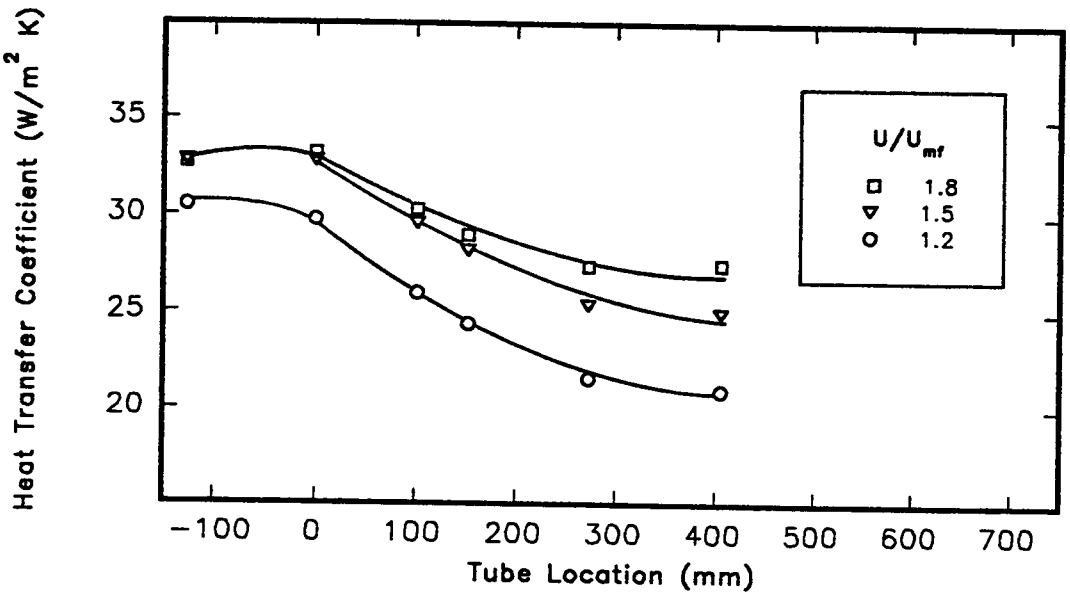

Fig. 4-14 Black body radiative heat transfer coefficients vs. tube location for T_{bed} = 1003 K and for mean particle size d_p = 2.0 mm

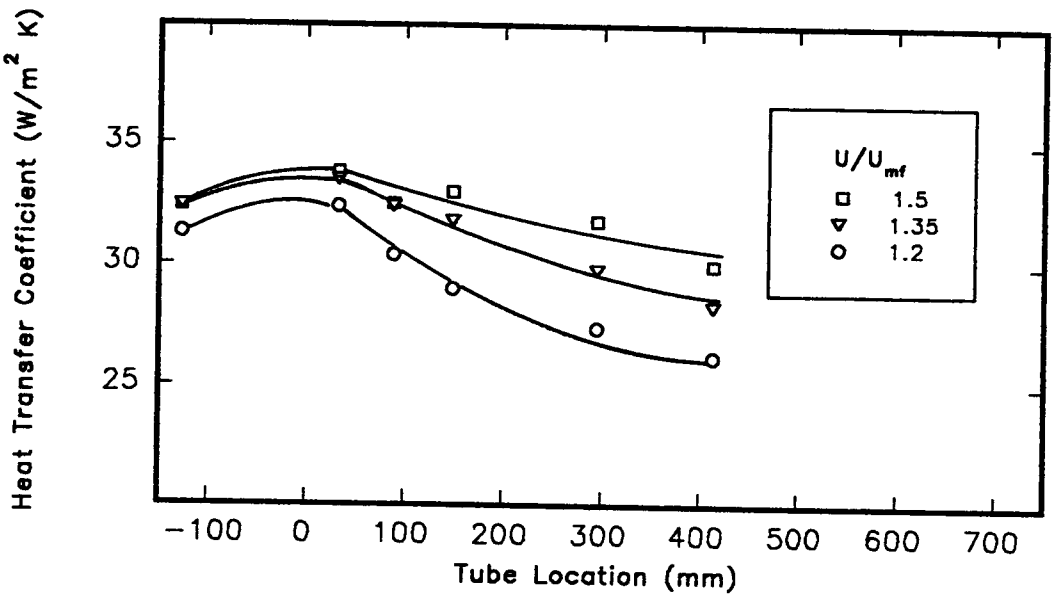

Fig. 4-15 Black body radiative heat transfer coefficients vs. tube location for T_{bed} = 1003 K and for mean particle size d_p = 2.9 mm

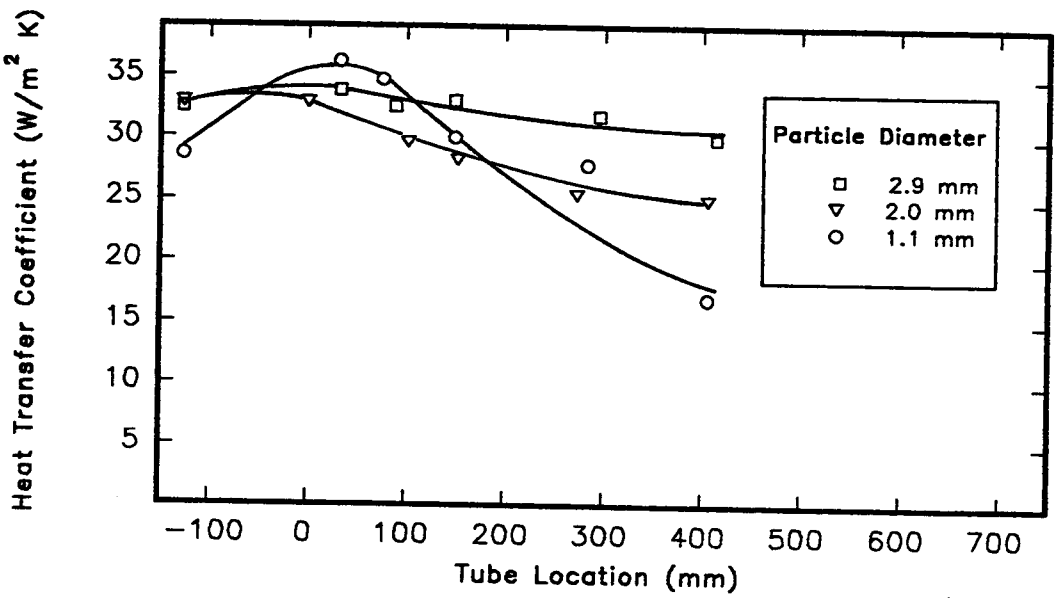

Fig. 4-16 Black body radiative heat transfer coefficients vs. tube location for T_{bed} = 1003 K and for U/U_{mf} = 1.5

4.11 REFERENCES

Alavizadeh, N., An experimental Investigation of Radiative and Total Heat Transfer Around a Horizontal Tube, Ph.D. Thesis, Dept. Mech. Eng., Oregon State Univ., 1985.

Alavizadeh, N., Adams, R.L., Welty, J.R., and Goshayeshi, A., An Instrument for Local Radiative Heat Transfer Measurement Around a Horizontal Tube Immersed in a Fluidized Bed, *J. Heat Transfer*, **112** (2), 486-491, 1990.

Bardakci, T. and Molayem, B., Experimental Studies of Heat Transfer to Horizontal Tubes in a Pilot-Scale Fluidized-Bed Combustor, *Canadian J. of Chem. Engr.*, **67**, 348-351, April 1989.

Baskakov, A.P., Radiative Heat Transfer in Fluidized Beds, in *Fluidization 2nd. Edition*, J.F. Davidson et. al. Eds., pp 465-472, Academic Press, London, 1985.

Biyikli, S., Tuzla, K., and Chen, J.C., A Phenomenological Model for Heat Transfer in Freeboard of Fluidized Beds, Can. *J. of Chem. Eng.*, **67**, 230-236, April 1989.

Biyikli, S., Tuzla, K., and Chen, J.C., Freeboard Heat Transfer in High-Temperature Fluidized Beds, *Powder Technology*, **53**, 187-194, 1987.

Biyikli, S., Tuzla, K., and Chen, J.C., Particle Contact Dynamics on Tubes in the Freeboard Region of Fluidized Beds, *AIChE J.*, **33** (7), 1225-1227, July 1987.

Biyikli, S., Tuzla, K., and Chen, J.C., Heat Transfer Around a Horizontal Tube in Freeboard Region of Fluidized Beds, *AIChE J.*, **29** (5), 712-716, Sept. 1983.

Byam, J., Pillai, K.K., and Roberts, A.G., Heat Transfer to Cooling Coils in the Splash Zone of a Pressurized Fluidized Bed Combustor, AIChE Symposium Series, Vol. 77, No. 208, pp 351-358, 1981.

Catipovic, N.M., Heat Transfer to Horizontal Tubes in Fluidized Beds, Ph.D. Thesis, Dept. of Chem. Eng., Oregon State Univ., March 1979.

Chung, T.-Y., Welty, J.R., Heat Transfer Characteristics for Tubular Arrays in a High-Temperature Fluidized Bed: An Experimental Study of Bed Temperature Effects, *Exper. Therm. and Fluid Sci.*, **3**, 388-394, 1990.

Doeblin, E. O., *Measurement Systems Application and Design*, rev. ed., McGraw-Hill, New York, 1975.

Dyrness, A., Glicksman, L.R., and Yule, T., Heat Transfer in the Splash Zone of a Bubbling Fluidized Bed, *Int. J. Heat Mass Transfer*, **35** (4), 847-859, 1993.

George, S.E. and Grace, J.R., Heat Transfer to Horizontal Tubes in the Freeboard Region of a Gas Fluidized Bed, *AIChE J.*,**28** (5), 759-765, 1982.

George, S.E. and Grace, J.R., Hear Transfer to Horizontal Tubes in Freeboard Region of a Gas Fluidized Bed, AIChE Meeting, San Francisco, No. 7E, 1979.

Gormar, H., Renz, U., and Verweyen, N., Heat Transfer to the Cooled Freeboard of a Fluidized Bed, Proc. of the 1989 Intl. Conf. on Fluidized Bed Combustion, A.M. Manaker Ed., Vol. 2, pp 1241-1244, Sponsored by ASME, San Francisco, CA, Apr 30 - May 3, 1989.

Hongshen, G., et. al., A Model and Experiments for Heat Transfer of Single Horizontal Tube in the Freeboard of Fluidized Bed, Proc. of the 1987 Intl. Conf. on Fluidized Bed Combustion, ed. J.P. Mustonen, Vol 2, pp 1159-1164, Sponsored by ASME, Boston, MA., 1987

Kortleven, A., Bast, J., and Meulink, J., Heat Transfer for Horizontal Tubes in the Splash Zone of a 0.6 x 0.6 m AFBC Research Facility, Proc. of the XVI Intl. Center of Heat and Mass Trans. Conf., Yugoslavia, 1984.

Kunii, D, Levenspiel, O, *Fluidization Engineering, 2nd. Edition,* pp 122, Butterworth-Heineman, Boston, 1991.

Lei, D.H.-Y., An Experimental Study of Radiative and Total Heat Transfer between a High Temperature Fluidized Bed and an Array of Immersed Tubes. Ph.D. Thesis, Dept. Mech. Eng., Oregon State Univ., January 1988.

Mitor, V.V., Matsnev, V.V., and Sorokin, A.P., Investigation of Heat Transfer in Bed and Freeboard of Fluidized Bed Combustors, Proc. of the Eighth Intl. Heat Trans. Conf., C.L. Tien, V.P. Carey, and J.K. Ferrell Eds., Vol. 5, pp 2611-2615, San Francisco, CA, 1986.

Pidwerbecki, D., Welty, J.R., Heat Transfer to a Horizontal Tube in the Splash-zone of a Bubbling Fluidized Bed, an Investigation of Particle Size Effects, to appear in *Journal of Experimental and Thermal Fluid Science* 1994.

Pidwerbecki, D., Welty, J.R., Splash-zone Heat Transfer in Bubbling Fluidized Beds - an Experimental Study of Temperature Effects, to appear in *Journal of Experimental and Thermal Fluid Science* 1994.

Renz, U., von Wedel, G., and Reinartz, A., Heat Transfer Characteristics of the FBC at Aachen Technical University, Proc. of the 1987 International Conf. on Fluidized Bed Combustion, J.P. Mustonen Ed., Vol. 1, pp 619-623, Sponsored by ASME, Boston, MA, May 3-7, 1987.

Shi, M.H., Heat Transfer to Horizontal Tube and Tube Bundle in Freeboard Region of a Gas Fluidized Bed, Proc. of the 1987 ASME/JSME Thermal Eng. Joint Conf., eds. P.J. Martso and I. Tanasawa, Vol. 4, pp 113, Honolulu, HI, March 22-27, 1987.

Wood, R.T., Kuwata, M., and Staub, F.W., Heat Transfer to Horizontal Tube Banks in the Splash Zone of a Fluidized Bed of Large Particles, *Fluidization*, R. Grace and J.M. Matsen Eds., pp 235-243, Plenum, NY, 1980.

Xavier, A.M. and Davidson, J.F., Heat Transfer to Surfaces Immersed in Fluidized Beds and in the Freeboard Region, AIChE Symposium Series, Vol.77, No. 208, pp 368-373, 1981.

5. Heat Transfer to a Horizontal Tube in the Splash-Zone of a Bubbling Fluidized Bed, an Investigation of Tube Location Effects. Part II: Predictive Correlation

5.1 ABSTRACT

A correlation which predicts the convective heat transfer coefficients for a horizontal tube located in the splash-zone of a high temperature bubbling fluidized bed has been developed. This paper is the second of a two-part series which describes the effects of different parameters on the heat transfer to a horizontal tube located in the splash-zone of high temperature bubbling fluidized beds. In Part I, the experimental study was described along with the data which were used in determining the form and constants for the empirical correlation developed herein. The array of experimental conditions used to formulate the correlation included three particle sizes of nominal 1.1, 2.0, and 2.9 mm diameter; four bed temperatures of 700 K, 810 K, 908 K, and 1003 K; and six tube locations ranging from the dense phase of the bed to the freeboard. Superficial velocities were varied from near minimum fluidization (U_{mf}) to over 2.0 U_{mf}. The correlation developed shows good agreement with the applicable data from other investigations.

5.2 KEY WORDS

splash-zone, high temperature, fluidized bed, horizontal tubes, predictive correlation

5.3 INTRODUCTION

A procedure and a correlation is presented for calculating the convective heat transfer coefficients from a bubbling high temperature fluidized bed of Geldart class D particles to a horizontal tube located in the splash-zone. Some correlations exist (Biyikli et al. (1989), Biyikli et al. (1987), Byam et al. (1981), Dyrness et al. (1993), George and Grace (1982), Shi (1987), Wood et al. (1980), Xavier and Davidson (1981)) which predict, over a limited range of operating variables, heat transfer coefficients in the splash-zone; however, none of these correlations can be applied to the Geldart class D particles in a high temperature bubbling fluidized bed.

The correlation proposed by Biyikli et al. (1989) was determined from data obtained at room temperature, for superficial velocities generally out of the range of bubbling fluidized beds, and is based upon parameters for which there are limited data, especially at elevated bed temperatures. Another correlation proposed by Biyikli et al. (1987) is applicable for high temperature fluidized beds and has the same form of the correlation proposed by George and Grace (1982), but the experimentally determined constants are based upon data which were obtained for superficial velocities generally outside the range of bubbling beds. Only a few of their data points are compatable with this study. The experimental conditions considered by Byam et al. (1981) were for a pressurized fluidized bed combustor, Xavier and Davidson's (1981) data were for slugging bed conditions, and Shi's (1987) work, which corresponds very closely with Biyikli's, generally was for superficial velocities beyond bubbling bed conditions. The work of Dyrness et al .(1993) was completed at room temperature in a fluidized bed employing various tube exchanger geometries and with particles of approximately 0.2 mm diameter. Direct comparison of the data is difficult, and the superficial velocity

ratios are beyond the current scope of interest. Wood et al. (1980) obtained data for a bed operating in the turbulent flow regime ($U/V_t \approx 0.5$).

George and Grace (1981) propose an empirical correlation which is in good agreement with their data, but the experimentally determined constants were obtained for a near-room-temperature, atmospheric pressure fluidized bed and for a limited range of particle sizes. The current effort is the only known work which outlines a procedure and a correlation for predicting the convective heat transfer to a horizontal tube in a high temperature bubbling fluidized bed of Geldart class D particles.

5.4 CORRELATION OF THE DATA

A relatively simple correlation has been developed which accurately relates the heat transfer coefficients to a horizontal tube in a high temperature fluidized bed. The particle size range for which the model was developed is from 1.1 to 2.9 mm, the temperature range is 800 to 1000 K, and the superficial velocity range is from 1.05 to 2.0 U_{mf}. The data used in developing this correlation are found in Part I (Pidwerbecki and Welty, (1994 c), Chapter 4) of this work.

5.4.1 Phenomenological Discussion:

The particles used in this study were representative of an actual fluidizing medium with a size range spanning the most commonly used Geldart class D particle sizes. The superficial velocity ranges chosen guaranteed a uniform bubbling bed, and the temperature ranges chosen represent those commonly found in power plant combustion applications. The tube locations within the splash-zone were chosen so that phenomenalogical changes could be analyzed with reasonable accuracy.

A sight glass, located on the top of the experimental facility, allowed a visual observation of the particle/tube interactions while the experiments took place. Some general features of this study are the following:

- Minimum fluidization velocity data were determined by both a visual inspection for minimum fluidization (the initial onset of bubbles forming) and pressure measurements along the bed height; the two methods corresponded very closely.
- The experimental facility consisted of a 0.3 m x 0.6 m x 1.3 m tall test section and a 0.9 m x 0.6 m x 1.3 m tall disengaging zone. During the experiments, the 1.1-mm particles occasionally reached the ceiling of the disengaging zone; the 2.0 and 2.9 mm particles routinely splashed against the disengaging zone ceiling. These observations, along with particle ejection observations made on 2 dimensional beds, led to certain assumptions made on initial particle ejection velocities which are discussed later in this chapter.
- Smaller particles tended to lodge on the lee side of the cylinder to a greater degree than did larger particles; the higher the superficial velocity, the greater the replacement frequency of the lee stack. Slug flow, for the 1.1 mm particles, occurred for superficial velocity ratios greater than approximately 2.4. Maximum superficial velocities studied for the 2.0 and 2.9 mm particles were limited by compressor capacity.

As shown in Part I of this series (Pidwerbecki and Welty (1994 c), Chapter 4), the convective heat transfer coefficients monotonically decrease from the dense phase value, h_b, to a free stream value, h_∞. The h_∞ values are roughly 2 - 3 times those determined by commonly accepted correlations for a cylinder in cross flow. This observation agrees closely with the results of others (Biyikli et al. (1987), Byam et al. (1981) and Renz et al. (1987)). Due to the complexities and chaotic nature of the particle-tube interaction in the splash-zone, a first principle analysis is prohibitive;

consequently, an empirical formulation with appropriate non dimensional variables is necessary.

5.4.2 Correlation:

Previous investigations (George and Grace (1981), Biyikli et al. (1987), and Shi (1987)) have resulted in an empirical formula for the splash-zone region of the form:

$$\frac{h-h_\infty}{h_b-h_\infty}=\frac{1}{1+C(X)^n} \tag{1}$$

where:

$$X=f(x, U, U_{mf}, \phi, C_d, Re, T_{bed})$$

and

"C and n" are experimentally determined constants.

The functional relationship of Eq.(1) also satisfies the boundary conditions:

$$h \Rightarrow h_b \text{ as } X \Rightarrow 0,$$

$$h \Rightarrow h_\infty \text{ as } X \Rightarrow \infty,$$

and

$$\frac{dh}{dX}=0 \text{ at } X=0; n>1$$

George and Grace (1981) assumed that the functional form of X could be described as the distance from the top of the tube to the mean expanded bed height (x) divided by the

value for x at which the non-dimensional heat transfer ratio (the left hand side of Eq.(1)) reached a value 0.025. These parameters are not well documented in the literature and are difficult to obtain for a wide range of operating conditions. Biyikli et al. (1987) and Shi (1987) described the functional form of X in terms of the distance between the tube within the freeboard and the static bed surface for which the average void fraction approaches 0.98. Most of the operating parameters for which the constants of Biyikli's (1987) correlation were obtained are radically different than in this work, and Biyikli's correlation does not agree with the data gathered in this work. Shi (1987) made slight improvements in Biyikli's correlation, however, his correlation still does not adequately correspond with the data gathered in the present study.

Kuni and Levinspiel (1991) and Dyrness et al. (1993) have stated that the gas velocity through bubbles in a bed of large particles is between 3 to greater than 10 times the minimum fluidization velocity. Terminal velocities for the particles in this work are within this expected gas velocity range. The proposed model is based on the assumption that a particle, ejected from the bed by a bubble eruption, will have an initial equivalent to the terminal velocity of the particle and that the maximum height which the particle will attain can be scaled according to simple ballistic theory, i.e.:

$$x_{max} \sim \frac{V_t^2}{2g}$$

The model also assumes that for a tube, located a distance x above the slumped bed height (tube centerline to slumped bed distance), the proper scaling factor which will correctly predict the heat transfer rate in the splash-zone is related to x_{max} by:

$$X = \frac{x}{x_{max}} * \frac{V_t^2}{U^2} \qquad (2)$$

where U is the average superficial velocity within the bed. The values of x_{max} and V_t are determined by the procedure described later in this work.

In order to evaluate the experimentally determined constants, C and n, Eq.(1) was rewritten as:

$$\log\left(\frac{h_b - h}{h - h_\infty}\right) = n \log(X) - \log(C) \qquad (3)$$

The constants C and n were determined by the method of least squares for each of the particle sizes. Values of n ranged between 2.0 and 1.8, hence, an average value of 1.9 was selected. The values of C varied with particle size, and the values obtained are as follows:

d_p = 1.1 mm, C = .11

d_p = 2.0 mm, C = 8.7

d_p = 2.9 mm, C = 12.1

n = 1.9 for all particle sizes

Figure 5-1 shows a logarithmic plot of the variation in $(h_b-h)/(h-h_\infty)$ with X for the 1.1 mm particles at different operating conditions. The data of Biyikli (1987) and George and Grace (1981) are also included and show good agreement. Note that the data of George and Grace tend to follow another coincident curve. This is likely the result of differences in the experimental configuration; George and Grace's data were measured for the first tube in a 16 tube bundle. There were insufficient data to

determine the effects of free-flow area and tube bundle arrangement for a more direct comparison. Biyikli's data are well described by the correlation. Figure 5-2 shows a similar plot for the data acquired in this work. Good agreement is noted between the correlation and the data for the different particle sizes. The RMS. and average absolute errors calculated between the correlation and the data are listed in Table 5-1.

Table 5-1.

Expected Correlation Error vs. Particle Size

d_p(mm)	RMS. Error	Average Error
1.1	21 %	15 %
2.0	21 %	18 %
2.9	16 %	13 %

These error values are comparable with those expected from correlations which predict the heat transfer within the dense phase of high temperature fluidized beds (Saxena (1989)). Figure 5-2 indicates that the 2.0 mm and 2.9 mm particles behave similarly, and the 1.1 mm particles follow the same trend, but follow a different curve. This can be explained, in part, by noting that the 1.1 mm particles should have the characteristics of Geldart class B - D particles, whereas the 2.0 and 2.9 mm particles are well within the Geldart class D range.

Figure 3 indicates how the constant C in Eqs. (1) and (2) varies with particle size. Use of Fig. 5-3 to determine C is recommended for applications where the particle size falls within the range of experimental conditions studied in this work.

5.4.3 Procedure for Calculation of V_t:

A simple procedure was used to estimate the values of V_t using the correlation and procedure proposed by Haider and Levenspiel (1989). The equations used to predict V_t are:

$$V_t = u_* \left[\frac{\rho_f^2}{g\mu(\rho_s - \rho_f)} \right]^{-1/3} \qquad (4)$$

where

$$u_* = \left[\frac{18}{d_*^2} + \frac{(2.3348 - 1.7439\phi)}{d_*^{0.5}} \right]^{-1} \qquad (5)$$

$$0.5 \leq \phi \leq 1$$

and

$$d_* = d_p \left[\frac{g\rho_f(\rho_s - \rho_f)}{\mu^2} \right]^{1/3} \qquad (6)$$

The particle sphericity, ϕ, was estimated from the values recommended by Saxena (1989). The sphericity values used for the particles in this work are shown in Table 5-2.

Table 5-2.

Sphericity of Particles vs. Particle Size
(From Saxena (1989))

d_p	ϕ
1.1 mm	.80
2.0 mm	.73
2.9 mm	.67

5.4.4 Procedure for Calculation of x_{max}:

A simplified methodology to determine x_{max} has been developed. Assumptions made in this part of the model include the following:

- Particle interactions within the splash-zone are ignored
- The particles are ejected perpendicular from the average bed surface with an initial velocity equal to the terminal velocity calculated by Eqs.(4, 5, and 6)
- The average gas velocity within the splash-zone is equal to the bulk fluidization velocity, U
- Bed expansion from fluidization can be ignored
- Fluid properties are evaluated at the bed temperature
- The effects of distributor plate design and the facility dimensions are negligible. The effects of available area (due to tube banks, etc.) were not addressed.

The equation for vertical motion of particles within the splash-zone is:

$$-F_d - W = mV_r \frac{dV_r}{dx} \qquad (7)$$

with the conditions

$$V_o = V_t$$

where F_d is the drag force and W is the weight of an individual particle, expressed as:

$$F_d = C_d \rho_f \frac{\pi d_p^2}{8} V_r^2 \tag{8}$$

$$W = \rho_s g \frac{\pi d_p^3}{6} \tag{9}$$

and

$$V_r = V - U \tag{10}$$

The quantity, V_r, is the relative velocity between the particles and the bulk fluid flow. The drag coefficient, C_d, is determined using the correlation of Haider and Levenspiel (1989):

$$C_d = \frac{24}{Re}\left[1 + [8.1716\exp(-4.0655\phi)] \times Re^{(0.0964+0.5565\phi)}\right] + \frac{73.67\,Re\exp(-5.0748\phi)}{Re + 5.378\exp(6.2122\phi)} \tag{11}$$

(maximum RMS deviation ≅ 4.4%)

Equations 7 - 11 were solved numerically to determine the maximum value for x, which equates to the term x_{max} listed in Eq. (2).

5.5 RESULTS AND DISCUSSION

Figures 5-4 through 5-8 show how the data relates to the correlation over the range of particle sizes, temperatures, and superficial velocities studied. Figure 5-4 indicates that the correlation closely reproduces the 1.1 mm particle size convective heat transfer data for splash-zone locations less than 300 mm, but begins to deviate for the tube located above this location. This deviation should be noted but, since the heat transfer coefficients at this region of the fluidized bed are small compared with those within the dense phase, the net effective error in determining the overall thermal output of a fluidized bed boiler would be small. The correlation also closely corresponds with the applicable data of other investigators even though their experimental conditions were somewhat different than those of this study. These comparisons indicate that the correlation is unrelated to the effects of distributor plate design and fluidized bed vessel dimensions; and is properly scaled to take into account the effects of particle density, sphericity, and bed temperature. Figures 5-4, 5-5, and 5-6 show that the correlation closely represents the data spanning the range of superficial velocity ratios (U/U_{mf}) for which fluidized beds are commonly operated and reconfirms the robustness of the correlation to variations in superficial velocities. Figures 5-7 and 5-8 indicate that the correlation is also robust to particle size variations and temperature variations (within the stated range of values).

Numerous correlations are available to predict the heat transfer coefficients within a high temperature bubbling fluidized bed (for a good overview, see Saxena (1989)), but the there are no known correlations which deal with a relatively low

Reynolds number bulk flow condition with large upstream turbulence (in order to determine the h_∞ values). It appears that the values for the heat transfer coefficients which are predicted from the commonly accepted correlations (McAdams (1954), for example) are low by a factor of 2 - 3 when a tube is subjected to extreme free-stream turbulence as is encountered within the splash-zone.

5.6 CONCLUSIONS

A correlation which predicts the convective heat transfer coefficients for a horizontal tube located in the splash-zone of a high temperature bubbling fluidized bed has been developed. The correlation is relatively simple to apply and requires a minimal number of empirical coefficients. Restated, the full form of the correlation is:

$$\frac{h-h_\infty}{h_b-h_\infty}=\frac{1}{1+C\left[\frac{x}{x_{max}}\left(\frac{V_t}{U}\right)^2\right]^{1.9}} \qquad (12)$$

where, for particle sizes studied, the values of C are:

d_p (mm)	C
1.1	.11
2.0	8.7
2.9	12.1

and the procedure for calculating x_{max} and V_t have been described in the paper. The use of Fig. 5-3 to determine C for various particle sizes is recommended for applications

where the particle size falls within the range of experimental conditions studied in this work. The range of conditions for which the model is applicable is:

$$1.1 \text{ mm} \leq d_p \leq 2.9 \text{ mm}$$

$$800 \text{ K} \leq T_{bed} \leq 1000 \text{ K}$$

$$1.05 \leq U/U_{mf} \leq 2.0$$

The model adequately correlates the heat transfer results reported in Part I of this paper as well as applicable results of other authors. The maximum RMS error for the data measured in this study is 21%. Due to the inability to correctly predict values for h_{∞}, a conservative RMS error estimate of 30% is recommended when using the model to predict the heat transfer coefficients in the splash-zone of a fluidized bed operating.

5.7 NOMENCLATURE

C	Constant in Eqs. (1), (3), and (12)
C_d	Drag Coefficient
d_p	Nominal particle diameter, mm
F_d	Drag force, N
g	Acceleration due to gravity, = 9.81 m/s^2
n	Constant in Eqs. (1) and (3)
Re	Reynolds Number based on equivalent spherical diameter of particle
	$= \frac{d_p V_r \rho_f}{\mu}$
T_{bed}	Average fluidized bed temperature, K
U	Average superficial fluidizing velocity, m/s

U_{mf} Minimum superficial fluidizing velocity, m/s

V Velocity of the particle at a particular location in the splash-zone, m/s

V_o Initial ejection velocity of the particle into the splash-zone, $\cong V_t$, m/s

V_r Relative velocity of particle in splash-zone, = V-U, m/s

V_t Terminal velocity of the particle, m/s

x Distance from the slumped bed surface to the tube centerline, m

x_{max} Parameter which describes the theoretical maximum distance a particle will travel into the splash-zone, m

W Weight of a particle with an average diameter of d_p, N

Greek Symbols

ρ_s density of particle, kg/m^3

ρ_f density of fluid, kg/m^3

μ viscosity of fluid, kg/m-s

ϕ particle sphericity, $\equiv s/S$

s is the surface area of a sphere having the same volume as the particle

S is the surface area of the particle

5.8 ACKNOWLEDGMENTS

We wish to express our appreciation to the National Science Foundation, Grant Number CTS-8803077, for supporting this research.

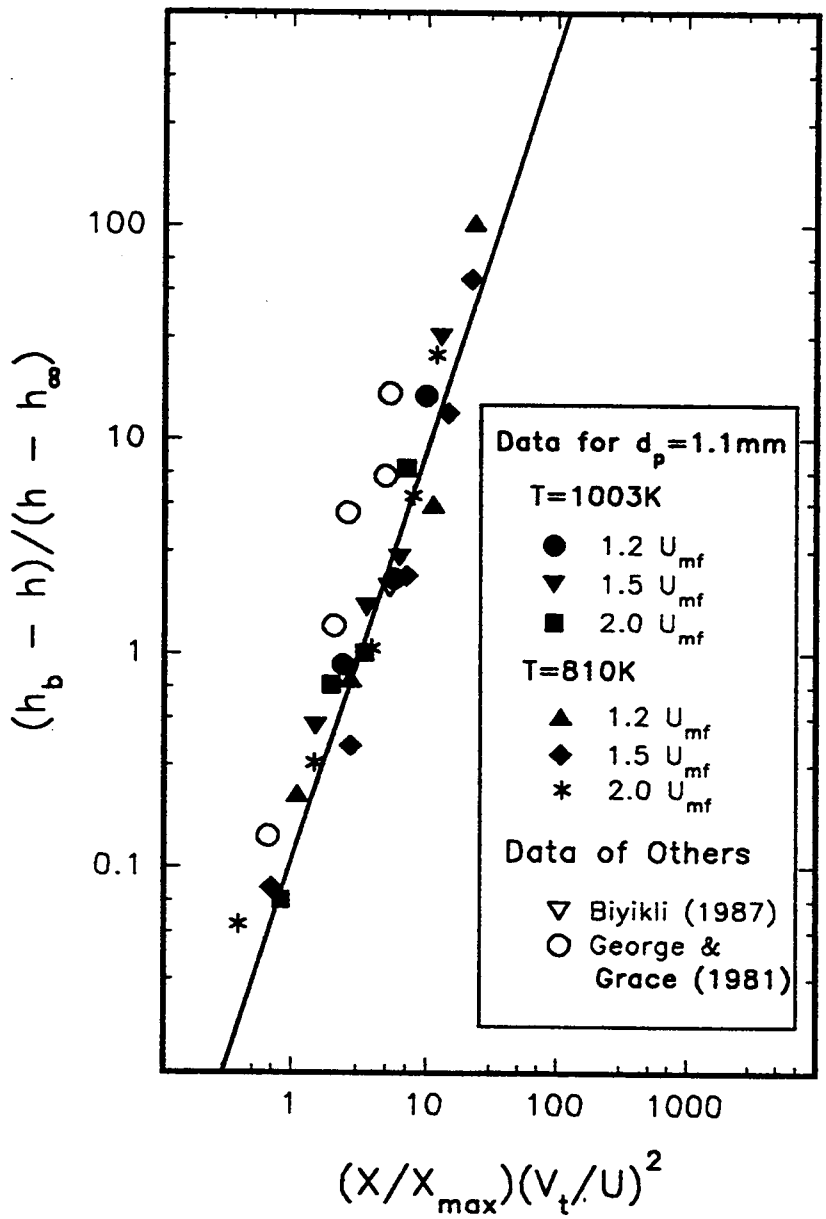

Fig. 5-1 Data for 1.1 mm particles fitted according to Eq. (3) for C = .11
Similar data of other investigators is also shown

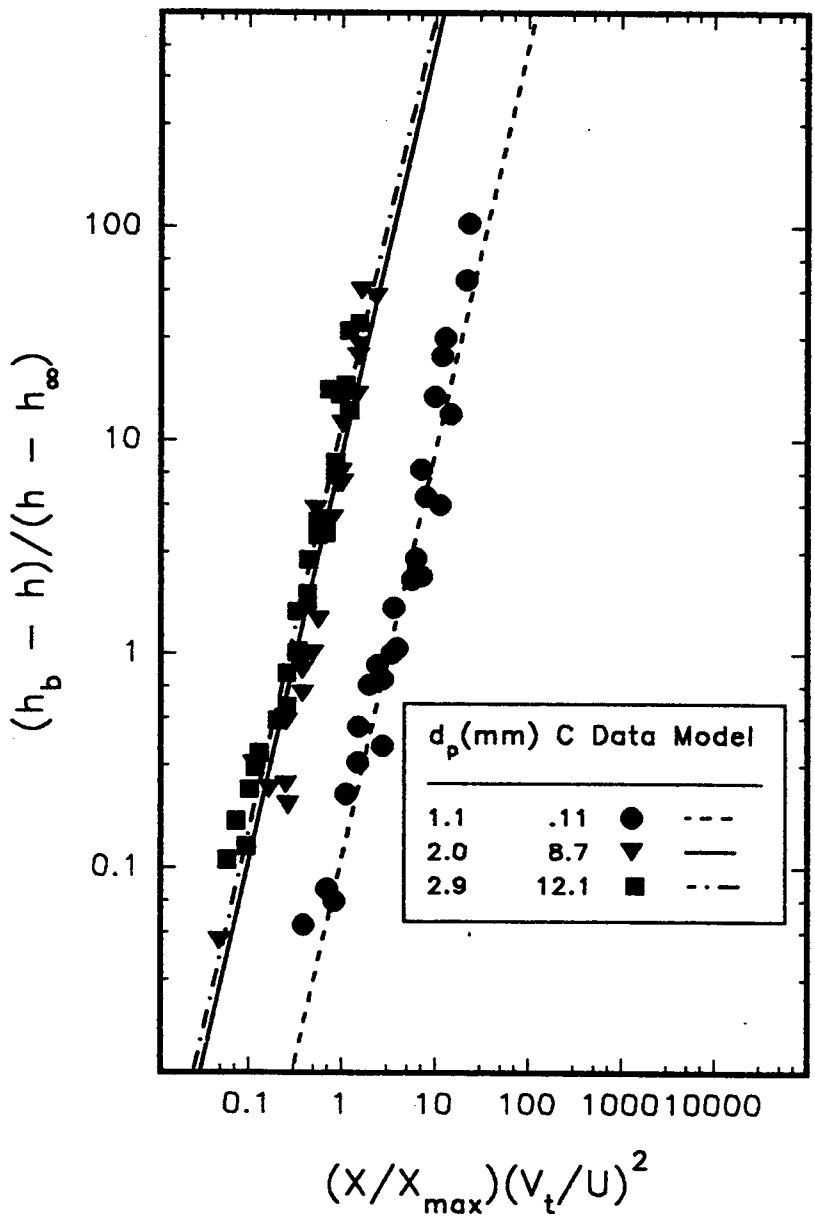

Fig. 5-2 Measured vs. predicted heat transfer coefficients (Eq. (3)) for the three particle sizes and for T_{bed} = 1003 K and T_{bed} = 810 K

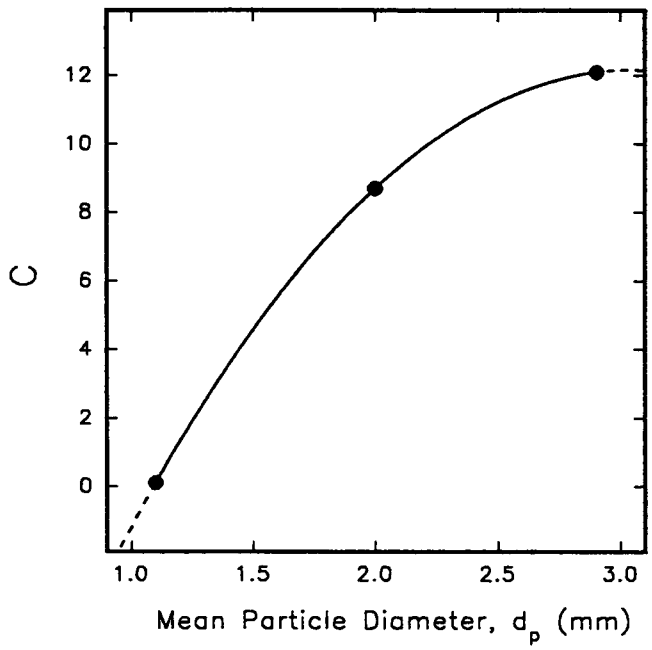

Fig. 5-3 Particle diameter vs. Constant C found in Eqs. (1), (3), and (12)

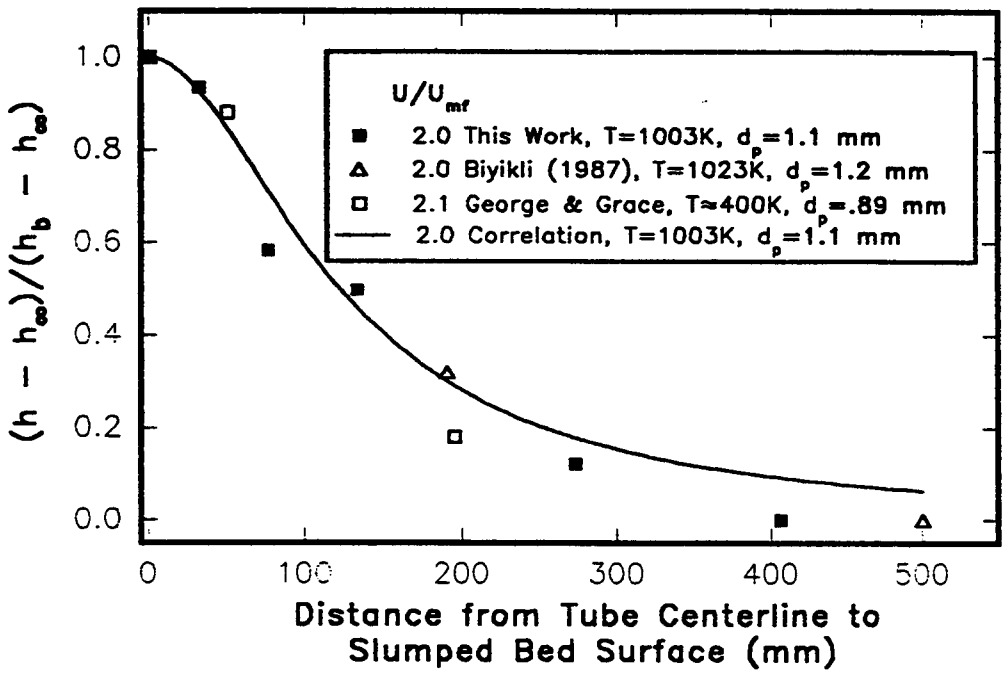

Fig. 5-4 Comparison between experimental dimensionless heat transfer coefficients and Eq. (1) with C = .11 and $U/U_{mf} \approx 2.0$

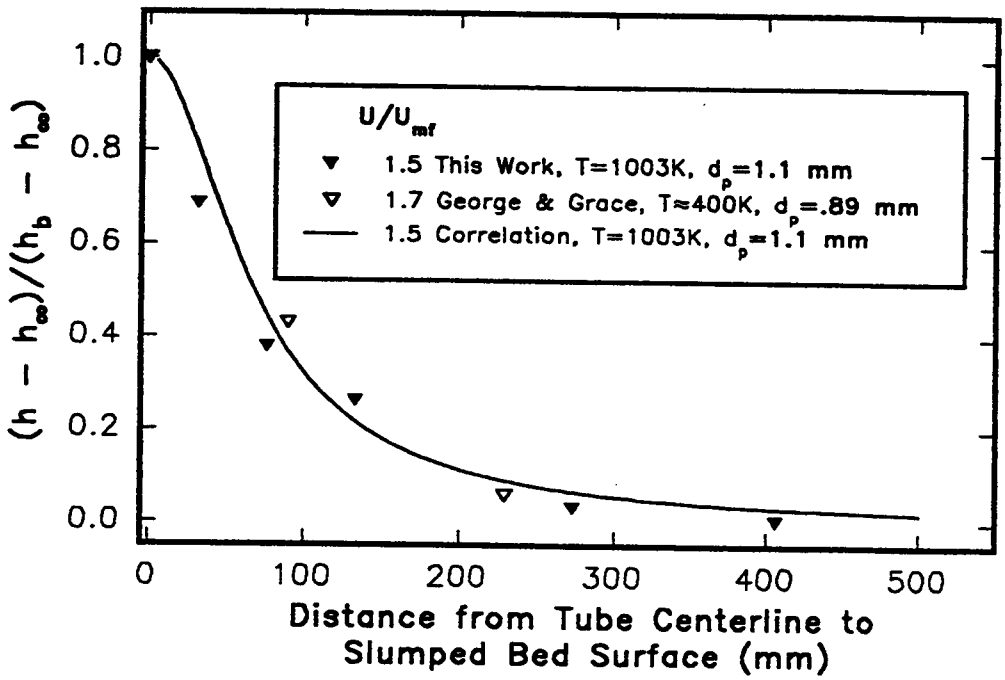

Fig. 5-5 Comparison between experimental dimensionless heat transfer coefficients and Eq. (1) with C = .11 and $U/U_{mf} \approx 1.5$

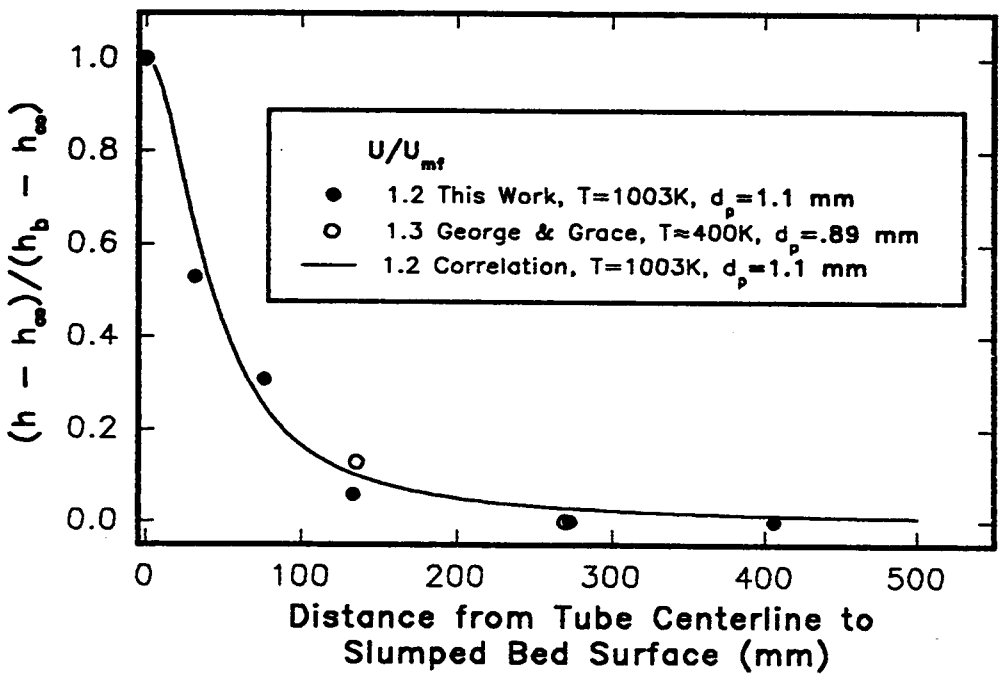

Fig. 5-6 Comparison between experimental dimensionless heat transfer coefficients and Eq. (1) with C = .11 and $U/U_{mf} \approx 1.2$

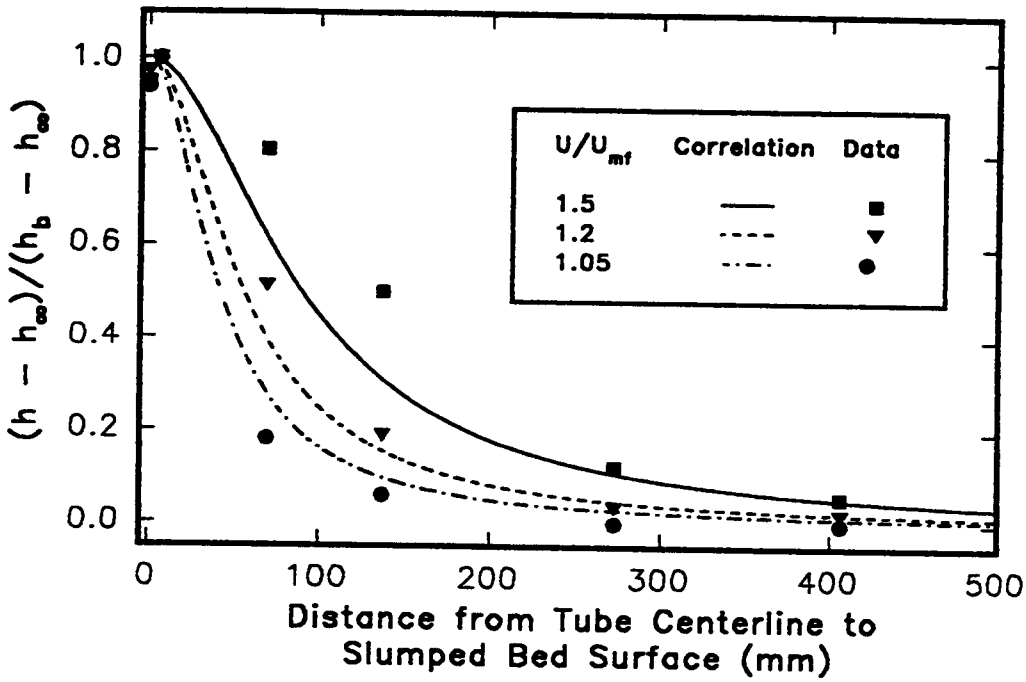

Fig. 5-7 Comparison between experimental dimensionless heat transfer coefficients and Eq. (1) for T_{bed} = 810 K, d_p = 2.0 mm and with C = 8.7

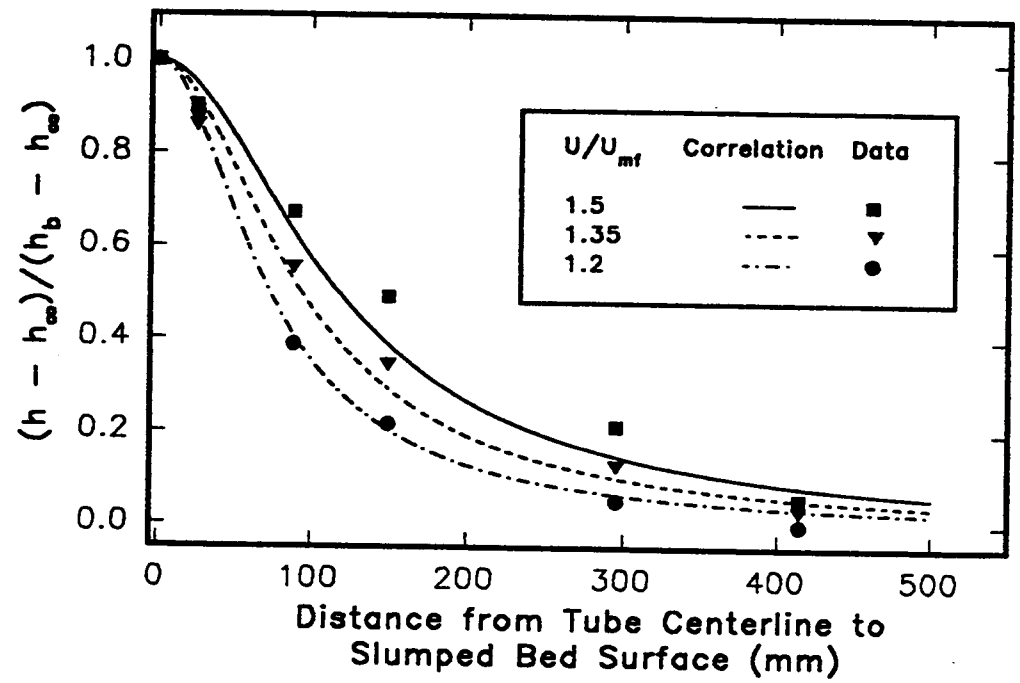

Fig. 5-8 Comparison between experimental dimensionless heat transfer coefficients and Eq. (1) for T_{bed} = 1003 K, d_p = 2.9 mm and with C = 12.1

5.9 REFERENCES

Biyikli, S., Tuzla, K., and Chen, J.C., A Phenomenological Model for Heat Transfer in Freeboard of Fluidized Beds, Can. *J. of Chem. Eng.*, **67**, 230-236, April 1989.

Biyikli, S., Tuzla, K., and Chen, J.C., Freeboard Heat Transfer in High-Temperature Fluidized Beds, *Powder Technology*, **53**, 187-194, 1987.

Biyikli, S., Tuzla, K., and Chen, J.C., Heat Transfer Around a Horizontal Tube in Freeboard Region of Fluidized Beds, *AIChE J.*, **29** (5), 712-716, Sept. 1983.

Byam, J., Pillai, K.K., and Roberts, A.G., Heat Transfer to Cooling Coils in the Splash Zone of a Pressurized Fluidized Bed Combustor, AIChE Symposium Series, Vol. 77, No. 208, pp 351-358, 1981.

Dyrness, A., Glicksman, L.R., and Yule, T., Heat Transfer in the Splash Zone of a Bubbling Fluidized Bed, *Int. J. Heat Mass Transfer*, **35** (4), 847-859, 1993.

George, S.E. and Grace, J.R., Heat Transfer to Horizontal Tubes in the Freeboard Region of a Gas Fluidized Bed, *AIChE J.*,**28** (5), 759-765, 1982.

Haider, A., and Levenspiel, O., "Drag Coefficient and Terminal Velocity of Spherical and Nonspherical Particles", *Powder Technology*, **58**, 63-70, 1989.

Kunii, D, Levenspiel, O, *Fluidization Engineering, 2nd. Edition,* pp 122, Butterworth-Heineman, Boston, 1991.

Pidwerbecki, D., Welty, J.R., 1993, Heat Transfer to a Horizontal Tube in the Splash-zone of a Bubbling Fluidized Bed, an Investigation of Particle Size Effects, to appear in *Journal of Experimental and Thermal Fluid Science*, 1994.

Pidwerbecki, D., Welty, J.R., Splash-zone Heat Transfer in Bubbling Fluidized Beds - an Experimental Study of Temperature Effects, to appear in *Journal of Experimental and Thermal Fluid Science*, 1994.

Pidwerbecki, D., Welty, J.R., Heat Transfer to a Horizontal Tube in the Splash-zone of a Bubbling Fluidized Bed, an Investigation of Tube Location Effects - Part I: Experimental Results, submitted to *Journal of Heat Transfer*, 1994.

Renz, U., von Wedel, G., and Reinartz, A., Heat Transfer Characteristics of the FBC at Aachen Technical University, Proc. of the 1987 International Conf. on Fluidized Bed Combustion, J.P. Mustonen Ed., Vol. 1, pp 619-623, Sponsored by ASME, Boston, MA, May 3-7, 1987.

Saxena, S.C., "Heat Transfer between Immersed Surfaces and Gas-Fluidized Beds", *Advances in Heat Transfer* Vol 19, 97-190, 1989.

Shi, M.H., Heat Transfer to Horizontal Tube and Tube Bundle in Freeboard Region of a Gas Fluidized Bed, Proc. of the 1987 ASME/JSME Thermal Eng. Joint Conf., eds. P.J. Martso and I. Tanasawa, Vol. 4, pp 113, Honolulu, HI, March 22-27, 1987.

Wood, R.T., Kuwata, M., and Staub, F.W., Heat Transfer to Horizontal Tube Banks in the Splash Zone of a Fluidized Bed of Large Particles, *Fluidization*, R. Grace and J.M. Matsen Eds., pp 235-243, Plenum, NY, 1980.

Xavier, A.M. and Davidson, J.F., Heat Transfer to Surfaces Immersed in Fluidized Beds and in the Freeboard Region, AIChE Symposium Series, Vol.77, No. 208, pp 368-373, 1981.

6. Conclusions and Recommendations

6.1 CONCLUSIONS

The experimental values of the time averaged convective and radiative heat transfer coefficients between a high temperature bubbling fluidized bed of Geldart class D particles and a horizontal tube located in the dense phase, splash-zone, and freeboard are reported. Of specific interest in this work are the effects of bed temperature, particle size, and tube location. A correlation is also presented which predicts, with reasonable accuracy, the convective heat transfer coefficients for a tube located in the splash-zone. This thesis is presented in a manuscript format, that is, chapters 2 - 5 are stand-alone works which were submitted to archival journals, complete with an all the requirements of the journals including a conclusion section. This section will reiterate, in a condensed format, the major findings of those chapters.

6.1.1 Chapter 2: Temperature Effects

The temperature effects were reported for a range of superficial velocities, tube locations, and for the 2.9 mm diameter particles. This particle size is representative of the effects which temperature has for all the particle sizes studied. The greatest convective heat transfer occurred within the dense phase of the fluidized bed (-127 mm location). The maximum convective heat transfer coefficients were obtained for the tube immersed in the bed and for superficial velocities between 2.4 to 2.7 m/s . The radiative

heat transfer coefficients were smallest at U_{mf} and increased to asymptotic limits at higher superficial velocities.

The tube located at 64 mm above the packed bed height exhibited characteristics of both the dense phase of the fluidized bed and the freeboard region. Circumferentially-averaged convective heat transfer coefficients increase from their minima at U_{mf} to maximum values at the higher superficial velocities. The maximum values indicated that the bed had expanded sufficiently so that the surroundings had little effect on the radiant contribution; thus the radiant transfer mechanisms were similar to those found in the dense phase of the bed. The 406 mm tube location exhibited characteristics of a tube in the freeboard region of a fluidized bed. Both the convective and radiative heat transfer coefficients increased linearly for the range of superficial velocities investigated. The convective heat transfer coefficients were approximately three times that expected for pure gas convection over a tube at the same bulk flow velocities.

6.1.2 Chapter 3: Particle Size Effects

The maximum convective heat transfer coefficients were realized for the 1.1 mm diameter particles located in the dense phase of the fluidized bed. The maximum convective heat transfer coefficients for the 2.0 mm particles and for the 2.9 mm particles were less than the 1.1 mm particles, similar in value, and also located in the dense phase. Convective heat transfer behavior of the 2.0 and 2.9 mm particles were similar and consistent with the characteristics of Geldart class D particles, while the 1.1 mm particles exhibited characteristics which are a combination of both Geldart class B and class D particle behavior.

Particle effects are not as pronounced for a tube located in the splash-zone, but

the superficial velocities have some effect upon the convective heat transfer coefficients. The gas convective component of the convective heat transfer coefficient is dominant for the 2.0 and 2.9 mm particles which caused less of a decrease in the convective heat transfer coefficient for these particles when compared with the 1.1 mm particles. This phenomena caused the overall convective heat transfer coefficients for the three particle sizes to have similar values for the tube located in the splash-zone. As the non-dimensional superficial velocity ratio was increased some change in the convective heat transfer coefficient was observed for all three particle sizes. This was a result of a decrease in the void fraction of the particles surrounding the tube with a corresponding increase in both the particle convective and gas convective contributions to the total convective heat transfer. Results show that for the tube located in the freeboard (406 mm), the bed particles have minimal effect, and the slight increase in the convective heat transfer is attributed to the increase in gas convection alone.

The maximum black body radiative heat transfer occurred either within the splash-zone or the dense phase of the fluidized bed but, the maximum values for either location are generally very similar. The data shows that the blackbody radiative heat transfer coefficients are likely to be of the same order, but somewhat less than those measured in the dense phase or the splash-zone of the fluidized bed. The blackbody radiative heat transfer coefficients for the tube located in the freeboard are specific to the fluidized bed test facility employed in this work and should be considered representative of typical values.

6.1.3 Chapter 4: Tube Location Effects

The coupled effects of particle size, superficial velocity, and tube location had the greatest influence on the convective heat transfer coefficients to the horizontal tube

located in all locations of the fluidized bed (dense phase, splash-zone, and freeboard). Temperature variations had less affect. The greatest overall heat transfer coefficients measured in this study occurred when the tube was located in the dense phase of the fluidized bed for the 1.1 mm particles. The 2.0 and 2.9 mm particles displayed similar behavior for convective heat transfer in the dense phase, but the convective heat transfer coefficients for these cases were significantly less than the values measured for the 1.1 mm particles. The smallest convective heat transfer coefficients occurred when the tube was located in the freeboard (the tube located the greatest distance from the bed) for all particle sizes.

The freeboard convective heat transfer coefficients were approximately two to three times greater than the values predicted by the correlations for a cylinder in single phase cross flow of a gas at the same temperature and bulk flow rate. A first-order analysis indicates that the expected flow rates caused by bursting bubbles could cause freeboard convective coefficients to be within the range of those values measured.

Superficial velocity, temperature, and tube location had the greatest influence on the radiative heat transfer coefficients, whereas particle size had minimal effect. The maximum radiative heat transfer coefficients were found when the tube was located slightly above the slumped bed level and the minimum coefficients were observed when the tube was located in the freeboard. Once again, the radiant heat transfer coefficients should only be considered representative of a similar apparatus. The in bed radiant coefficients, however, can be considered general, and are well within the limits determined by Baskakov (1985).

6.1.4 Chapter 5: Predictive Correlation

A relatively simple correlation requiring minimal number of empirical coefficients was developed which adequately predicts the convective heat transfer coefficients for a horizontal tube located in the splash-zone of a high temperature bubbling fluidized bed. The full form of the correlation is:

$$\frac{h-h_\infty}{h_b-h_\infty}=\frac{1}{1+C\left[\frac{x}{x_{max}}\left(\frac{V_t}{U}\right)^2\right]^{1.9}}$$

The values of C determined for the particle sizes studied are:

d_p (mm)	C
1.1	.11
2.0	8.7
2.9	12.1

and the procedure for calculating x_{max} and V_t are described in depth in chapter 5.. The maximum RMS error for the data measured in this study is 21%, however due to the inability to correctly predict values for h_∞, a conservative RMS error estimate of 30% is recommended when applying the model.

6.2 RECOMMENDATIONS

In completing this work, the following items which could be examined in future investigations were noted.

- Splash-zone measurements using a short time constant heat flux sensor (say, a gage capable of approximately 100 samples/sec.) mounted on a tube would provide a much deeper insight on the two phase fluid mechanic/heat transfer phenomena between the bed and the tube surface (instantaneous heat transfer measurements and emulsion packet residence time). Possibly, a capacitance probe could be used in conjunction with the tube providing information on the instantaneous and time average void fraction within the splash-zone. Instantaneous Radiant heat transfer data could also provide a great deal of information which could be applied, in conjunction with the instantaneous convective heat transfer results, to a general model of the total energy transport within the splash-zone.
- There is a dearth of information and correlations which addresses the convective heat transfer for a tube exposed to a highly turbulent free stream flow. These fundamental works would be very helpful for a wide variety of engineering applications.
- The present work could be extended to cover a wider array of particle sizes, bed temperatures, bed materials, tube arrangements (tube arrays), etc. These works should include both convective and radiative measurements and would be of practical importance in the design of fluidized bed combustors.
- The fluidized bed test facility could be optimized to operate more efficiently for the intermediate particle size ranges ($0.1 \leq d_p \leq 1$ mm) by installing smaller gas burner nozzles.

- A more detailed analysis on the particle ejection velocities from the bed surface could be used to improve the accuracy of the correlation proposed in this study.

Bibliography

1. Alavizadeh, N., An experimental Investigation of Radiative and Total Heat Transfer Around a Horizontal Tube, Ph.D. Thesis, Dept. Mech. Eng., Oregon State Univ., 1985.

2. Alavizadeh, N., Adams, R.L., Welty, J.R., and Goshayeshi, A., An Instrument for Local Radiative Heat Transfer Measurement Around a Horizontal Tube Immersed in a Fluidized Bed, *J. Heat Transfer*, **112** (2), 486-491, 1990.

3. Bardakci, T. and Molayem, B., Experimental Studies of Heat Transfer to Horizontal Tubes in a Pilot-Scale Fluidized-Bed Combustor, *Canadian J. of Chem. Engr.*, **67**, 348-351, April 1989.

4. Baskakov, A.P., Radiative Heat Transfer in Fluidized Beds, in *Fluidization 2nd. Edition*, J.F. Davidson et. al. Eds., pp 465-472, Academic Press, London, 1985.

5. Biyikli, S., Tuzla, K., and Chen, J.C., A Phenomenological Model for Heat Transfer in Freeboard of Fluidized Beds, Can. *J. of Chem. Eng.*, **67**, 230-236, April 1989.

6. Biyikli, S., Tuzla, K., and Chen, J.C., Freeboard Heat Transfer in High-Temperature Fluidized Beds, *Powder Technology*, **53**, 187-194, 1987.

7. Biyikli, S., Tuzla, K., and Chen, J.C., Particle Contact Dynamics on Tubes in the Freeboard Region of Fluidized Beds, *AIChE J.*, **33** (7), 1225-1227, July 1987.

8. Biyikli, S., Tuzla, K., and Chen, J.C., Heat Transfer Around a Horizontal Tube in Freeboard Region of Fluidized Beds, *AIChE J.*, **29** (5), 712-716, Sept. 1983.

9. Byam, J., Pillai, K.K., and Roberts, A.G., Heat Transfer to Cooling Coils in the Splash Zone of a Pressurized Fluidized Bed Combustor, AIChE Symposium Series, Vol. 77, No. 208, pp 351-358, 1981.

10. Catipovic, N.M., Heat Transfer to Horizontal Tubes in Fluidized Beds, Ph.D. Thesis, Dept. of Chem. Eng., Oregon State Univ., March 1979.

11. Chung, T.-Y., Welty, J.R., Heat Transfer Characteristics for Tubular Arrays in a High-Temperature Fluidized Bed: An Experimental Study of Bed Temperature Effects, *Exper. Therm. and Fluid Sci.*, **3**, 388-394, 1990.

12. Doeblin, E. O., *Measurement Systems Application and Design*, rev. ed., McGraw-Hill, New York, 1975.

13. Dyrness, A., Glicksman, L.R., and Yule, T., Heat Transfer in the Splash Zone of a Bubbling Fluidized Bed, *Int. J. Heat Mass Transfer*, **35** (4), 847-859, 1993.

14. Geldart, D., Types of Gas Fluidization, *Powder Technology*, **7**, 285-291, 1972.

15. George, S.E. and Grace, J.R., Heat Transfer to Horizontal Tubes in the Freeboard Region of a Gas Fluidized Bed, *AIChE J.*,**28** (5), 759-765, 1982.

16. George, S.E. and Grace, J.R., Hear Transfer to Horizontal Tubes in Freeboard Region of a Gas Fluidized Bed, AIChE Meeting, San Francisco, No. 7E, 1979.

17. Gormar, H., Renz, U., and Verweyen, N., Heat Transfer to the Cooled Freeboard of a Fluidized Bed, Proc. of the 1989 Intl. Conf. on Fluidized Bed Combustion, A.M. Manaker Ed., Vol. 2, pp 1241-1244, Sponsored by ASME, San Francisco, CA, Apr 30 - May 3, 1989.

18. Haider, A., and Levenspiel, O., "Drag Coefficient and Terminal Velocity of Spherical and Nonspherical Particles", *Powder Technology*, **58**, 63-70, 1989.

19. Hongshen, G., et. al., A Model and Experiments for Heat Transfer of Single Horizontal Tube in the Freeboard of Fluidized Bed, Proc. of the 1987 Intl. Conf. on Fluidized Bed Combustion, ed. J.P. Mustonen, Vol 2, pp 1159-1164, Sponsored by ASME, Boston, MA., 1987

20. Kortleven, A., Bast, J., and Meulink, J., Heat Transfer for Horizontal Tubes in the Splash Zone of a 0.6 x 0.6 m AFBC Research Facility, Proc. of the XVI Intl. Center of Heat and Mass Trans. Conf., Yugoslavia, 1984.

21. Kunii, D, Levenspiel, O, *Fluidization Engineering, 2nd. Edition,* Butterworth-Heineman, Boston, 1991.

22. Lei, D.H.-Y., An Experimental Study of Radiative and Total Heat Transfer between a High Temperature Fluidized Bed and an Array of Immersed Tubes. Ph.D. Thesis, Dept. Mech. Eng., Oregon State Univ., January 1988.

23. Mitor, V.V., Matsnev, V.V., and Sorokin, A.P., Investigation of Heat Transfer in Bed and Freeboard of Fluidized Bed Combustors, Proc. of the Eighth Intl. Heat Trans. Conf., C.L. Tien, V.P. Carey, and J.K. Ferrell Eds., Vol. 5, pp 2611-2615, San Francisco, CA, 1986.

24. Pidwerbecki, D., Welty, J.R., Heat Transfer to a Horizontal Tube in the Splash-zone of a Bubbling Fluidized Bed, an Investigation of Particle Size Effects, to appear in *Journal of Experimental and Thermal Fluid Science* 1994.

25. Pidwerbecki, D., Welty, J.R., Splash-zone Heat Transfer in Bubbling Fluidized Beds - an Experimental Study of Temperature Effects, to appear in *Journal of Experimental and Thermal Fluid Science* 1994.

26. Pidwerbecki, D., Welty, J.R., Heat Transfer to a Horizontal Tube in the Splash-zone of a Bubbling Fluidized Bed, an Investigation of Tube Location Effects - Part I Experimental Results, submitted to *Journal of Heat Transfer*, 1994.

27. Pidwerbecki, D., Welty, J.R., Heat Transfer to a Horizontal Tube in the Splash-Zone of a Bubbling Fluidized Bed, an Investigation of Tube Location Effects - Part II Predictive Correlation, submitted to *Journal of Heat Transfer*, 1994.

28. Renz, U., von Wedel, G., and Reinartz, A., Heat Transfer Characteristics of the FBC at Aachen Technical University, Proc. of the 1987 International Conf. on Fluidized Bed Combustion, J.P. Mustonen Ed., Vol. 1, pp 619-623, Sponsored by ASME, Boston, MA, May 3-7, 1987.

29. Saxena, S.C., "Heat Transfer between Immersed Surfaces and Gas-Fluidized Beds", *Advances in Heat Transfer* Vol 19, 97-190, 1989.

30. Shi, M.H., Heat Transfer to Horizontal Tube and Tube Bundle in Freeboard Region of a Gas Fluidized Bed, Proc. of the 1987 ASME/JSME Thermal Eng. Joint Conf., eds. P.J. Martso and I. Tanasawa, Vol. 4, pp 113, Honolulu, HI, March 22-27, 1987.

31. Wood, R.T., Kuwata, M., and Staub, F.W., Heat Transfer to Horizontal Tube Banks in the Splash Zone of a Fluidized Bed of Large Particles, *Fluidization*, R. Grace and J.M. Matsen Eds., pp 235-243, Plenum, NY, 1980.

32. Xavier, A.M. and Davidson, J.F., Heat Transfer to Surfaces Immersed in Fluidized Beds and in the Freeboard Region, AIChE Symposium Series, Vol.77, No. 208, pp 368-373, 1981.